THERMOCLINE VARIABILITY IN THE ARABIAN SEA AND ITS EFFECTS ON ACOUSTIC PROPAGATION

Thesis submitted in partial fulfilment of the requirements
for the degree of **Doctor of Philosophy**
in **Physical Oceanography**

K. G. RADHAKRISHNAN
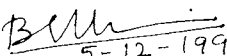Naval Physical and Oceanographic Laboratory, Cochin 682 021

at

COCHIN UNIVERSITY OF SCIENCE AND TECHNOLOGY
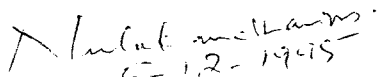COCHIN – 682 022

December 1995

CERTIFICATE

This is to certify that this thesis on **Thermocline variability in the Arabian Sea and its effects** on acoustic **propagation** is an authentic record of research work carried out by Mr K G Radhakrishnan, under our supervision and guidance at the Naval Physical and Oceanographic Laboratory, Cochin 682 021 for the Ph.D degree of the Cochin University of Science and technology and no part of it has previously formed the basis for the award of any other degree in any other University.

Research Supervisors

Dr Basil Mathew
Scientist-D
NPOL, Cochin 682 021

Dr K S N Namboodiripad
Reader
CUSAT, Cochin 682 016

CONTENTS

PREFACE

Typical vertical profiles of temperature consist of a near surface well mixed layer, layer of strong vertical gradient followed by a weak gradient layer. The area of large vertical gradients in temperature is refered to as thermocline which is ubiquitous in the Arabian Sea. The thermocline structure in the Arabian Sea exhibits large spatial and temporal variations in association with the seasonally reversing monsoon winds and currents, upwelling and sinking, eddies and fronts, etc. The influence of these factors on the thermocline structure have not been adequately described. In the thesis attempts have been made to study the spatial and temporal variations of thermocline structure in the Arabian Sea.

Speed of sound in sea water depends on various oceanographic parameters such as temperature, salinity and pressure (depth). The horizontal and vertical gradients of these parameters result in the variation of sound speed structure and hence its propagation. The effect of salinity variations on sound speed is considerably less than the temperature variations. The role of thermocline variability on the acoustic propagation is not clearly understood for the Arabian Sea. In this thesis attempts have also been made to study influences of thermocline structure on acoustic propagation. The thesis contains six chapters. A brief outline of the work carried out in each chapter is given below.

In the introductory chapter the description of the area of study (Arabian Sea) and various factors affecting thermocline variability are discussed. As these

variabilities and their influence on propagation in the Arabian Sea are not understood well, attempts are made to highlight this aspect. In addition to this the previous works relevant to the present study are reviewed.

In chapter II climatology of the thermocline characteristics such as top, thickness, average temperature, gradient, etc. are described utilising an extensive data base. The preparation of this data base compiled from different sources is described. The variations of thermocline structure in the Arabian Sea on an annual cycle is analysed and interpreted.

Climatic mean study indicated that the processes controlling the thermocline dynamics are different for the coastal and open ocean areas. In chapter III regions off west coast of India are identified to investigate this aspect. The monthly cross shelf variations of thermocline characteristics at the selected locations in this region are studied based on a unique data set.

The short term variability of the thermocline characteristics at the selected locations based on time series data are studied in chapter IV. The role of dynamic stability on mixing characteristics in the thermocline is highlighted. The thermocline oscillations and their different harmonics are identified to study their influence on the acoustic propagation.

After establishing various factors causing thermocline variability the acoustic propagation aspects are studied in the Vth chapter. A range-dependent parabolic equation model is used to simulate the propagation conditions. Case studies for internal waves, eddy and typical thermocline structures

identified at different locations are made to highlight their role on sound transmission.

The major findings and their importance are summarised in the last chapter along with the future outlook.
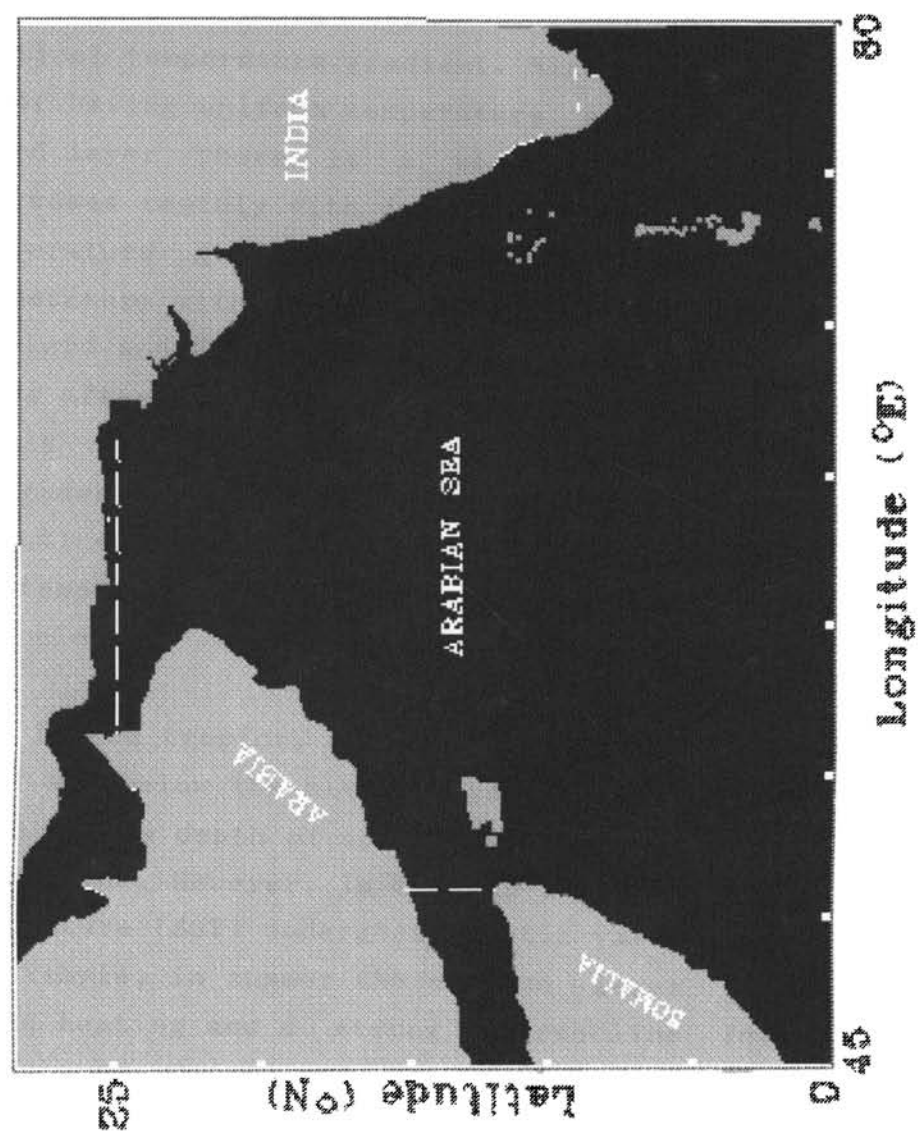
CHAPTER I

INTRODUCTION

1.1 THERMAL STRUCTURE IN THE OCEAN

In the ocean, a typical temperature profile consists of a surface well mixed layer, a layer of sharp temperature drop with increasing depth followed by a zone of weak vertical temperature gradient. Mixed layer is the turbulent layer having uniform temperature and salinity. Below the mixed layer, there is a zone in which the temperature decreases rapidly with depth and the depth at which the temperature gradient is maximum (rate of decrease of temperature with increase of depth) is called *thermocline* (Pickard and Emery, 1982). However in the actual observation it is often difficult to determine this depth precisely mainly because there is a zone in which temperature decreases rapidly with increasing depth. Hence it is easier to notice a thermocline zone as a range of depth over which the temperature gradient is large compared with that above and below.

In the tropics, usually the sea surface is warm (28°-32°C) and below the mixed layer a strong thermocline is found upto a depth of about 200m. This is called the *main thermocline*. However, in the sub-tropics, the sea surface temperature (SST) undergoes drastic variations with season. For example, in summer the surface layer is subjected to strong heating and a strong thermocline forms below the mixed layer. However, during winter the surface layers cools and the thermocline disappears. Hence the thermocline during summer is called *seasonal thermocline*. In the polar regions,

1
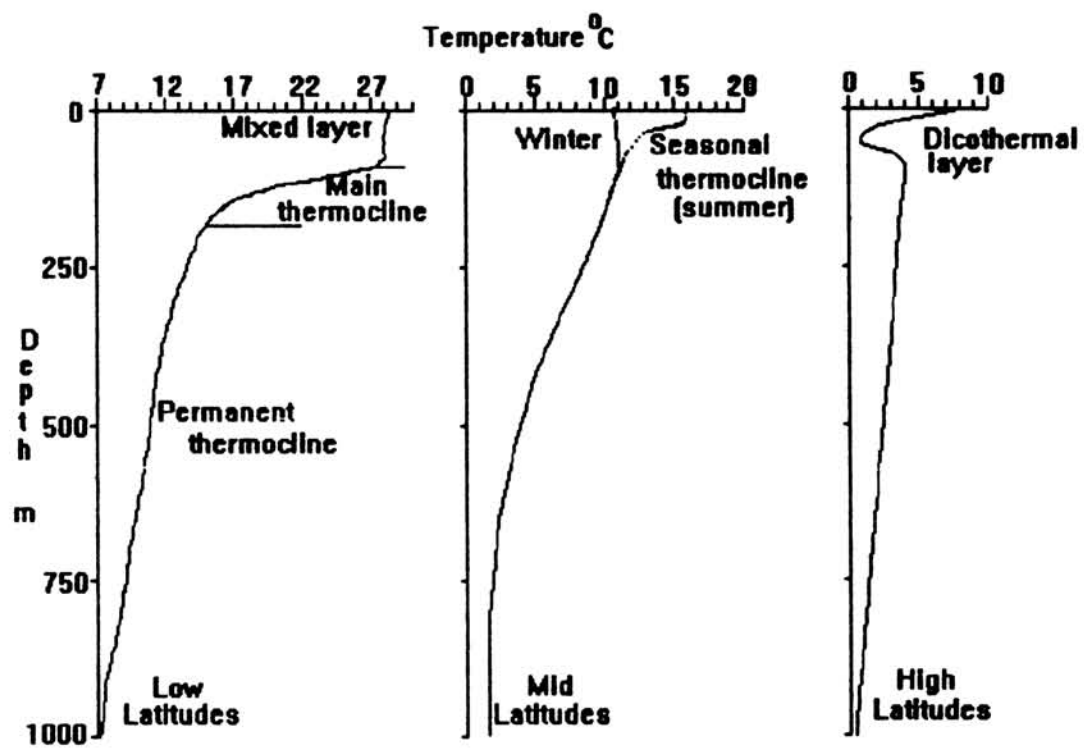
Fig.1.1 Schematic diagram of temperature profile in the Ocean

practically there is no thermocline and in winter the surface layers are colder than the underlying water. However with the advent of summer, the surface layers get heated and a zone of cold water is formed at about 50-100m depth called the *dicothermal layer* (Fig.1.1).

In the tropics and sub-tropics between about 200 and 1000m the temperature decreases with depth. Though the vertical thermal gradients are much weaker than the main thermocline (in the tropics), it is present in all seasons and hence it is called the *permanent thermocline*.

It is well known that deeper waters of the ocean are formed in the polar regions. During winter, the waters of the polar regions becomes colder and denser and it sinks. These waters then spreads along the bottom layers in all ocean basins. On the other hand the upper layers of the tropical and sub-tropical waters get warmed and the heat is expected to be transferred to the lower layers. However this does not seem to take place mainly because the downward transfer of heat at low and mid latitudes is offset by the simultaneous upward movement of cold water (formed near the polar region and advected to middle and low latitudes) from below. It is presumed that the two processes are in long term balance and thermocline is a permanent feature of much of ocean's upper layer. However, the characteristics of thermocline vary widely in space and time due to a variety of factors.

1.2 THERMOCLINE STUDIES IN THE ARABIAN SEA

Arabian Sea is the northwest part of the tropical Indian Ocean with land boundaries in the west, north and east. The domain of study extends from the equator to $25^{\circ}N$

2

and 45°E to 80°E excluding the marginal seas, Red Sea and Persian Gulf.

In tropics, Arabian Sea is a region where the main thermocline is a ubiquitous feature. The sea surface temperature exceeds 29°C during pre-monsoon (Hastenrath and Lamb,1979) in the entire Arabian Sea while it cools significantly to about 23-24°C in the northern Arabian Sea during winter. The winter cooling and summer heating in the northern Arabian Sea causes drastic variations in thermocline characteristics. However in the central Arabian Sea and coastal regions, except northern Arabian Sea, most of the cooling occur during Summer (Colborn,1975) which in turn drastically alter the thermocline characteristics compared to pre-monsoon months. The most significant variations of thermocline from June to August are the shoaling of thermocline off Somalia and Arabia and concomitant deepening in the south central Arabian Sea (Hastenrath and Greischar,1989). However, they have not made attempts to explain the physical processes governing the thermocline variability.

The Arabian Sea is a region of a number of unique oceanographic phenomena. One of the important characteristics of this region is the occurrence of seasonally reversing monsoon winds. During south west monsoon season (June to September) winds are southwesterly which reverse to northeasterly during north east monsoon season (November-February). The Arabian Sea responds both thermodynamically and dynamically to the reversals of winds. Some of the major oceanographic features observed are summer and winter cooling, strong upwelling and sinking, undercurrents, watermass intrusions, meso-scale eddies (clockwise and anticlockwise), and internal waves. All these

features are known to influence the ocean thermal structure
in spatial and temporal domains (Colborn,1975; Duing and
Leetmaa,1980; Schott,1983; Rao et al.,1989).

Associated with onset and progress of the summer
monsoon large cooling of the surface layer take place mainly
due to evaporative cooling and off shore spreading of cold
upwelled water (Krishnamurti,1981; Duing and Leetmaa, 1980).
As a result thermocline is encountered at deeper depths
except near the coast where it shoals. During the monsoon
season entrainment of cold waters from the thermocline into
the mixed layer due to wind, wave and buoyancy mixing
results in the erosion of the top layers of thermocline
(Murthy et al.,1983; Ramesh Babu and Sastry,1984). The
deepening of thermocline is mostly attributed to the mixing
in the upper layers caused by wind wave action and
convective over turning by buoyancy flux, convergence due to
clockwise surface wind stress curl and enhanced vertical
shear in the horizontal flow. (Wyrkti,1971; Colborn,1975;
Rao et al.,1976; Sastry and Ramesh Babu,1979; Robinson et
al.,1979 ; Rao,1987; Rao and Mathew 1990).

Vertical motions in the sea also influence thermocline
characteristics. The thermocline shoals and sometimes even
surfaces during the periods of upwelling (divergence) while
it deepens during the periods of convergence (sinking). The
process of upwelling commences in the early part of summer
monsoon while sinking occur mostly in winter. The effect of
the latter process is manifested as the deepening of
thermocline. Moreover, the thermocline gradient also gets
affected by these vertical motions. During the periods of
upwelling, usually a undercurrent is noticed in the lower
thermocline (counter to surface flow) which drastically
alters the thermocline gradient in the lower thermocline. In

the Arabian Sea, the prominent regions of upwelling and sinking are off Somalia (Bruce,1974; Schott,1983) off Arabia (Bruce,1974; Smith and Bottero,1977; Swallow,1984; Elliot and Savidge,1990; Bauer et al.,1991; Brock et al.,1991) and off the westcoast of India (Sharma,1968; Banse,1968; Wyrtki,1973).

A common feature of upwelling system is the presence of an undercurrent flowing opposite to the surface current (Yoshida and Mao,1957). The region of undercurrent are marked by isotherm downsloping in the subsurface levels and upsloping of isotherms in the surface levels towards the coast. The undercurrent is northward flowing (along west coast of continents) strong currents ($\cong$ 2 Knots) usually found at the continental shelf break associated with coastal upwelling (Hart and Currie,1960). The undercurrents get weaker from south to north along the west coast of India, and ceases to be noticed at about 20°N (Shetye et al.,1990). This undercurrent carries low saline waters from southwestern Bay of Bengal/Equatorial Indian Ocean origin. Studies of Antony (1990), Mohan Kumar et al.,(1995) and Hareesh kumar and Mohan kumar (1995) have clearly established the presence of northward undercurrent along the southwest coast of India. This current is responsible for strong shear leading to mixing in the lower thermocline. This results in the spreading of isotherms in the lower thermocline (reduction of thermocline gradient). They are also responsible for the formation of fine scale structure (step and inversion) in the thermocline (Hareesh kumar et al.,1995). The equatorial undercurrent with its core about 50-100m depth causes spreading of thermocline (Sharma,1968).

The formation, interaction and advection of different watermasses can also cause variations in the thermocline

characteristics. The intrusion of warm/cold water into the thermocline causes warming/cooling of the thermocline in that area. The Arabian Sea high salinity watermass is formed in the northern Arabian Sea and spreads southward in the upper thermocline zone (Rochford,1964; Wyrtki,1971). At the source region it has a temperature of about $30^{\circ}C$ and salinty 36.5 PSU. The Persian Gulf watermass (temperature $27^{\circ}C$ and salinity 39.5 PSU at the source) enters the northern Arabian Sea and spreads in the lower thermocline zone (Rochford,1964; Wyrtki,1971). The Red Sea watermass (temperature $20^{\circ}C$ and salinity 39.7 PSU at source) is mostly found below the main thermocline (Wyrtki,1971; Brock et al.,1992). Further, the low saline Bay of Bengal/Equatorial Indian Ocean watermass (temperature $28^{\circ}C$ and salinity 32.5 PSU at source) also enters the Arabian Sea (Darbyshire,1967; Pankajakshnan and Ramaraju,1987) but its influence is mostly limited to the mixed layer. During southwest monsoon the saline waters of pacific ocean origin enters the western Arabian Sea along with the Somali current (Swallow et al.,1983)

Ocean currents and their associated field of pressure, temperature and density vary in both time and space throughout the ocean. The variability is distributed unevenly with dominant spatial scales in the range of tens to hundreds of kilometers and temporal scales in the range of weeks to months. The meandering and filmenting of intense current systems, semi-attached and cast-off ring currents, advective vortices extending throughout the entire water column, lens vortices, planetary waves, topographic waves and wakes etc., are commonly referred to the generic term *eddies* (Robinson,1983). A knowledge of the actual description of ocean currents and their evolution in time on eddy scales is of considerable interest for practical

purposes.

Arabian Sea is well known for its rich eddy structures (Duing,1972). They are zones of large horizontal and vertical temperature variability. In associate with these features one can expect large changes in the thermocline characteristics (Duing 1972; Swallow,1983). They are classified as cold core and warm core eddies depending on their core temperatures. In contrast to weak thermocline gradients at the core, sharp thermocline are observed at the peripheries of both cold core and warm core eddies. During the early stages of southwest monsoon, two clockwise eddies form off the Somalia coast (Swallow et al.,1983). By July-August, the eddy in the southern region move towards north and merge with the northern eddy (Swallow et al.,1983). However, in some years, both the eddies keep their identity till the end of southwest monsoon (Schott,1983). Das et al.,(1980) resolved eddies based on the hydrographic survey in the northern Arabian Sea in February and March-April 1974. They found eddies of about 200km diameter. Bruce et al.,(1980) reported a warm-core eddy to the northeast of Socotra having approximately 500km diameter based on three synoptic XBT (eXpendable Bathy Thermogaph) sections in June 1978. Studies based on the hydrographic sections covered by ATLANTIS II in 1964-65 and other drifter trajectories revealed that eddies are likely to be found anywhere in the Arabian Sea, with horizontal dimensions in the range 200-500km, vertical extent of some hundreds of meters, and typical surface currents of 20-30cm s^{-1}(Swallow, 1983).

Internal waves are sub-surface waves which propagate along the interface separating fluid layers of different densities within the sea. They may be generated by the flow

of deep ocean currents over topographical features such as
seamounts or the edge of the continental shelf break, the
moving low atmospheric pressure systems and related short
period variations in the wind stress and non-linear transfer
of energy from surface waves, etc. Internal waves owe their
existance to the density gradient and the gravitational
restoring force. The frequency spectra of internal wave are
bounded by the inertial frequency (Sin $\phi/12$) and
Brunt-Vaisala frequency,

$$N = \sqrt{- g\left[\frac{1}{\rho} \frac{\partial \rho}{\partial z} + \frac{g}{C^2} \right]} \text{ rad s}^{-1}$$

where, ϕ : latitude, g : acceleration due to gravity, C :
speed of sound, ρ : density, ∂z and $\partial \rho$ are the depth
difference and corresponding density difference.

Several studies were carried out to understand the
characteristics of the internal waves and its causative
factors (Varkey,1980; Charyulu et al.,1994; Murthy et
al.,1992; Murthy and James,1995). In the coastal waters off
Cochin Rao et al.,(1995) reported the presence of internal
waves throughout the water column with its maximum amplitude
(20 to 30m) in the pycnocline. During the summer monsoon
season, Murthy et al.,(1992) observed high frequency
internal waves with significant spectral peacks at 0.5 to 2
cycles/hour in the deep waters off Ratnagiri and Karwar.
Recently Murthy and Ananth (1994) reported diurnal activity
of internal waves with intense activity during night. One of
the notable results is that the local winds are not
responsible for the generation of internal waves. Based on
current measurements made in the coastal waters off Bombay,
Varkey (1980) reported the presence of internal tides (12

8

hrs). Similar observations were also reported by Shenoi and Antony (1991).

1.2.1 IMPORTANCE OF THERMOCLINE STUDIES

The thermocline studies have got a wide variety of applications in the field of fisheries, underwater surveillance, Ocean Thermal Energy Conversion, Ocean Engineering, etc. In the present study major focus has been given to understand the thermocline characteristics with special emphasis on acoustic propagation in the Arabian Sea. The speed of sound in sea water is an oceanographic variable that determines the behaviour of sound propagation in the ocean. Sound speed varies as a function of water temperature, salinity and pressure (or depth). The speed of sound in the sea water increases with an increase in any of the above three parameters. Since temperature variations are rapid in the thermocline regions, the associated sound propagation is also expected to have large variability in this zone. The thermocline characteristics which influence acoustic propagation have not been adequately studied well for the Arabian Sea. Typical parameters which are commonly used to describe thermocline characteristics are top,thickness, gradient and oscillations in the thermocline (internal waves). All these parameters are known to have impact on the sound propagation.

Top of the thermocline generally coincides with the bottom of the surface mixed layer, the depth at which temperature is 1°C lower than at the surface (Wyrtki,1971; Colborn,1975; Robinson et al.,1979; Hastenrath and Merle,1987). Hence, the factors which control the mixed layer can also be used to explain the variability of the thermocline top. After careful scrutiny top of thermocline

9

is defined as the depth at which the vertical temperature gradient is more than 0.04 ^{o}C m^{-1} for the present study.

Thickness of the thermocline is the vertical separation between top and bottom of the thermocline (Colborn, 1975; Hasternrath and Greischar, 1989). Several authors have given criteria to define the bottom of the thermocline. According to Wyrtki (1964) it is the depth at which the vertical temperature gradient drops to $0.03^{o}C$ m^{-1}. Defant (1936) for his study in Atlantic Ocean and Colborn (1975) after studying several gradient limits for the Indian ocean prescribed $0.02^{o}C$ m^{-1} as the lower boundary criterion. In a recent study, Hastenrath and Merle (1987) suggested it as the level from which downward temperature decreases by less than $2^{o}C$ over an interval of 50m. After analysing the data set of Arabian Sea, a gradient criterion of $0.04^{o}C$ m^{-1} drop in temperature is found more suitable for defining the lower boundary of thermocline in the Arabian Sea. This criterion is followed for the present study.

Thermocline gradient is the ratio of temperature difference between top and bottom of the thermocline over its thickness (Hastenrath and Greischar,1989). In the present study it is computed by taking the temperature differences between two successive layers of 10m each which was then averaged over the entire thermocline.

1.3 OCEAN ACOUSTICS

Sound is the only form of energy which propagates to very long ranges within the volume of the oceans. This is due to the fact that low frequency is less attenuated and travel more distances. Research and exploratory activities

10

on underwater life and other resources, communication, sea bottom mapping, remote control and monitoring of underwater equipment etc. utilise sound energy. Ocean acoustics has developed into a multi-disciplinary branch of science as there are several commercial and military applications of underwater sound.

Speed of sound and transmission loss are two most important acoustic parameters of the ocean medium. Sound speed in sea water increases with increase in temperature, salinity and pressure (depth). It is possible to calculate sound speed using the equation of state of sea water (Fofonoff and Millard, 1984). But the relations involved are cumbersome and computations are time consuming. Hence empirical relations are used for the calculation of sound speed (Wilson,1960; Del Grosso and Mader,1972; Del Grosso,1974; Medwin,1975; Chen and Millero,1977; Mackenzie,1981). Direct measurements of sound speed are also possible with commercially available velocimeters. Sound speed is given by (Mackenzie,1981)

$$C= 1448.96 + 4.591T - 5.304 \times 10^{-2} T^2 + 2.374 \times 10^{-4} T^3 +$$
$$1.340(S-35) + 1.630 \times 10^{-2} D + 1.675 \times 10^{-7} D^2 -$$
$$1.025 \times 10^{-2} T(S-35) - 7.139 \times 10^{-13} TD^3$$

Where C is the sound speed (m s^{-1}), T is the temperature (°C), S is the salinity (PSU), and D is the depth (m). This equation is followed for sound speed computations in the present study.

Vertical variations in sound speed in the ocean are in general much larger than horizontal variations. This vertical variation in sound speed (sound speed profile)

11

results in refraction of sound energy as it propagates in the medium resulting in various propagation characteristics.

Propagation of sound in the sea over long ranges is always by some form of ducted or guided propagation in which maximum energy is confined within the boundaries of the duct. These ducts are called sound channels, or wave guides in general. The deep sound channel (DSC), the surface duct, and the shallow water channel are the important types of wave guides that exist in the ocean. Phenomena associated with long range sound propagation in deep waters are discussed by many authors (Urick,1983; 1982; Brekhovskikh and Lysanov,1982). Lens-like action of the water column causes the formation of zonal patterns of energy distribution with high and low intensity areas. These are associated with the existence of convergence zones and shadow zones.

Transmission loss is a measure of sound intensity available at a point relative to the intensity at the source. It is represented in decibels (dB). There are two components for transmission loss viz., spreading loss and attenuation. Spreading loss is related to geometrical focusing and de-focusing of energy as it travels away from the source. Attenuation has two components: volume absorption and loss due to boundary interactions. Volume absorption involves the conversion of elastic energy into heat and represents a true loss of the energy to the medium. The processes leading to absorption are viscosity and molecular relaxation processes involving magnesium sulphate and boric acid (Urick,1982). The boundary interaction losses are surface- and bottom-scattering losses and reflection loss at the bottom. Other mechanisms determining transmission loss are volume scattering by inhomogeneities,

diffraction, and leakage out of sound channels.

There are different methods for studying the propagation characteristics. Analysis of field experimental data help to reveal propagation features under various environmental conditions. Though expensive and difficult to conduct, experiments at sea provide realistic data. Theoretical studies and mathematical models of sound propagation help in interpreting and predicting propagation features observed in the environment. A range of mathematical methods exist for propagation modeling. There are simple analytical models and complex numerical models. Prediction of expected propagation conditions are useful in the planning of many underwater and related activities. They are used in purely research oriented work, in commercial applications, and in military requirements.

The theoretical basis underlying all mathematical models of acoustic propagation is the wave equation. Mathematical models of sound propagation can be conveniently grouped into two types: range-independent and range-dependent. In range-independent models a simplified mathematical model of the environment is used for obtaining a relatively quick estimate of transmission loss. Examples of such simplifying assumptions are constant water depth, range-independent sound speed profile etc. In range-dependent models, variations in water depth and sound speed profiles with range are also taken into account and hence are more general and realistic. But the computational efforts are phenomenally large compared to range-independent models. Most common range-independent models are usually based on either ray theory or normal mode theory (Urick,1983). If the environment varies both in range and depth, the wave equation is to be solved numerically. The

Parabolic Equation (PE-IFD) model (Lee and McDaniel,1988) is an example.

1.3.1 OCEANIC INHOMOGENEITIES AND ACOUSTICS

In reality, the ocean is an extremely complex and variable medium. In such a complex environment more complex models of propagation incorporating statistical characteristics of the variations might be necessary to obtain reliable predictions of the sound field. Ocean currents, internal waves and small-scale turbulence perturb the horizontally stratified character of the sound speed and cause spatial and temporal fluctuations in sound propagation. Boundaries of large currents, such as the Gulf stream and Kuroshio, represent frontal zones separating watermasses with essentially different characteristics. Within these frontal zones, temperature, salinity, density and sound speed suffer strong variations and hence the acoustic propagation (Levenson and Doblar,1976). Large eddies in the ocean are mostly observed near intense frontal currents. The parameters of synoptic eddies vary over rather wide range. The diameter of an eddy ranges from 25 to 500km. Analysis of propagation studies through a cyclonic gulf stream eddy revealed considerable variations in the propagation conditions (Vastano and Owens, 1973). Considerable fluctuations of the intensity and phase of sound waves arise in the presence of internal waves (Stanford,1974). We know that such characteristics of the ocean water as salinity, temperature, density, and current velocity do not vary smoothly with depth, but in discontinuous fashion. Such fine layered structure leads to multipath of sound transmission and hence cause additional fluctuations of phase and amplitude to the sound signal (Stanford,1974). Thicknesses of these layers typically vary

from tens of centimetres to tens of metres.

Propagation of sound in the ocean is usually accompanied by the fluctuation in the amplitude and phase of the transmitted signal. The fluctuations are manifestations of not only the changing patterns of interaction with the bottom and surface, but also of the propagation of the energy through time-varying inhomogeneities in the ocean medium. Internal wave-induced variability has been found to be a very significant source of sound intensity fluctuation and has received considerable attention. There are several studies to predict the influence of internal wave field on acoustic transmission (De Saubies, 1976, 1978; Munk and Zachariasen, 1976; Flatte and Tappert, 1975; Flatte' et.al., 1979; Colosi et al., 1994). Most of the work on this subject deals with deep ocean environments. In the shallow water the modelling of internal wave fields runs out to be inappropriate, partly due to the strong influence of the atmosphere (wind stress) and the fact that the waveguide properties of these environments are considerably different from those of the deep ocean (Ali,1993). Using ray theoretical transmission loss computations and observed internal wave data, a transmission loss contrast of 22-30 dB are reported by several authors (Lee ,1961; Baxter and Orr,1982; Murthy and Murthy, 1986). Porter, et al., (1974), Pinkel and Sherman (1991) and Rubenstein and Brill (1991) studied sound speed fluctuations and corresponding spectrum of internal wave field. They simulated transmission loss data in these environments and compared them with experimental data.

The temperature fluctuations caused by eddies significantly alter the sound speed in the ocean, producing a transient range-dependent acoustic environment; the direct

effect of the Doppler shifting by currents could also be of some relevance. On the other hand, the alterations of sound propagation by eddy currents can be used to infer the distribution of the currents themselves if travel times and something about the structure of the temperature field are known. This is the basis of the acoustic tomography technique.

Hamilton (1974) is considered to be the first to encounter the manifestation of this variability, eddy, during the experiment on long range propagation of sound along two paths (Antigue-Eluethra, Antigue-Bermuda) in the Sargasso sea. Clark and Kronengold (1974) carried out detailed experiments to study the fluctuations of amplitude and phase of an acoustic signal at short and long ranges across the Florida Strait and along the Eluethra-Bermuda route, respectively. Both these studies were accounted for by the fact that the sound paths intersected various synoptic-scale inhomogeneities of the oceanic structure. There are several experimental studies across the Gulf Stream eddy (Weinberg and Zabalgogeazcoa, 1977 ; Beckerle et al., 1980).

The effect of an eddy manifests itself not only in local changes of amplitude and phase of a sound signal but also in displacements of the boundaries of convergence zones and acoustic shadow zones as a whole. The convergence zones correspond to the areas of substantial concentration of sound energy related to the arrival of one or several sound rays at each point of such a zone; in the shadow zones there are no rays or intensities of the signals arriving along them are small. In the recent study through the Gulf Stream eddy Mellberg et al.,(1990) observed a change of more than 5dB in sound intensity level and a shift of 10km in the

16

location of first convergence zone in a time varying acoustic field..

Any eddy is a distribution of not only the sound speed field but also of currents. These currents can either accelerate or decelerate the propagation of a sound signal. Moreover, the length of the sound path and its orientation relative to the eddy are important for the propagation of sound. Attempts were made by Henrick (1980) and Itzikowitz et al.,(1982) to consider all these effects jointly on sound propagation. Several theoretical and experimental studies (Munk,1980; Weinberg and Clark,1980; Baer,1981) have been made to understand the horizontal (lateral) refraction of sound rays produced by oceanic eddies.

Oceanic microstructure induced variability has been found to be a very significant source of sound intensity fluctuations and has received considerable attention in these years (Melberg and Johannessen,1973;Lysanov and plotkin,1987; Potter,1991). Shulkin et al.,(1979) observed a fluctuation of acoustic intensity of the order of 5-10dB at a range of 210m for a high frequency(60kHz) sound source. Including the effect of oceanic microstructure to a model for predicting internal wave fluctuations Ewart (1980) observed a very good agreement between model simulations and the experimental results. However, in a study by Unni and Kaufman (1980) pointed out that the presence of microstructure adds little to the phase fluctuations.

Even though the importance of the oceanographic features on acoustic propagation has been realised, systematic studies addressing this aspect are rather few for the Indian Ocean. Prasanna Kumar et al.,(1992) have analysed the sound speed structure and propagation characteristics of

a cold core eddy in the Bay of Bengal. They noticed a travel time delay of the order of 200 milliseconds for an acoustic ray passing through the eddy. Ramana Murty et al.,(1993) studied acoustic characteristics of the Bay of Bengal waters. Eigen rays, rays connecting the source and receiver, are identified in the deep sound channel and their turning depth, path length, travel time etc. were computed in the study. They also studied intensity fluctuation along the eigen rays due to both refraction and volume absorption by the medium. Prasanna kumar et al.,(1994) also carried out similar work in Bay of Bengal. In their study, a climatological mean sound speed profile was developed after analysing hydrographic data collected from this area. This climatological profile was used for studying the acoustic characteristics. Somayajulu et al.,(1994), based on acoustic simulation studies in the Arabian Sea, attributed the fluctuations in the travel time of the eigen rays in the deep sound channel to the sound speed fluctuations in this region.

1.4 OBJECTIVES OF THE STUDY

The variability of thermocline characteristics has profound influence on underwater acoustic propagation. As the thermocline characteristics affect the transmission of sound enormously, apriori knowledge of its characteristics is very essential for the conduct of ocean acoustics studies. The review of available literature clearly points out that studies are rather fragmentary as far as the distribution of thermocline characteristics and acoustic propagation aspects in the Arabian Sea are concerned.

The prime objective of this study is to identify the

18

generic features of thermocline variability and to highlight
different oceanographic aspects causing this variability.
After having identified the features, temporal and spatial
distribution of the thermocline characteristics on a basin
scale is studied in detail. This gives an idea of the
thermocline structure viz. topography, gradient and
thickness. It is worth mentioning here that the analysis
were carried out with extensive data bases to bring out
salient features observed in the thermocline.

The role of thermocline features on acoustic
propagation is not studied well for the Arabian Sea. This
problem can be addressed in two ways viz. experimental
studies at sea and mathematical modeling. Logistics involved
in the planning and conduct of experimental studies are
enormous especially for range dependent scenario. The
advantage of using theoretical models is that with the
available environmental information a realistic assessment
of propagation can be attained. Keeping these aspects in the
background, in the present study an attempt has also been
made to study the propagation under different oceanic
conditions.

The unique nature of the Arabian Sea is discussed
highlighting various oceanographic features controlling the
thermocline characteristics in the introductory chapter. In
addition to this all the previous works pertaining to the
thermocline variability are reviewed.

In the next chapter to bring out the oceanographic
features, which cannot be identified by synoptic
observations at a particular location, climatological
aspects of the thermocline characteristics for the entire
Arabain Sea is studied. This was carried out utilising an

extensive temperature data base. The variations in the thermocline structure in the Arabian Sea on an annual cycle is analysed and interpreted. This study showed that the thermocline characteristics for the deep and coastal waters are distinct.

In the third chapter thermocline characteristics for the coastal waters are exclusively studied focusing west coast of India. This study has shown the importance of onshore/offshore processes in controlling the thermocline characteristics. To investigate this aspect thermocline characteristics are studied based on a unique data set.

To identify the oscillations in the thermocline, mainly caused by internal waves, its characteristics at the selected locations based on time series data are presented in chapter 4. The role of dynamic stability on mixing characteristics in the thermocline is highlighted. The thermocline oscillations and their different harmonics are identified.

After establishing various factors causing thermocline variability the acoustic propagation aspects are studied. A range-dependent parabolic equation model is used to simulate the propagation conditions. Case studies for internal waves, eddy and typical thermocline structures identified at different locations are made to highlight their role on sound transmission.

The major findings and their importance are summarised in the last chapter of the thesis.

CHAPTER II

THERMOCLINE CLIMATOLOGY OF THE ARABIAN SEA

2.1 INTRODUCTION

Studies on thermohaline variability of the Arabian Sea received considerable momentum after the International Indian Ocean Expedition (IIOE). Based on these data sets, watermass structure in the Arabian Sea was analysed by Rochford (1964), Gallaghar (1966), Darbyshire (1967), Wyrtki (1971), Sastry and D'Souza (1971,72) and Sharma (1976). However, most of the studies on thermal structure were limited to either selected locations or seasons (Colon,1964; ? Warren et al.,1966; Taft and Knauss,1967; Banse,1968; Saha,1974). Colborn (1975) made a climatological study of the Indian Ocean thermal structure utilising all available data till then. The data sets collected during other observational programs, particularly MONSOON-77, INDEX-79 and MONEX-79 have considerably improved our understanding of the thermal structure variability on synoptic time scales. These experiments were also confined to certain locations in the Arabian Sea during pre-monsoon or monsoon seasons (Quadfasel and Schott,1982; Swallow et al.,1983; ? Schott,1983; Rao et al.,1990).

Climatological studies of thermocline variability in the Arabian Sea have not received much attention till recently. In most of the earlier studies importance is given to address the variability of surface mixed layer characteristics (Molinary,1986(a,b); Rao et al.,1989; McCreary and Kundu,1989). More recently, Brock et al.,(1991)
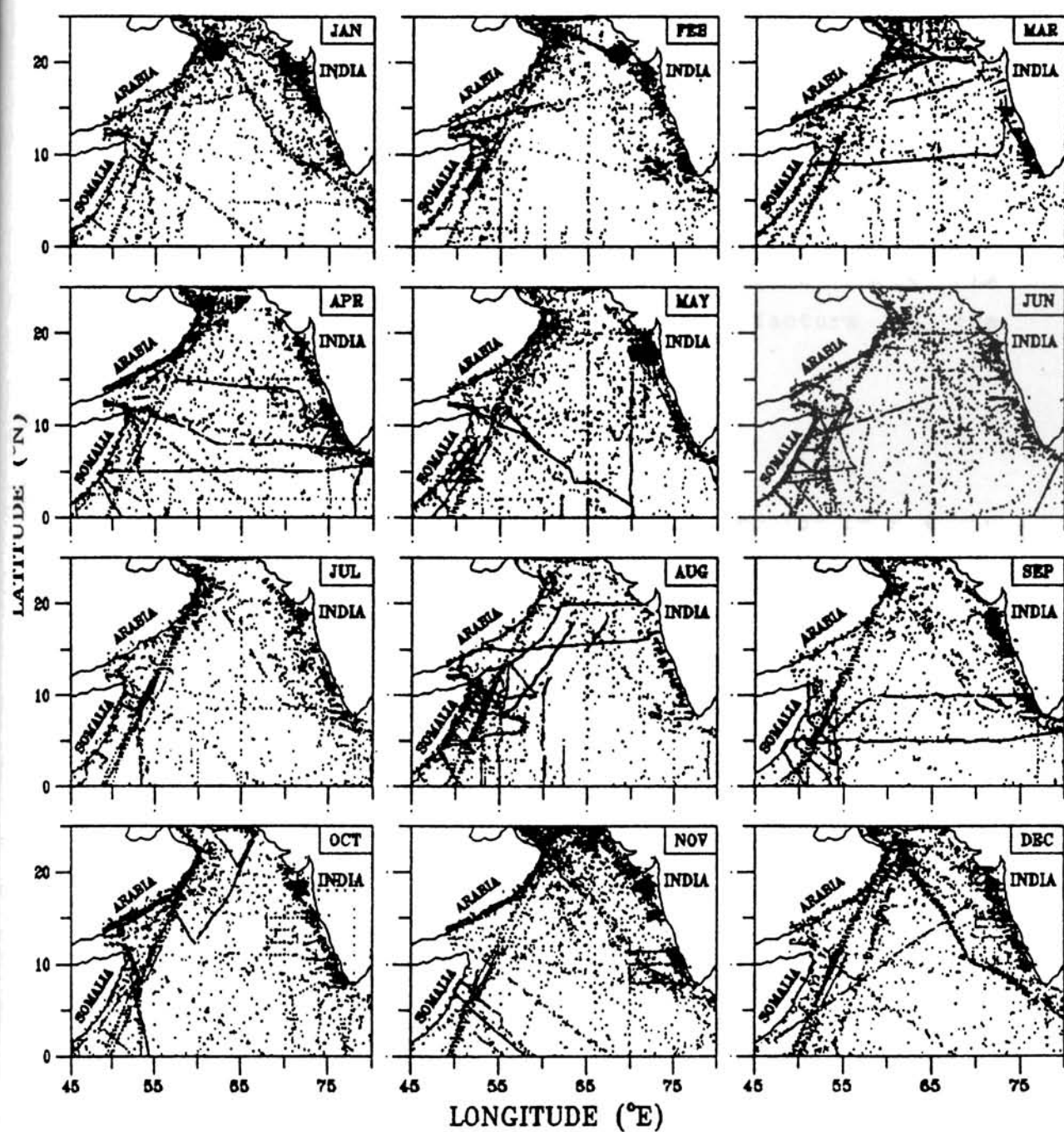
Fig. 2.1 Distribution of temperature data (dots corresponding to vertical profiles)

made a detailed study on watermass structure off the Arabia coast in the upper 500m during summer monsoon. In a recent work, Hastenrath and Greischar (1989) presented the climatic distribution of thermocline structure in the form of an atlas for the Indian Ocean. However, they have not attempted to explain the physical processes responsible for the observed thermocline variabilities. In reality there are many factors like pre-monsoon warming, summer cooling, upwelling, sinking and eddies which are known to influence the thermocline variability. In this chapter, attempts are made to infer the influence of these factors on the thermocline characteristics.

2.2 DATA

Individual temperature profiles utilised for this study are obtained from the National Oceanographic Data Centre, Indian National Oceanographic Data Centre, First Global GARP Expedition, Oceanovax, Indo-Polish expedition and from ships of opportunity. The domain of study extends from the equator to $25°N$ and $45°E$ to $80°E$ excluding the marginal seas, Red Sea and Persian Gulf. The data set used were collected during the period 1931 to 1992.

In the temperature file, data sets collected using Mechanical Bathythermograph, Expendable Bathythermograph, Salinity-Temperature-Depth recorder and Nansen cast are merged together. Since the data sets utilised for this study are from different years and collected using different instruments, a preliminary check and subsequently a detailed statistical quality control is performed to remove any spurious data. The details of the quality control procedures used are discussed below.

As a first step, locations, date, and ship codes of all stations are checked to eliminate duplicate data. Then the data which are grossly in error is eliminated by range checking. Various range criteria are used for temperature at different depth levels following Levitus (1982). Further, each temperature profile is checked for inversion. Except in selected areas like the vicinity of Red Sea and Persian Gulf, profiles having thermal inversion greater than $1^{\circ}C$ are eliminated. Then the vertical profiles of temperature are interpolated using Lagrangian interpolation scheme to obtain values at every 10m depth. Following Levitus (1982) statistical check is performed to eliminate erroneous data for each $2^{\circ}x2^{\circ}$ grid. By this process, 7237 spurious data profiles were eliminated. After the quality control, temperature data sets contain 47,695 profiles. Station locations of these temperature profiles for each month are presented in Fig.(2.1). Finally, monthly mean profiles of temperature for each $2^{\circ}x2^{\circ}$ grids were computed.

2.3 MONTHLY THERMOCLINE CHARACTERISTICS

To study the basin scale variability of the thermocline characteristics in the Arabian Sea and the factors influencing its variability, monthly evolution of top, thickness, average temperature and gradient of the thermocline are described in the following sections.

2.3.1 TOP OF THE THERMOCLINE

Top of the thermocline is computed for each 2° X 2° grid and its monthly distribution is presented in Fig.(2.2). During December - February, the circulation pattern in the Arabian Sea is anticlockwise (KNMI,1952). This gyre causes the redistribution of thermal field resulting in sinking
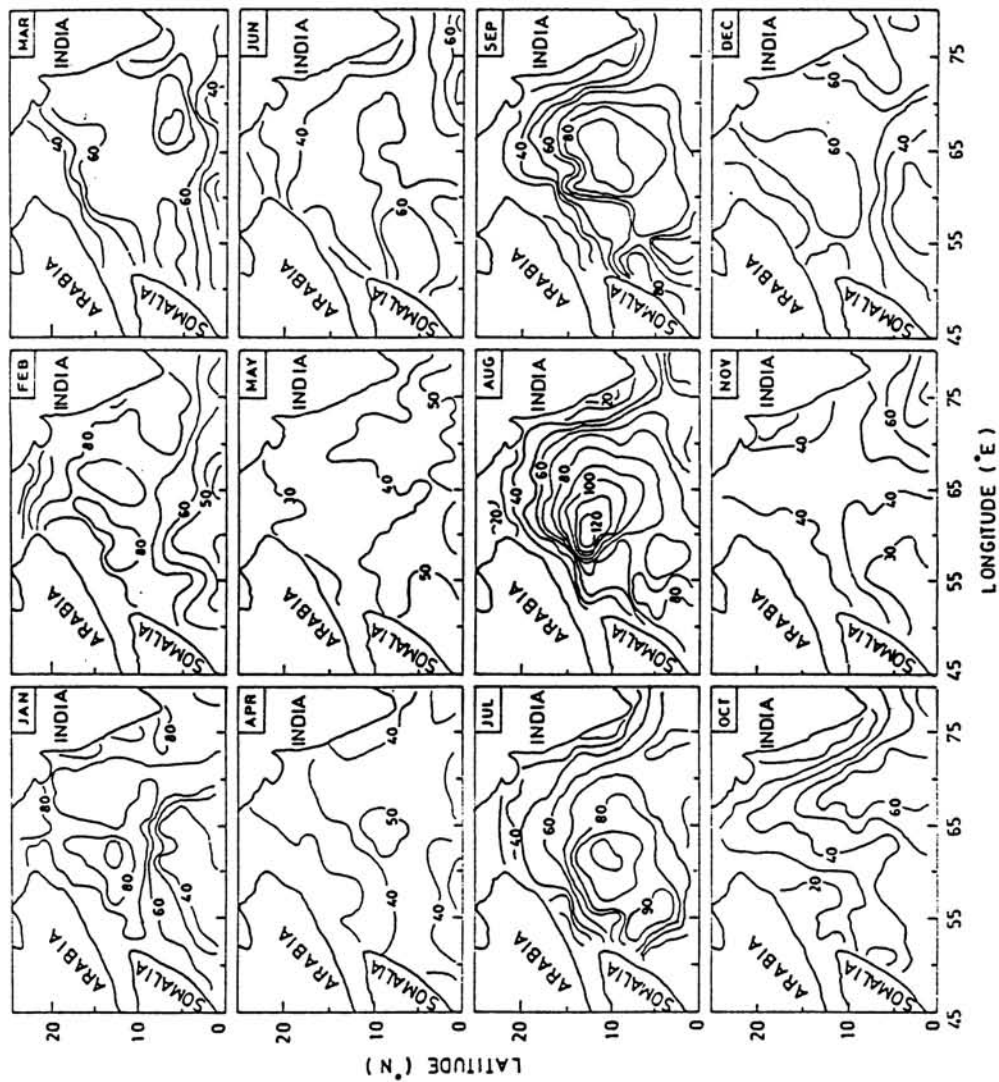
Fig. 2.2 Monthly distribution of the thermocline top (m)

(convergence) near the coastal regions and divergence in the central Arabian Sea. Hence, the thermocline is found to be deep (>70m) all along the coastal region during this period while it is shallow (<50m) near the equator. In the nothern Arabian Sea (north of 20°N) drastic net heat loss (Hastenrath and Lamb,1979), enhanced the vertical mixing and thereby deepened the thermocline to over 80m.

During the pre-monsoon months (April-May), entire thermocline shoals in the Arabian Sea (30-40m) under strong surface heating (Hastenrath and Lamb,1979; Mohan Kumar,1991), which stabilise the surface layers and reduce the vertical mixing. With the onset of summer monsoon (by June), thermocline shoals further (<30m) near the coastal regions which continues till October. The process of upwelling observed off Somalia (Swallow and Bruce, 1966; Schott, 1983), off Arabia (Currie et al.,1973; Smith and Bottero, 1977; Swallow,1984; Elliot and Savidge, 1990; Bauer et al.,1991; Brock et al.,1991) and off the west coast of India (Banse,1968) results in the formation of shallow thermocline (<30m) near the coastal regions.

On the otherhand, top of the thermocline continues to deepen in the central Arabian Sea ($\cong$ 60°E and 10°N) during the summer monsoon season with deepest thermocline occurring in August (>120m). This can be explained in terms of the increased mechanical and buoyant mixing (Hastenrath and Lamb 1979), erosion of top of the thermocline due to entrainment (Ramesh Babu and Sastry, 1984), convergence caused by negative wind stress curl (Rao et al.,1993) and the clockwise gyre in the Arabian Sea. One of the major findings of this analysis is that strong spatial variability is noticed during July-September in the entire Arabian Sea. This suggests the importance of two physical processes, viz.

24

upwelling near the coasts and sinking in the central Arabian
Sea in controlling the top of the thermocline. Top of the
thermocline exhibits minimum variability in the entire
Arabian Sea during pre-monsoon months (April-May) and
post-monsoon period (November), suggesting weak dynamic
processes.

2.3.2 THERMOCLINE THICKNESS

The monthly distribution of the thermocline thickness
presented in Fig.(2.3) also reveals marked variations across
the Arabian Sea. One of the notable findings is the
occurrence of thin thermocline (< 40m) in the northern
Arabian Sea (north of 20°N) throughout the year. The thin
thermocline in the northern Arabian Sea is caused by a
variety factors. The northern Arabian Sea is the source
region of Arabian Sea High Salinity Watermass(ASHSW). This
watermass at the source region has a salinity about 36.5 PSU
and temperature about 30°C (Brock et al.,1992) which sinks
and occupies the mid-thermocline region as it advects
southward (Rochford,1964). The Persian Gulf water which
enters the nothern Arabian Sea has a core depth of about
200m in the northern Arabian Sea (Fig.2.3a). This watermass
has a temperature of about 27°c and salinity about 39.5 PSU
at the source region (Brock et al.,1992). Between these two
high saline waters, there is a relatively low salinity zone.
The Persian Gulf watermass is denser than the ASHSW and
hence the latter occupies a deeper (200m) depth (Fig.2.3a).
Since the diffusion of temperature is much greater than that
of salinity (Pond and Pickard,1983), near the core of
Persian Gulf watermass the layer between these two
watermasses are warmed much faster than it gains salinity.
This reduces the thermocline gradient (Fig.2.3a) and hence
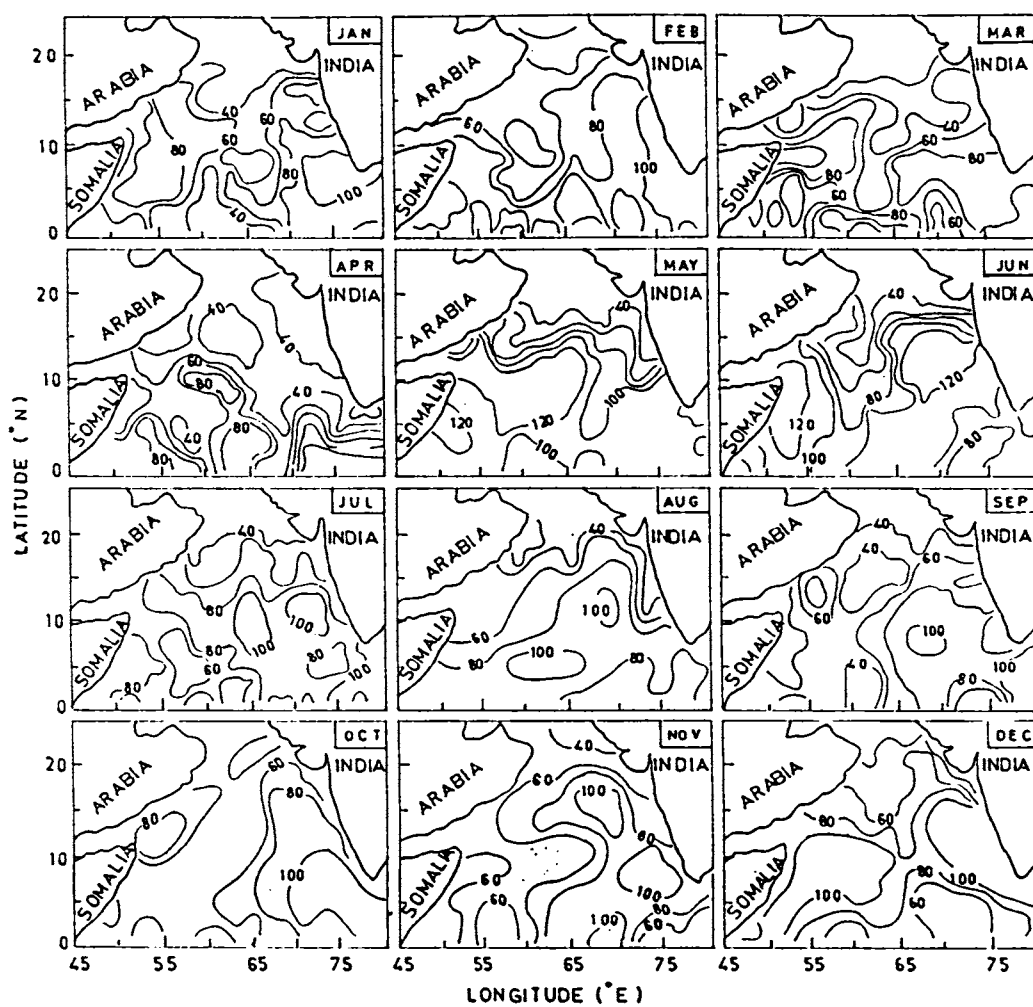reduction in the thickness of the thermocline.

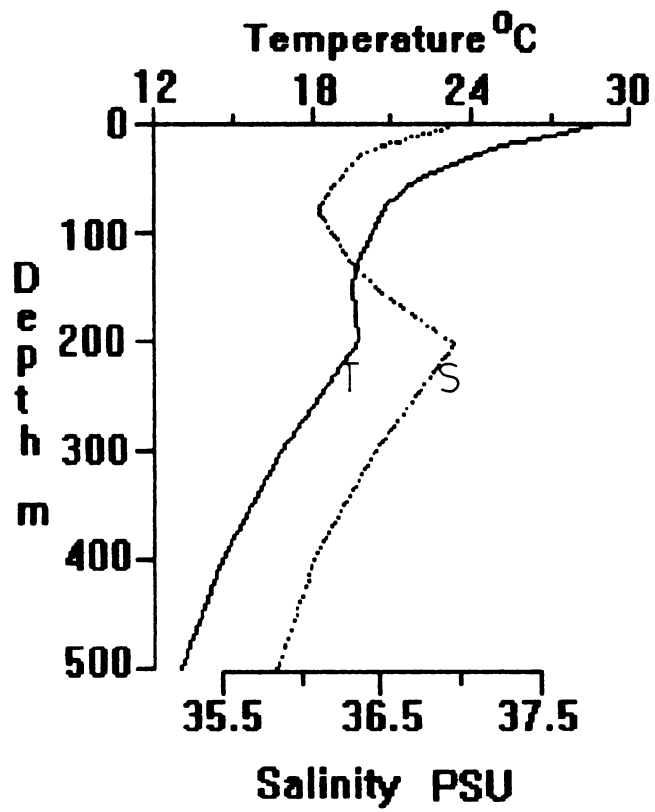Fig. 2.3 Monthly distribution of the thermocline thickness (m)

Fig.2.3a Typical temperature and salinity profile in the Northern Arabian Sea (22°22'N, 60°05'E)

Northern Arabian Sea (22°22'N, 60°05'E)

It is interesting to note that the thermocline
thickness increases in the coastal regions of Somalia ($\cong$
120m in June), southern Arabia ($\cong$ 100m in June) and west
coast of India ($\cong$ 120m in June) during the summer monsoon
season. The presence of northward flowing undercurrent along
the southwest coast of India (Antony,1990; Muralidharan et
al., 1995; Hareesh Kumar and Mohan Kumar,1995) and southward
flowing undercurrent off Somalia (Leetmaa et al.,1982;
Schott and Quadfasel,1982; Schott,1983; Quadfasel and
Schott,1983) during the periods of upwelling has been
established. Moreover, during this period, surface
circulation is southerly along the west coast of India
(KNMI,1952; Cutler and Swallow,1984) and northerly along the
east coast of Somalia(Swallow and Bruce,1966; Schott,1983)
and Arabia (KNMI,1952; Wyrtki,1973; Swallow,1984). These
opposing flows produce divergence and convergence in the
surface and subsurface levels respectively. The combined
effect of these two process increases the thickness of the
thermocline in the coastal regions. The variability of
thermocline thickness is more complex in the equatorial
region due to the presence of number features. For instance,
thermocline thickness is less than 60m during
December-February and thickens to values over 80m during
March-April due to the presence of equatorial undercurrent
(Reverdin,1987).

2.3.3 AVERAGE TEMPERATURE IN THE THERMOCLINE

The annual variation of the average temperature in the
thermocline (Fig.2.4) is found to vary between 19°C and
24°C. During the pre-monsoon months (April-May) and
post-monsoon period (November), minimum variation is
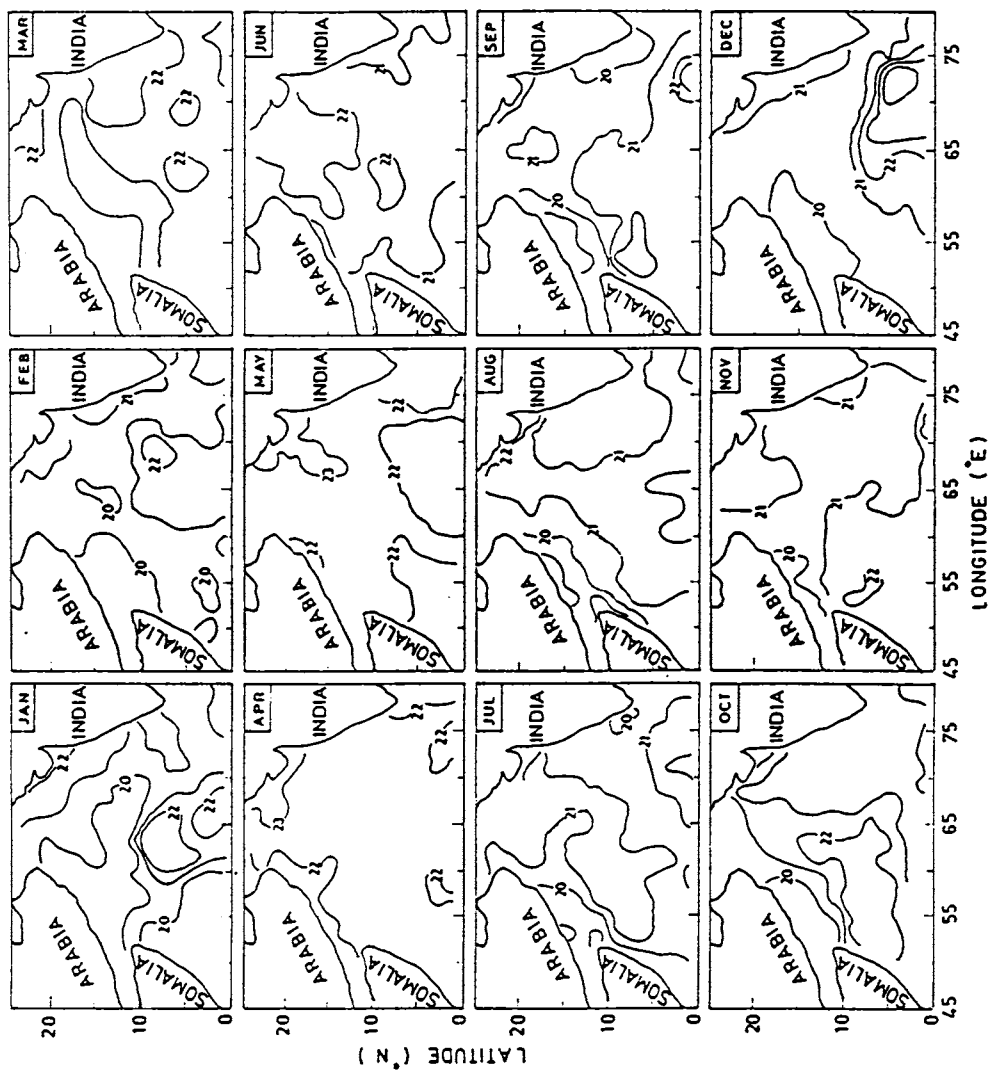observed in the entire Arabian Sea (22° to 23°C and 20° to

Fig. 2.4 Monthly distribution of the thermocline temperature (°C)

21°C respectively) suggesting weak dynamic processes. Comparatively large temperature during pre-monsoon season may be caused by oceanic heat gain (Hasternrath and Lamb 1979).

With the onset of summer monsoon, temperature in the entire Arabian Sea decreases. The minimum temperature is noticed in the coastal regions off the Southwest coast of India ($\cong$ 20°C in September), Arabia ($\cong$ 19°C in September) and Somalia ($\cong$ 19°C in August), which are the regions of intense upwelling. After the withdrawal of summer monsoon, temperature in the thermocline increased in the entire Arabian Sea due to post monsoon warming (Hastenrath and Lamb,1979). During winter, the prevailing northerly currents, which is a part of the anticlockwise gyral circulation, carries warm waters in to the eastern Arabian Sea. The intrusion of these waters, in the form of a tongue, is clearly evident from December. In January this tongue shifted westward due to the prevailing flow pattern and became organised but without appreciable temperature change.

2.3.4 THERMOCLINE GRADIENT

On an annual cycle, thermocline gradient (Fig.2.5) exhibits large variations in the Arabian sea (0.04° to 0.14° C m^{-1}). In all months, thermocline gradient increased towards equatorial Arabian Sea (0.04°C m^{-1} north of 20°N to 0.12° C m^{-1} south of 5°N). The weak gradients observed in the northern Arabian Sea (<.04°C m^{-1}) could be related to the combined effect of ASHSW and warm saline waters from Persian Gulf into the thermocline, which makes the thermocline more diffused.Near the equator the thermocline gradients exceeds $\cong$0.1°C m^{-1} throughout the year. It is more during winter compared to summer off Somalia and southwest
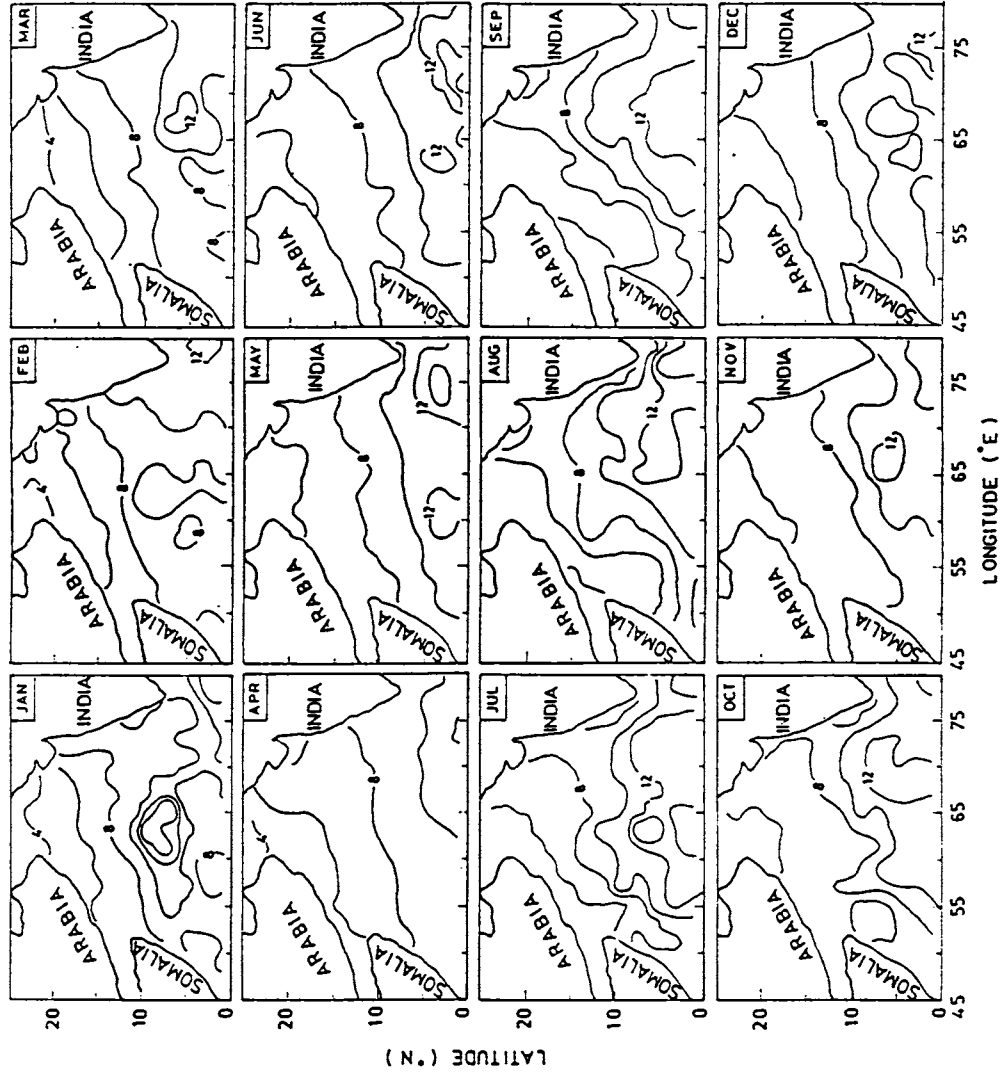
27

Fig. 2.5 Monthly distribution of the thermocline gradient ($\times 10^{-2}$ $^{\circ}$C m^{-1})

coast of India. The presence of equatorial Indian Ocean /
Bay of Bengal watermass over the ASHSW off the southwest
coast of India is responsible for the large gradient. The
relatively lower gradient in the equatorial Indian Ocean
during the early part of the year (January to June) could be
related to the spreading of thermocline associated with
equatorial undercurrent (Montgomery and Stroup,1962). The
equatorial undercurrent is found to be presented in Indian
Ocean between January and June (Leetmaa and Stommel, 1980).
However, during summer monsoon the currents of equatorial
Indian Ocean is broadly eastward resulting in deep
thermocline and stronger vertical gradients. This is
consistent with deep and shallow thermoclines during winter
and summer respectively (Fig.2.2). Another interesting
result is that the large variability in thermocline gradient
($\cong$ 0.04 $^{\circ}$C m^{-1} near the coasts to 0.12 $^{\circ}$C m^{-1} in the central
Arabian Sea) is noticed during July-September throughout the
Arabian Sea. This suggest the significance of upwelling near
the coasts, sinking in the central Arabian Sea and the
prevailing circulation pattern in controlling the thermal
structure. The contours of thermocline gradient are zonally
distributed suggesting large variations in the east-west
direction mostly during summer monsoon period.

2.3.5 DEPTH OF 25°C ISOTHERM

The depth of 25°C isotherm is taken to study the
vertical displacement of thermocline on an annual cycle
(Fig.2.6). It is noticed between 0 and 120m in the Arabian
Sea. On an annual scale, the 25°C isotherm exhibits maximum
variation in the central Arabian Sea ($\cong$ 60m in November to
120m in August) and minimum in the northern Arabian Sea (20m
in March to 50m in December). The occurrence of this
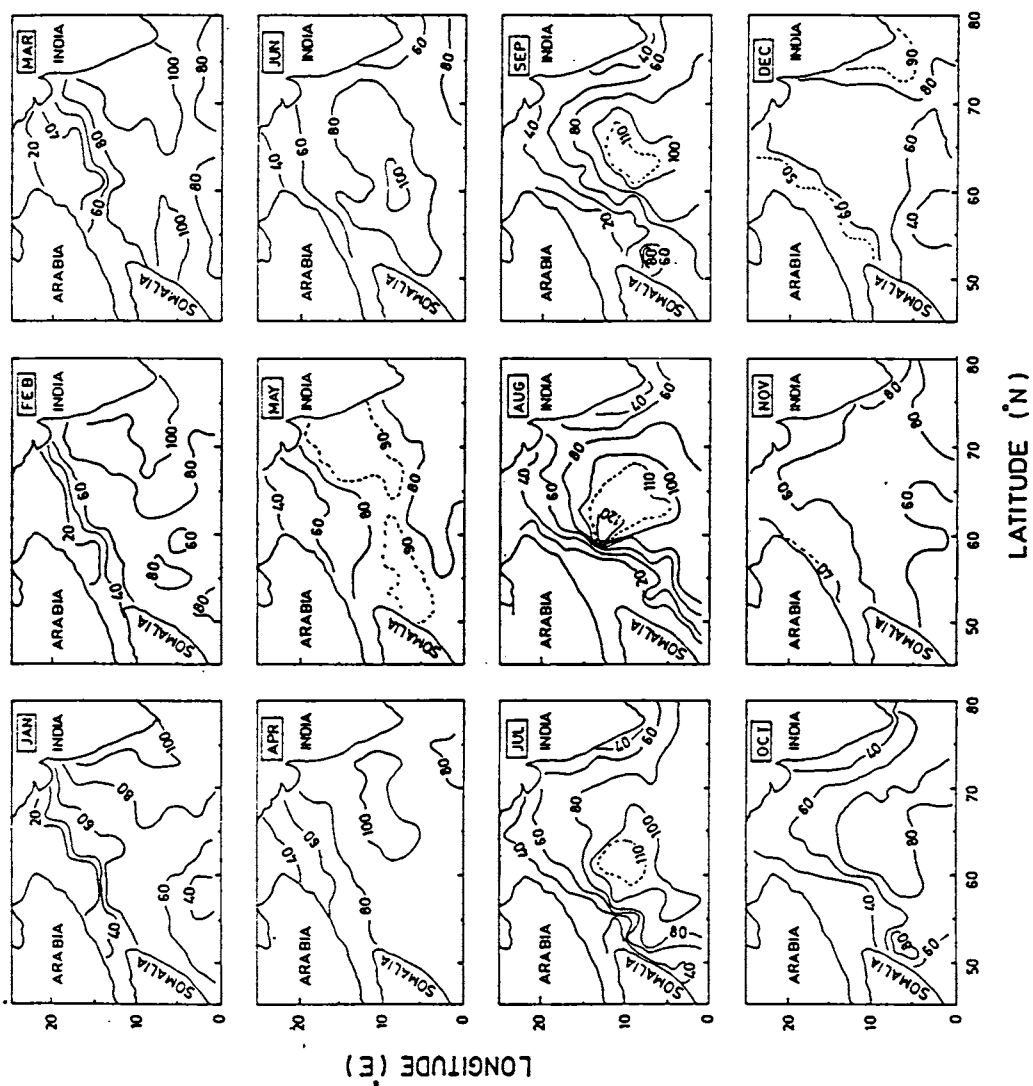isotherm at shallower depths (0m) in the northern Arabian

Fig. 2.6 Monthly distribution of depth of 25°C isotherm (m)

Sea (north of 20°N) is due to increased net heat loss (Hastenrath and Lamb,1979) which cools the upper layers of the water column. Just before the onset of monsoon (May) this isotherm is found between 40 and 90m. With the onset of summer monsoon, when there is intense upwelling in the coastal regions, it shoaled (< 40m in July off Cochin, < 20m in August off Arabia and < 20m in August off Somalia). On the otherhand, the increased vertical mixing and convergence induced by the surface wind stress curl (Hastenrath and Lamb 1979) in the central Arabian Sea deepens the isotherms (values over 120m in August). During this period, marked zonal variations are noticed between the southwest coast of India and Somalia. However, these variations are weak for the rest of the year. This brings out the importance of upwelling in the coastal regions and sinking in the central Arabian Sea. Another factor responsible for the large zonal variations is the flow pattern during this period. In winter, this isotherm deepens in the entire coastal regions (except northern Arabian Sea) with varying magnitudes (100m in January off the southwest coast of India, 50m in December off Somalia and Arabia) due to sinking.

2.3.6 THERMOCLINE CHARACTERISTICS AT SELECTED AREAS

From the above discussion it is clear that there is drastic spatial variations in the thermocline characteristics for the entire Arabian Sea. The variations are more in the coastal regions due to complex coastal dynamical processes. Hence, it would be of interest to concentrate more at the coastal stations. To study the thermocline behavior in the coastal and deep stations, typical areas were selected in the coastal belt and open ocean (Fig.2.7). The areas selected are: Area I (Cochin), Area II (Bombay), Area III (Karachi), Area IV (Arabia), Area
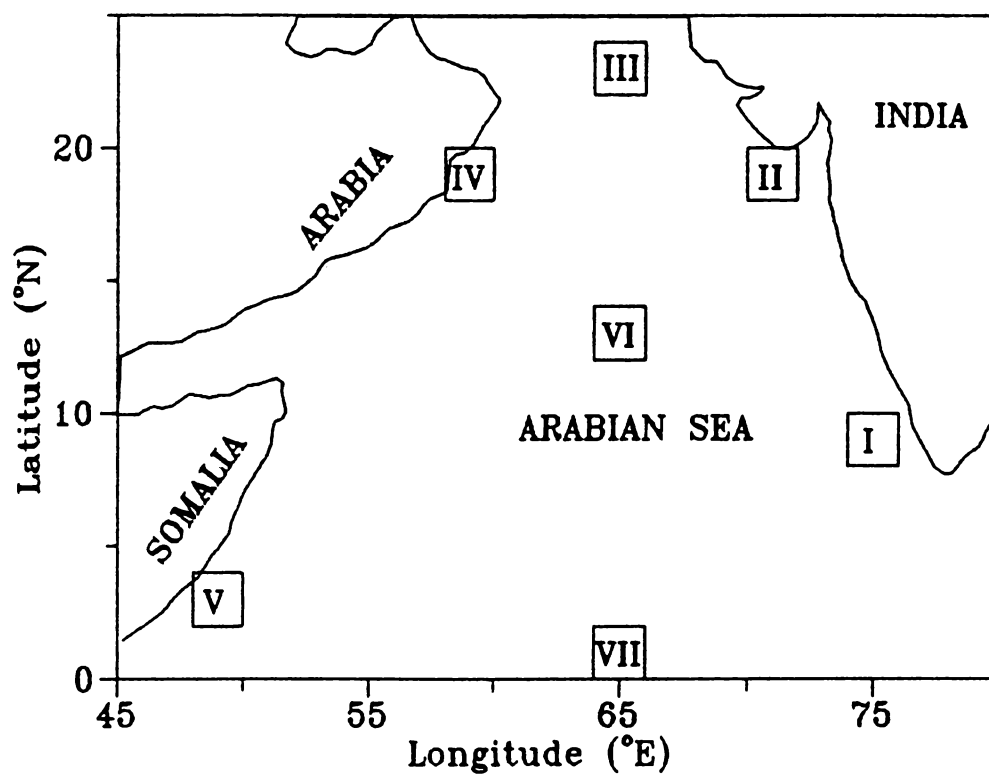
Fig. 2.7 Typical areas selected in deep and coastal waters

V (Somalia), Area VI (Central Arabian Sea) and Area VII (equatorial Arabian Sea).

The top of the thermocline (Fig.2.8a) exhibits a bi-modal distribution with a varying magnitude at all locations except in Areas III and VII. The thermocline is deepest ($\cong$ 100m) in Areas II and III during January-February mainly due to winter cooling and sinking. On the otherhand, in Area VI the maximum depth is noticed during the summer monsoon season (>100m in August). Increased vertical mixing processes and convergence induced by the surface wind stress curl (Hastenrath and Lamb,1979) are the prime mechanisms responsible for the deeper thermocline in this region. In Areas I and IV, shallower thermocline is noticed during April-May (25m) and August-September (15m), which are the periods of pre-monsoon heating and coastal upwelling respectively. In Area III, thermocline is around 25m during March to September and deepens to over 100m in January-February due to drastic heat loss across the air-sea interface (winter cooling). In Area VII, a continuous deepening of the thermocline is noticed from February which continues upto October (25 to 60m) and shoals thereafter. In Area VI, thermocline is shallow during April-May and September-October which are the pre- and post monsoon heating periods respectively. Moreover, the annual range of the top of the thermocline is also maximum in this region ($\cong$ 80m).

Unlike the top of the thermocline, average gradient in the thermocline (Fig.2.8b) does not exhibit a bimodal distribution at any locations. It varies between $\cong$ 0.04 to $0.14^{\circ}C$ m^{-1} with maximum values observed in Area V ($0.14^{\circ}C$ m^{-1} in February) and minimum in Area IV ($0.04^{\circ}C$ m^{-1} in August). In Areas III and IV, the thermocline gradient is
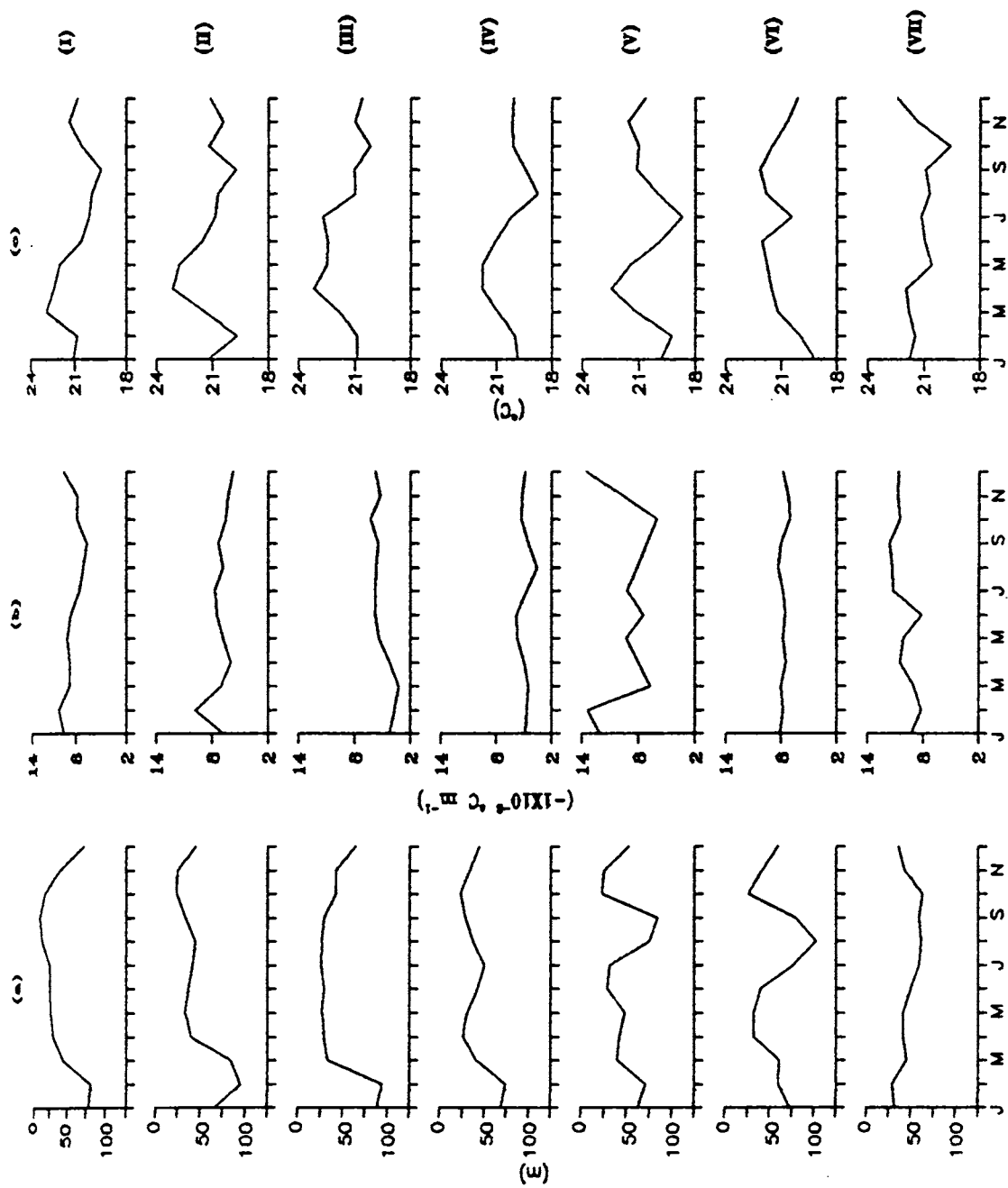
Fig. 2.8 Monthly distribution of (a) thermocline top
(b) thermocline thickness (c) thermocline temperature
at the selected locations.

weak ($<0.05^\circ$C m^{-1}) during most part of the year. In the Area VI, the average gradient remains the same $\cong$ 0.08°C m^{-1} throughout the year. The maximum gradient fluctuation is observed in the Area V (0.08°C m^{-1}) while minimum variations are observed in Areas VI ($<0.01^\circ$C m^{-1}), III (0.03°C m^{-1}), IV (0.02°C m^{-1}) and VI ($<0.01^\circ$C m^{-1}).

The average temperature of the thermocline (Fig.2.8c) also exhibits a bi-modal distribution with a varying degree of magnitudes at all locations, except in Area VII. On an annual cycle, average temperature of the thermocline varies between 18° and 24°C. It is maximum during pre-monsoon heating months and minimum during the summer monsoon season and winter. Maximum thermocline temperature is noticed in Areas II and III ($\cong$ 23.5°C in April-May), and minimum in Areas I, IV & V ($\cong$ 19.5°C in September, $\cong$ 18.5°C in August and $\cong$ 18.5°C in July respectively), in the coastal regions. The reduction in temperature is due to upwelling while that in the central Arabian Sea (Area VI), it is due to drastic heat loss during summer monsoon. One of the interesting features is that the annual variation of thermocline temperature is more in the coastal regions ($3-4^\circ$ C) compared to open ocean ($2-3^\circ$C).

CHAPTER III

THERMOCLINE CHARACTERISTICS OFF THE WEST COAST OF INDIA

3.1 INTRODUCTION

Seasonal variability in the temperature field is quite large off the west coast of India where vertical motions are significant (Sharma,1968,1978; Banse,1968; Darbyshare,1967; Narayana Pillai et al.,1980; Shetye,1984). The annual cycle of temperature and density fields off the west coast of India suggest the occurrence of upwelling during March-August and sinking during November to February (Sharma,1966;1968;1978; Narayana Pillai et al.,1980; Mathew,1981; Shetye,1984; Hareesh Kumar,1994). The upwelling/sinking commences in the southern region and progresses northward with time lags of the order of few months (Hareesh Kumar,1994). During the periods of upwelling a northward flowing undercurrent develops at the shelf edge which brings waters from the equatorial Indian Ocean (Antony,1990). The major transformations due to upwelling are the upward displacement of thermocline with an increase/decrease in the gradient of the upper/lower thermocline while sinking causes downward displacement of thermocline.

One of the notable features of the watermass structure in the eastern Arabian Sea is the presence of a high saline watermass, the Arabian Sea High Salinity Watermass, throughout the year (Hareesh Kumar,1994). Another prominent watermass found in this region is the low saline waters from the Bay of Bengal and Equatorial Indian Ocean during winter
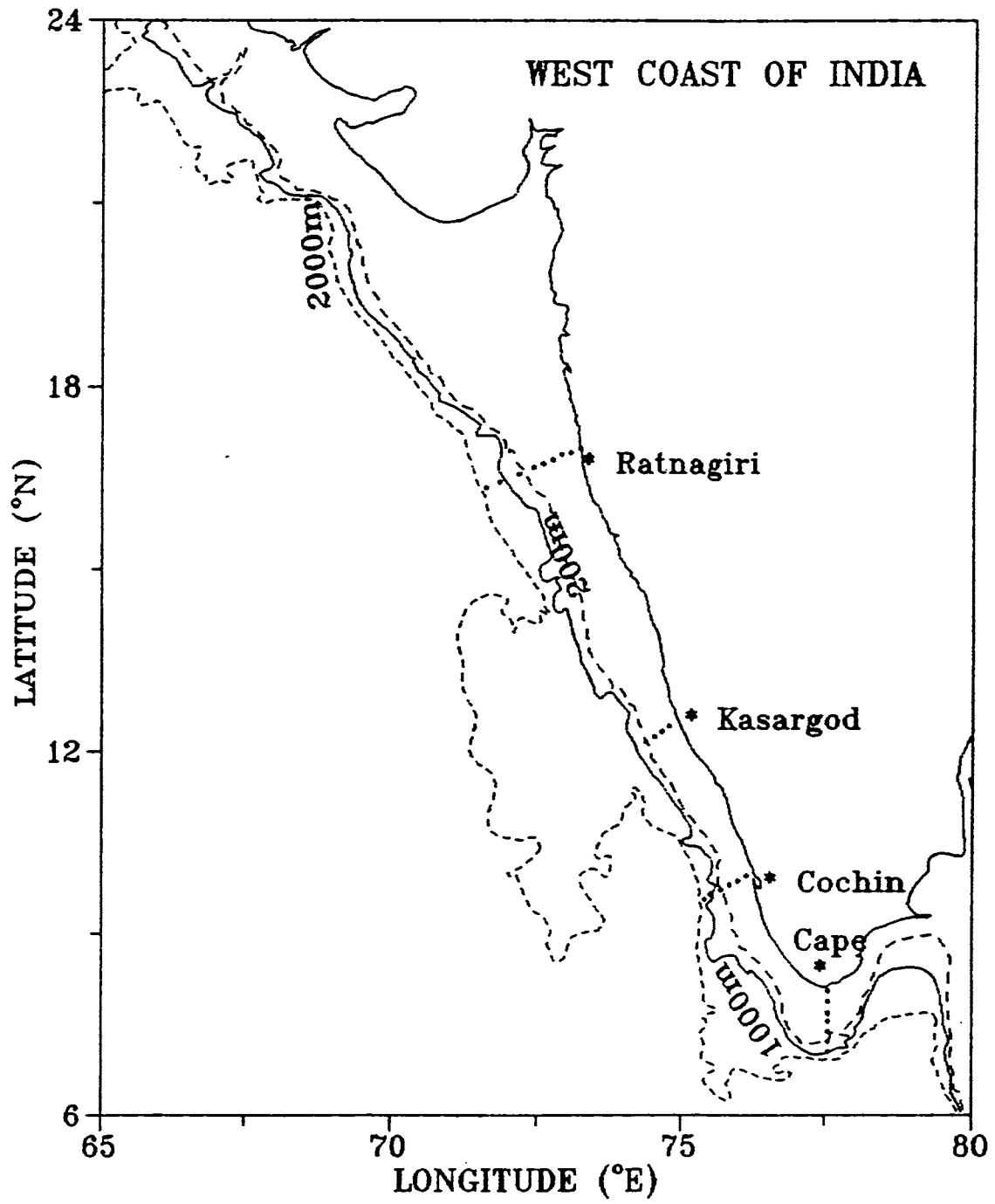
Fig. 3.1 Station location map

(Darbyshire,1967; Wyrtki,1971; Johannessen et al.,1981; Pankajakshan and Ramaraju,1987). Several studies have been carried out to understand certain aspects of coastal upwelling and watermass structure off the west coast of India during summer monsoon season (Shetye et al.,1990; Hareesh Kumar,1994). However the available studies are either limited in time or space and do not adequately describe the thermocline features. In this chapter an attempt is made to describe the thermocline characteristics and to highlight the important watermasses on an annual cycle.

3.2 DATA

Data sets used for this study consist of temperature and salinity profiles collected in coastal region (within 200 m depth zone) from 6° N to 24° N in the eastern Arabia Sea. The details of the temperature data set are presented in Chapter 2. The domain of the present study is limited to off the west coast of India where vertical motions are dominant. The salinity profiles obtained from hydrocasts corresponding to the temperature profiles are extracted from the data set discussed in Chapter 2. To remove outliers in the data, quality control is carried out following Levitus (1982). After quality control the temperature and salinity profiles are sorted for each month.

Hydrographic observations made during a special experimental programme of FAO/UNDP (1971-1978) Pelagic Fisheries Project (Narayana Pillai et al.,1980) are also utilised for the present work to study the cross-shore variations. During this programme hydrographic measurements were carried out at selected stations normal to the west coast of India (Fig.3.1). The same stations were occupied at

33

least seven to eight times in a year. This provided a very good data base to study the seasonal evolution of the thermocline characteristics off the west coast of India.

3.3 CROSS-SHELF VARIATIONS OF TEMPERATURE FIELD

It is well known that large variations in the thermal structure are mainly related to nearshore-offshore dynamic processes. In order to study these aspects, the monthly cross shelf variation of temperature at selected locations normal to the coast (Ratnagiri, Kasargod, Cochin, and Cape Comorin) are presented.

The monthly cross-shelf variation of temperature off Ratnagiri shows deep thermocline (>60m) from January to March. The temperature above the thermocline is about $27^{\circ}C$ during this period (Fig.3.2). In this zone, isotherms slope upwards towards the coast from May to December indicating upwelling. During this period, temperature gradient is strong ($\cong 0.36^{\circ}Cm^{-1}$ in October) in the upper thermocline ($\cong$ 50m) close to the coast. The upward movement of the isotherms is inhibited by the downward mechanical and buoyant mixing processes (Hastenrath and Lamb,1979; Mohan Kumar,1991) resulting in strong gradient. A mild downward slope of isotherms below 125m is seen in December. This is an indirect evidence of the northward flowing undercurrent associated with coastal upwelling which significantly reduces the vertical temperature gradient ($<0.04^{\circ}C$ m^{-1}) in the lower part of the thermocline. The intensity of upwelling is maximum during August to September resulting in the formation of cold upper layer temperatures ($<27^{\circ}C$ near the coast). The isotherms descend in January indicating the sinking process in the thermocline. During this period a four fold reduction in the temperature gradient ($0.36^{\circ}Cm^{-1}$

34

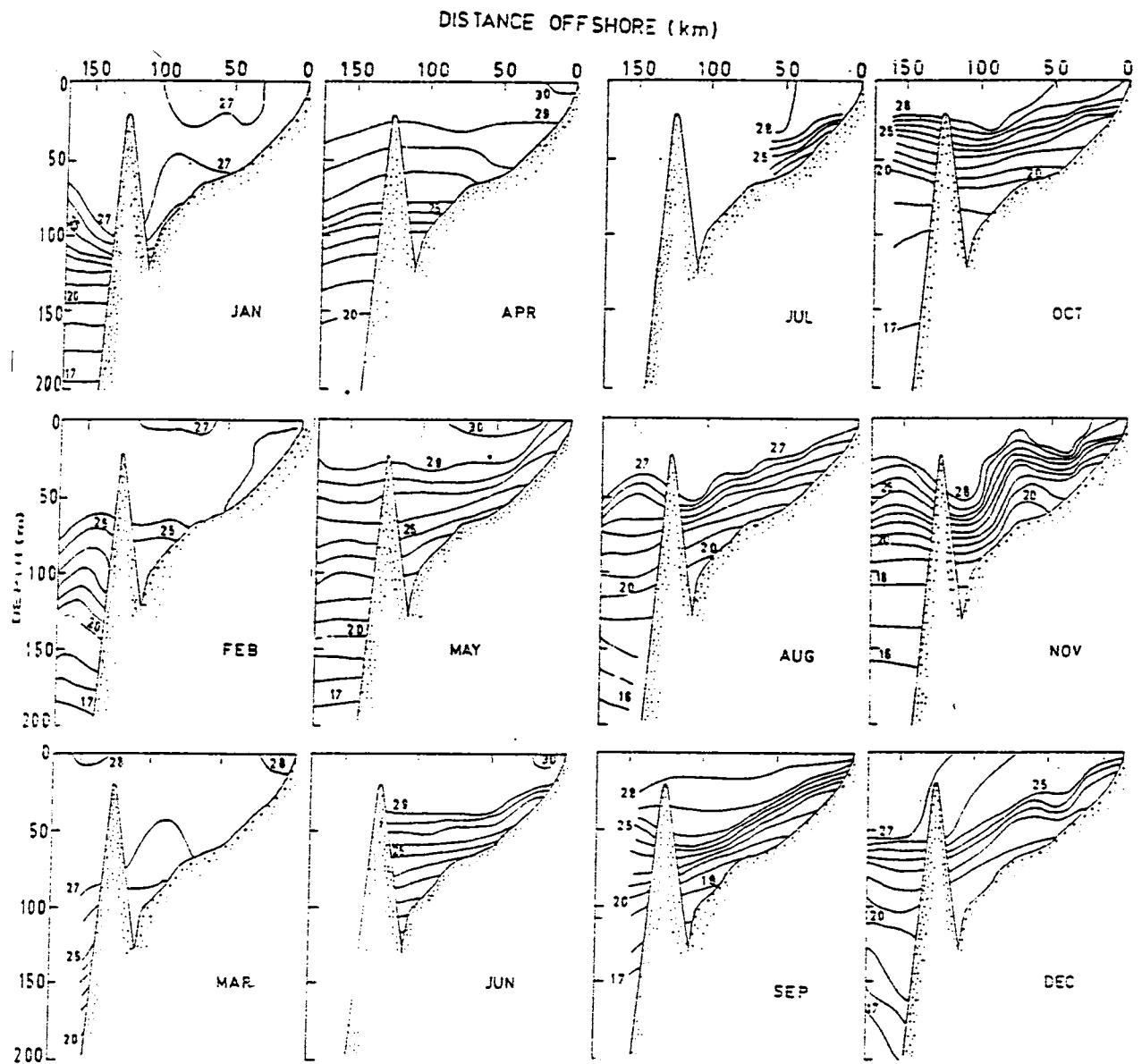Fig. 3.2 Monthly Cross-shelf variations of temperature off Ratnagiri(°C)

to $0.08^\circ C$ m^{-1}) within the thermocline is observed. This suggests that with the evolution of sinking process the thermocline diffused considerably. The diffused thermocline can be traced till upwelling gathers momentum.

The monthly cross-shelf variation of temperature off Kasargod shows deep thermocline (>60m) having a mixed layer temperature of $28^\circ C$ from December to February (Fig.3.3). During pre-monsoon months (March to May) thermocline shoals to depth less than 25m due to the accumulation of heat in the surface layers. The warm temperature zone (>$30^\circ C$) is thought to be a part of the Indian Ocean warm pool which is formed prior to onset of summer monsoon (Seetharamayya and Master,1984; Joseph, 1990). During this period a thick thermocline ($\cong$ 190m) with very weak gradients ($0.075^\circ C$ m^{-1}) are noticed. From March onwards the isotherms slope upward towards the coast in the upper thermocline (<150 m) and continues till October indicating southerly surface flow and upwelling. During this period strong gradient is noticed in the upper thermocline with maximum values occurring in September ($0.2^\circ C$ m^{-1}). The lower thermocline (>150m) is characterised by down sloping of isotherms suggesting the presence of northward undercurrent. The intense shear mixing with southerly surface current and northerly undercurrent causes weak gradients in the lower thermocline ($\cong$ $0.08^\circ C$ m^{-1}). From December to February isotherms slope downward towards the coast in the entire thermocline suggesting intense sinking and northward surface current. During this period uniform and weak gradient is noticed in the entire thermocline.

A deep thermocline (>100m) with surface layer temperatures of $28^\circ C$ is observed in December off Cochin Fig.(3.4). The influence of intense surface heating during
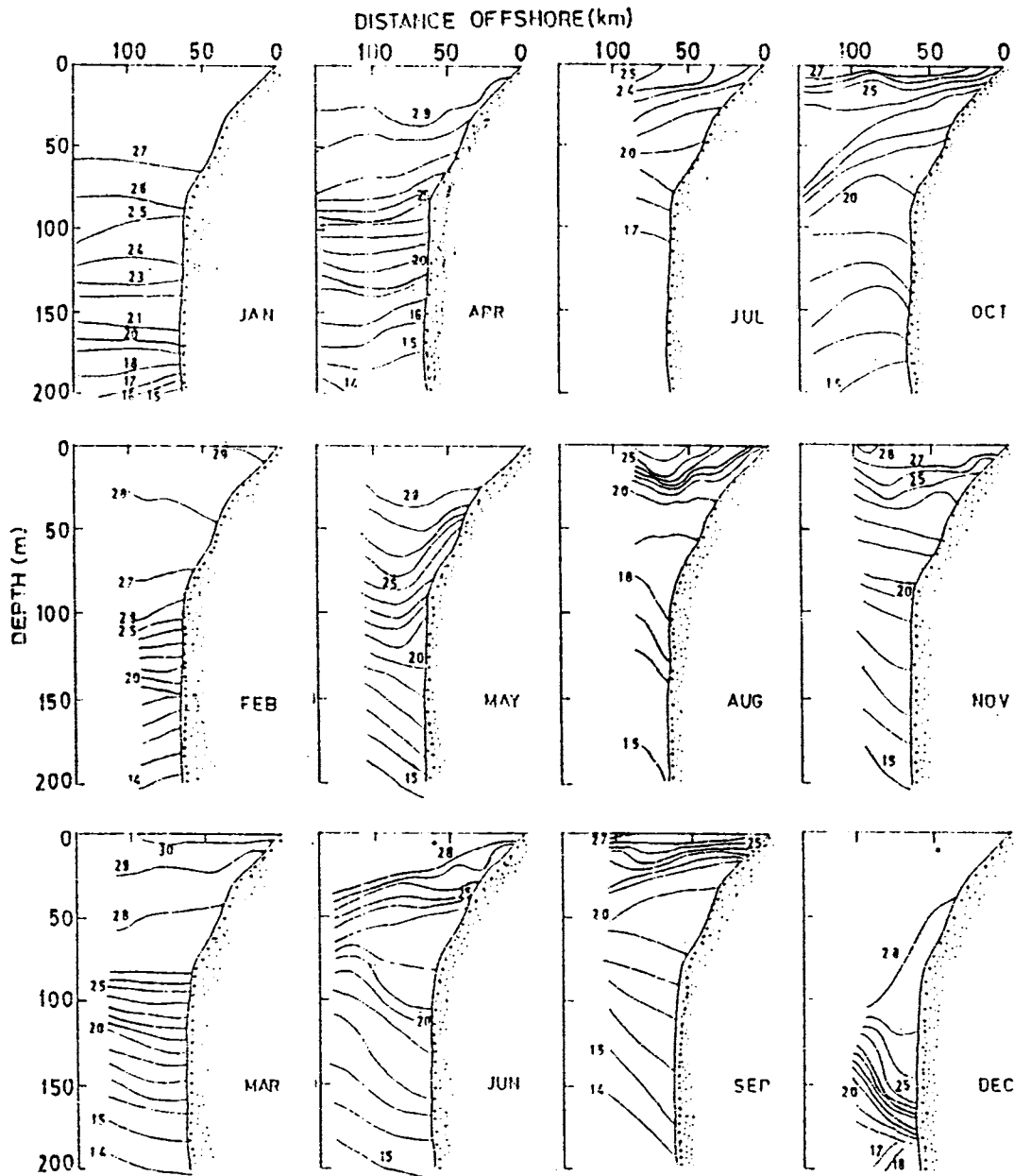
Fig. 3.3 Monthly cross-shelf variations of temperature off Kasargod(°C)

pre-monsoon period is reflected in the surface layer with temperature exceeding $29^{\circ}C$ between March and May. The surface layer temperature off Cochin is lower (by $\cong 1^{\circ}C$) than that of Kasargod during this period probably because the Indian Ocean warm water pool is centered off Kasargod-Mangalore during most of the year (Joseph,1990). In the thermocline the effect of upwelling is evident from March onwards, as inferred from the upsloping of isotherms towards the coast. The maximum effect of upwelling is noticed during July-August as indicated by the shallow thermocline (<10m), low surface temperature (<$25^{\circ}C$) and maximum gradient in the upper thermocline ($0.2^{\circ}C$ m^{-1}). The upward movement of isotherms continue till October. Moreover, the downward sloping of isotherms in the lower thermocline (>60m) suggests the presence of northward flowing undercurrent. The temperature gradient in this zone is very weak ($0.03^{\circ}C$ m^{-1} in August) compared to the upper thermocline ($0.2^{\circ}C$). The reduction in gradient in this zone is mainly due to the increased shear mixing between the southerly surface current and northerly undercurrent.

The effect of sinking is evident during November to December when the entire thermocline slopes downward towards the coast. An interesting feature is the sharp thermocline gradient ($0.15^{\circ}C$ m^{-1}) during the periods of sinking which is not observed at the other stations. Weak cross-shore temperature gradients in the thermocline from January to April suggest weak flow.

The monthly cross shelf variation of temperature off Cape Comorin (Fig.3.5) is characterised by deep thermocline (>70m) with near surface temperature more than $27^{\circ}C$ during December to January. It may be noted that depression of isotherms with sharp thermal gradient ($0.3^{\circ}C$ m^{-1}) is
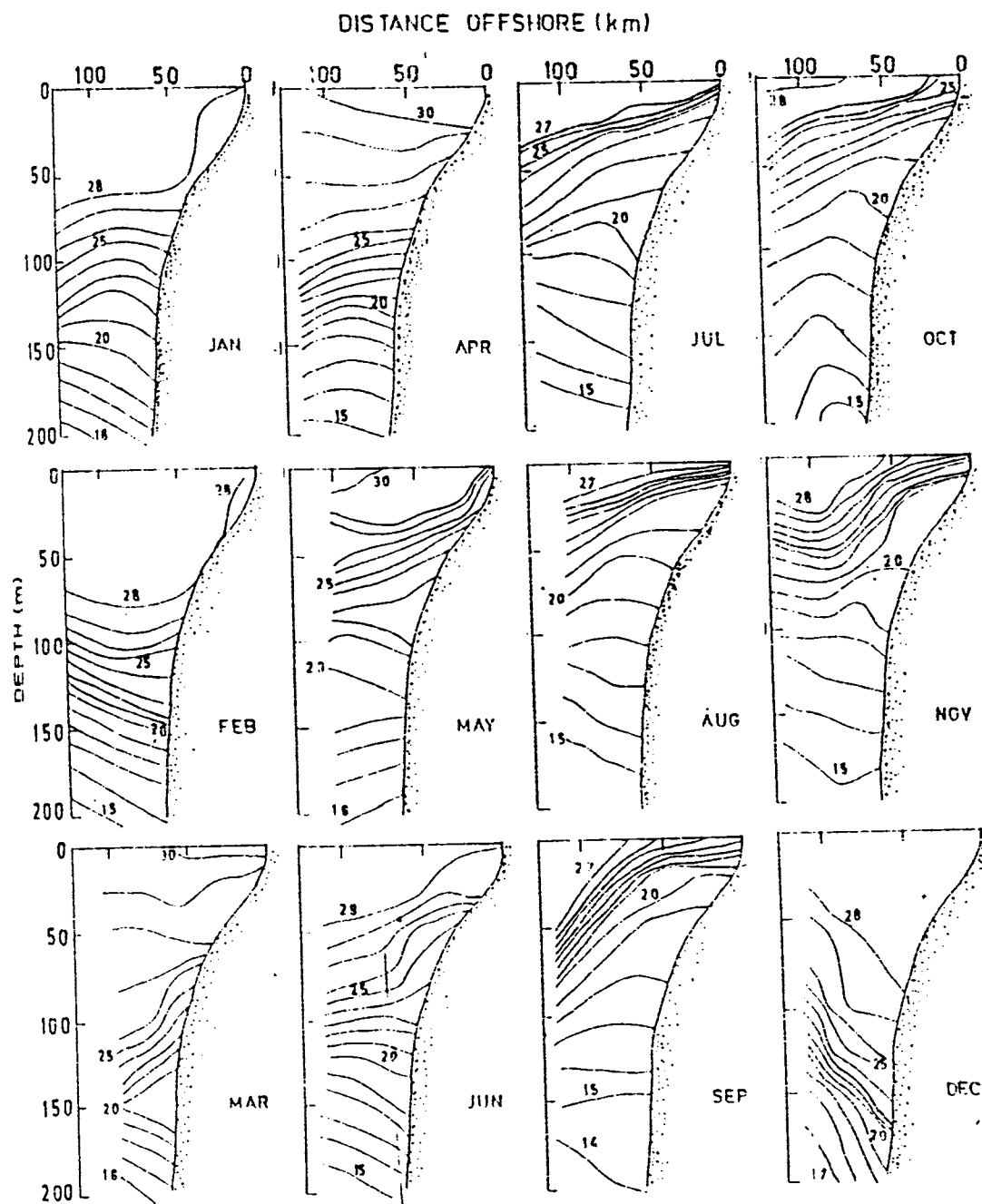
36

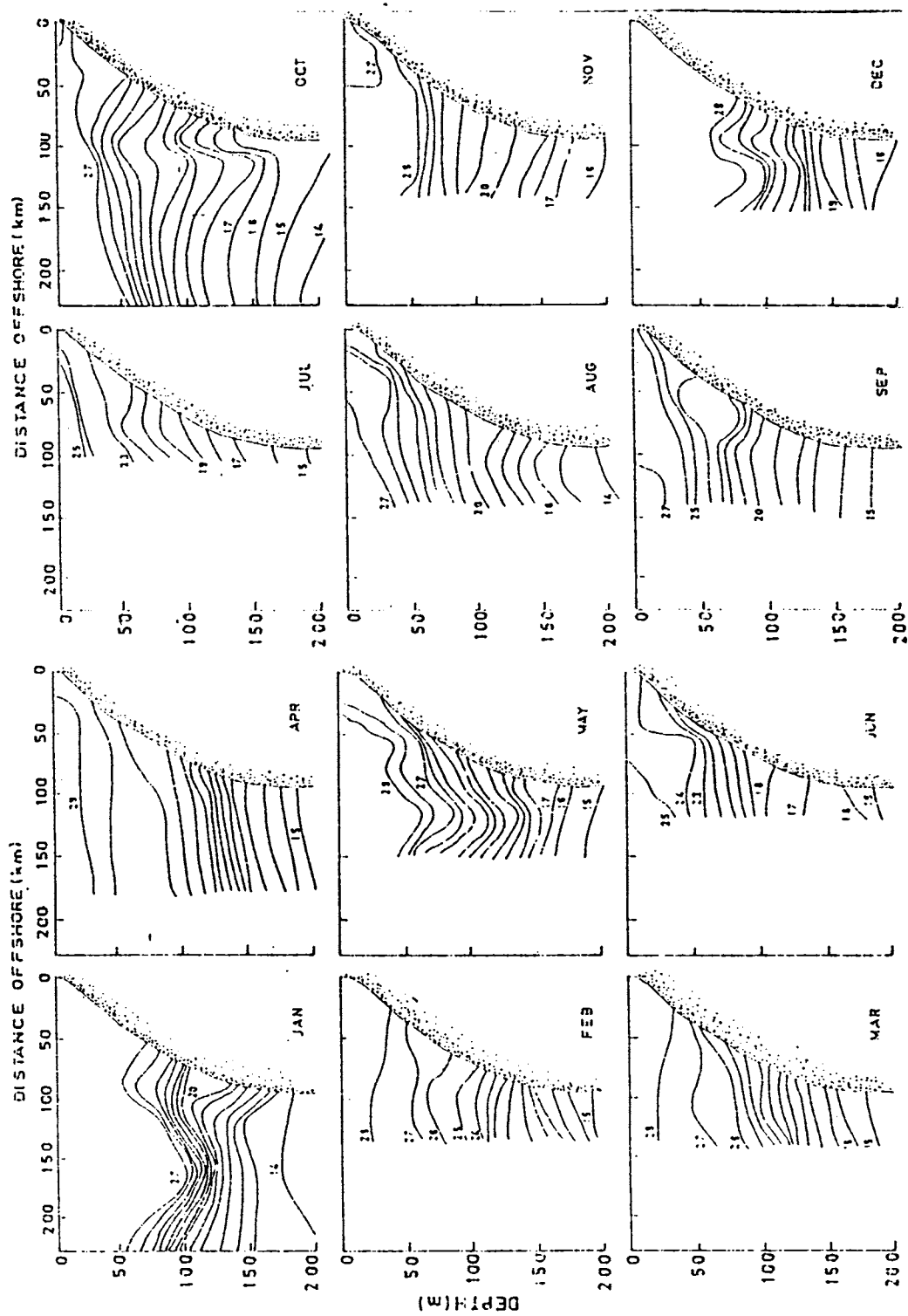Fig. 3.4 Monthly cross-shelf variations of temperature off Cochin(°C)

Fig. 3.5 Monthly cross-shelf variations of temperature off Cape Comorin (°C)

observed 150 km away from the coast occurring in January resulting in the shrinking of thermocline. This indicates the presence a clockwise (warm core) eddy of about 100km diameter centred about this location. Comparison between upwelling and sinking processes suggests that the former process lasts for the greater part of the year (March-October) compared to the latter (November-February). This clearly establish dominance of the upwelling process over sinking as far as the thermocline variabilities are concerned. Another aspect that has to be noted is the weak thermal gradients ($\cong$ 0.07°C m^{-1}) and deeper thermocline (>70m) during the periods of sinking.

A comparison of the thermocline structure at different locations off the west coast of India shows strong gradient in the upper thermocline during the periods of upwelling. However, the downsloping of isotherms in the lower thermocline is prominent only off Cochin, Kasargod and Ratnagiri during this period indicating a well developed northward undercurrent. The thermocline surfaces near the coast (25°C isotherm) at all locations except off Ratnagiri, suggesting strong upwelling off the southwest coast of India compared to northern locations. The higher surface layer temperature associated with the Indian Ocean warm pool is found more near Kasargod compared to other locations during April-May, which is in confirmity with Joseph (1990).

3.4 THERMOCLINE STRUCTURE AT SELECTED LOCATIONS IN THE SHELF WATERS ON AN ANNUAL CYCLE

In order to obtain the evolution of thermocline features in coastal regions (depths <200m) on an annual cycle, depth-time sections of monthly mean temperatures at selected locations off the west coast of India (Fig.3.1) are
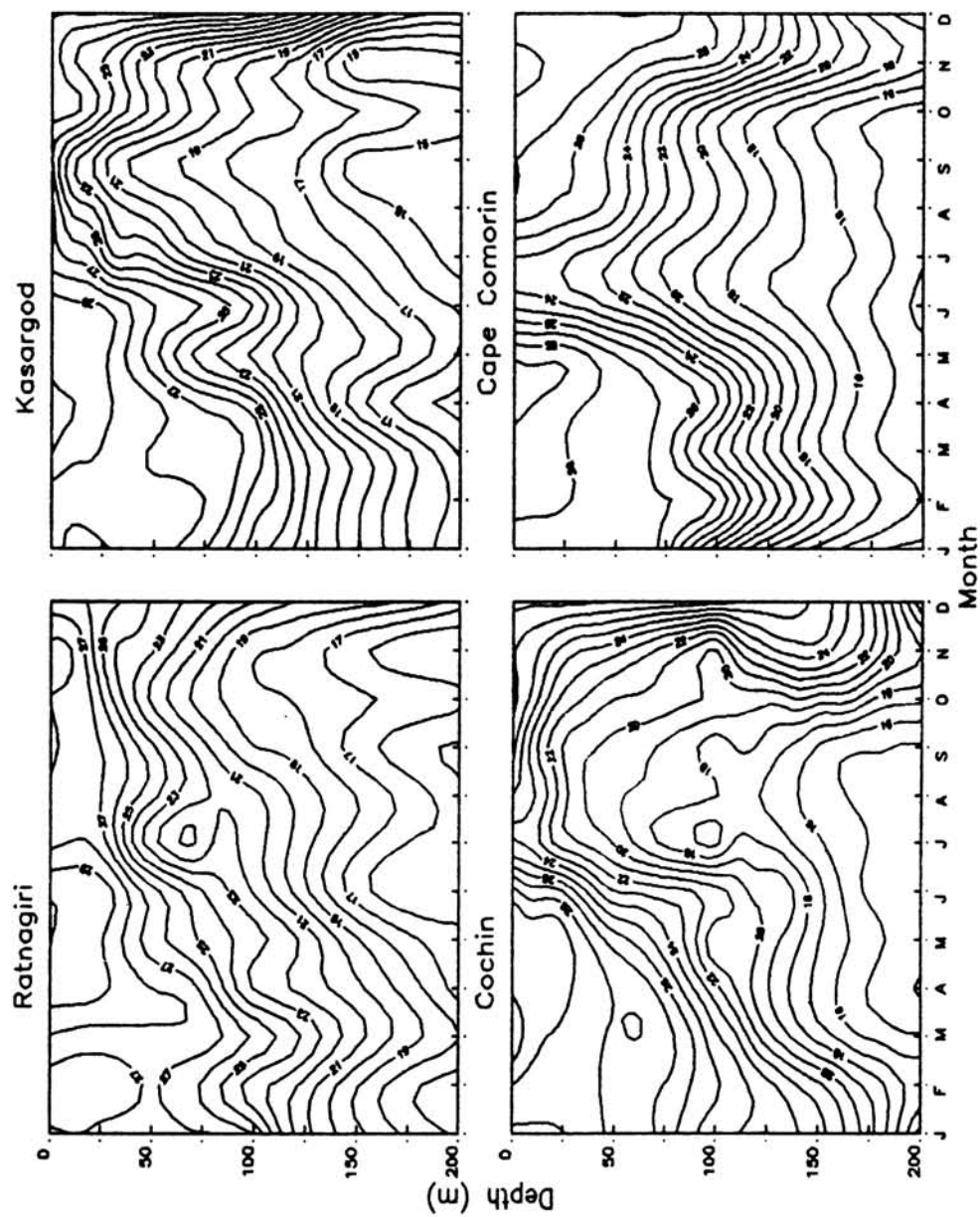
Fig. 3.6 Depth-time sections of temperature at selected locations (°C)

presented in Fig.3.6.

The isotherms start ascending in the thermocline zone at all locations from pre-monsoon period suggesting the commencement of upwelling. However, this process is found to occur with certain time lag. It can be seen that isotherms in the thermocline zone off Cape Comorin ascend from March/April onwards and surface by June (Fig.3.6). However, the surfacing of thermocline occurs during July-August and in September off Cochin and Kasargod respectively. However, off Ratnagiri, upward motion of thermocline continues up to November. The downward movement of thermocline starts by October, October-November and November off Cape Comorin, Cochin and Kasargod respectively.These results indicate that there is an approximate time lag of one month for the surfacing of the thermocline between sucessive locations from south to north. The surfacing of thermocline lead to significant cooling ($\cong$ 6°C off Cape Comorin and Cochin, $\cong$ 4°C off Kasargod). The secondary warming in the surface layers during the post monsoon season (Colborn,1975; Hastenrath and Lamb,1979; Mohan Kumar, 1991) prevents the surfacing of thermocline off Ratnagiri.

The average thermocline temperature is found to be minimum in September ($\cong$ 17°C) off Cochin and maximum ($\cong$ 24°C) in March off Kasargod. Further, the annual range of temperature is minimum off Ratnagiri (3°C) and is maximum off Cochin (5°C) where effect of upwelling is more pronounced. The temperature gradients on an annual cycle show large variations at all locations due to upwelling and sinking except off Ratnagiri. This is due to the fact that vertical motion off Ratnagiri is weak compared to other stations (where the thermocline does not surfaces). At all locations the gradients are strong in the upper thermocline

during the upwelling periods. Reduction in the gradient in the lower thermocline is due to the presence of northward flowing undercurrent. This can be inferred from the depth-time section of temperature (Fig.3.6) also where spreading of isotherms are noticed in the depth range of 80-150m.

Another interesting feature noticed is the large vertical displacement of isotherms (Fig.3.6) in the upper thermocline ($\cong$ 110m for 23°C isotherm) compared to the lower part of the thermocline ($\cong$ 30 m for 16°C isotherm). The combined effect of upwelling and sinking causes large displacement in the upper thermocline. The increased vertical mixing caused by the southerly surface currents (KNMI, 1952; Cutler and Swallow, 1984) and northerly undercurrent (Antony,1990) reduces the vertical displacement of isotherms in the lower part of thermocline, thereby reducing its amplitudes.

3.5 VERTICAL MOVEMENTS IN THE THERMOCLINE

The analysis reveals that the upper and lower thermoclines undergo upward and downward motions of varying magnitudes in an annual cycle. To compute the rate of vertical motion (Table 3.1) in the upper and lower thermoclines $23^{\circ}$and 18°C isotherms were chosen. The reason for choosing these isotherms is that they persist throughout the year at all locations and are seen in the upper and lower thermoclines respectively. It is worth mentioning here that there are no previous studies available describing the vertical motions in the upper and lower thermoclines for the west coast of India.

The rate (per month) of upward movement of 23°C

39

isotherm is 30m (110m in April to 20m in July) off Cape
Comorin. The corresponding values are 23m (130m in February
to 15m in July), 20m (125m in March to 10m in September) and
11m (130m in March to 40m in November) off Cochin, Kasargod
and Ratnagiri respectively. Contrary to upward movement, the
downward movement of this isotherm is found to be rapid
(Table 3.1). For instance, the rate of downward movement is
33m (65m in September to 130m in November) and 78m (15m in
September to 170m in November) off Cape Comorin and Cochin
respectively. The corresponding values are 30m (13m in
September to 103 in December) off Kasargod and 23m (40m in
October to 110m in January) off Ratnagiri.

TABLE 3.1

Rates of Vertical movement 23°C and 18°C isotherms

Locations	Rate (m month^{-1})	
	23°C	18°C
Cape	30 (33)	17 (31)
Cochin	23 (78)	21 (72)
Kasargod	20 (30)	15 (47)
Ratnagiri	11 (23)	12 (60)

(Values in paranthesis indicate the rate of downward
movement)

Similar analysis were carried out for 18°C isotherm,
which represent the lower thermocline (Fig.3.6 and Table
3.1). During upwelling periods this isotherm is observed at
its deepest depth (146m) in April-May which shoals to 103m
in July at a rate of 17m off Cape Comorin. The corresponding
values are 21m (183m in Februay to to 66m during

July-August), 15m (175m in March to 86m in September) and
12m (198m in March to 100m in November) off Cochin, Kasargod
and Ratnagiri respectively. The downward movement of $18^{\circ}C$
isotherm is 31m (113m in September to 190m during
November-December), 72m (90m in September to 198m during
October-November), 47m (106m during October-November to 176m
in December) and 60m (100m during October-November to 190m
in December) respectively off Cape Comorin, Cochin, Kasargod
and Ratnagiri.

This suggests that rate of downward movements of
isotherms in the thermocline is about 2 to 5 times faster
than that of upward movements. Moreover, the rate of upward
movements are more in the upper thermocline (30m per month
for $23^{\circ}C$ isotherm) compared to the lower thermocline (17m
per month for $18^{\circ}C$ isotherm). The reasons for the low rate
of upward movement in the lower thermocline is discussed in
section 3.4. However, during the periods of sinking, except
off Cochin and Cape, the rate of downward movements are more
in the lower thermocline. Moreover, the rate of downward
movement is appreciably higher off Cochin compared to any
other locations along the west coast of India.

3.6 T-S CHARACTERISTICS WITHIN THE THERMOCLINE OFF THE WEST COAST OF INDIA

The thermocline characteristics in the Arabian Sea is
influenced by the presence of various watermasses during
different times of the year (Wyrtki,1971; Darbyshire,1967;
Sastry and D'Souza,1972). Individual hydrographic data
available off the west coast of India are utilised to map
the T-S diagrams (Fig.3.7) in order to identify some of the
major watermasses in the thermocline and their monthly

Fig. 3.7 T-S Characteristics within the thermocline for coastal waters (depth <200m)
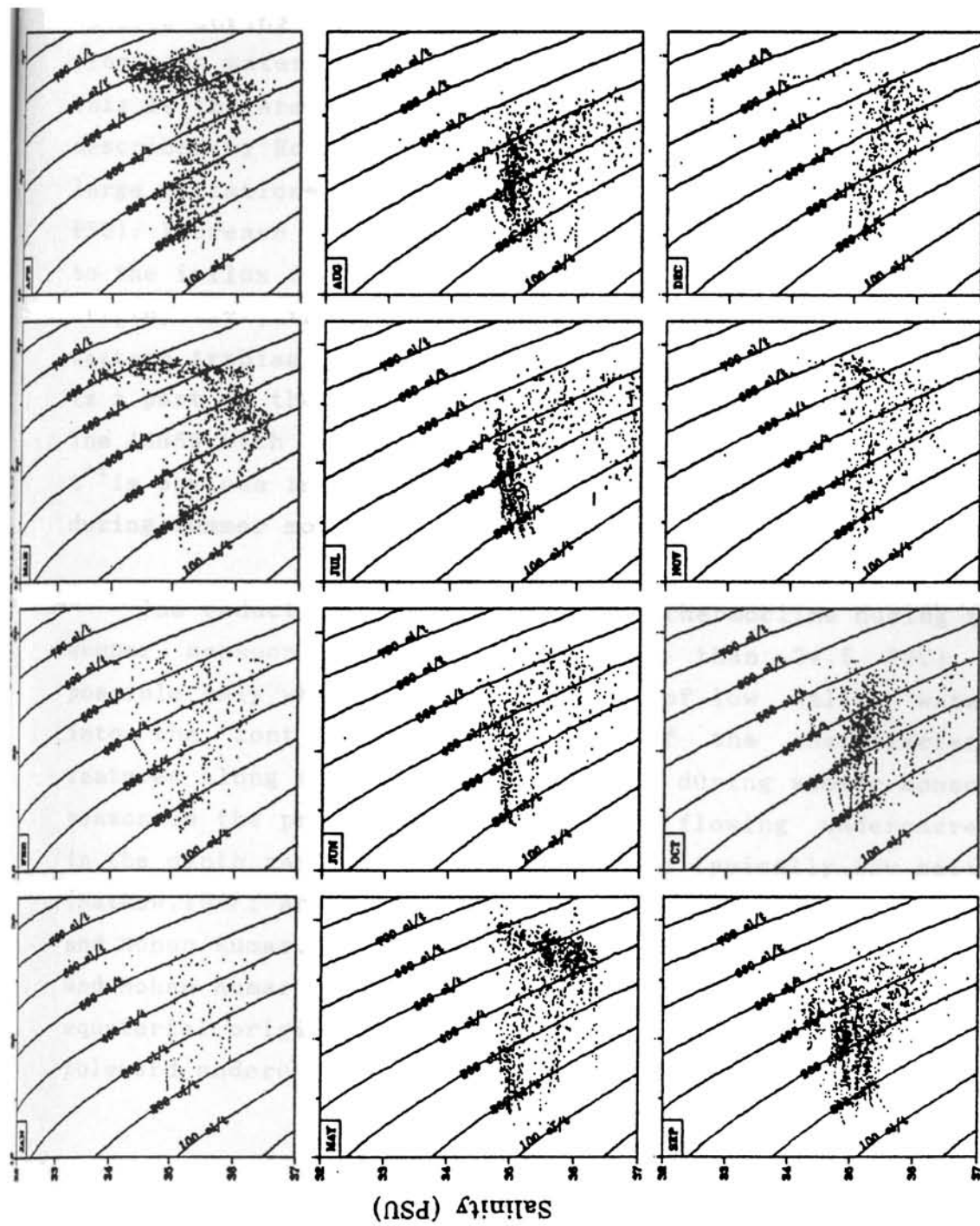
evolution. The T-S plots show minimum scatter during May-June and September-October while relatively larger scatter is noticed during the rest of the year suggesting the presence of a number of watermasses having different T-S characteristics.

Prior to the onset of monsoon (May), salinity within the thermocline is between 35-36.25 PSU. The minimum scatter noticed during this period suggests the presence of a prominent watermass with its core centred around 400 cl t^{-1}. This is the Arabian Sea High Sslinity Watermass (ASHSW) as described by Rochford (1964). During the monsoon season large variations are noticed in the salinity field (34.25-37 PSU). Increase of salinity in the thermocline is mainly due to the influx of high saline waters of northern Arabian Sea origin, viz., the ASHSW. This watermass brought into the eastern Arabian Sea by the prevailing southerly flow, which is a part of the clockwise gyre (Culter and Swallow, 1984). The ASHSW with temperature (22-26°C) centered around 400 cl t^{-1} is obvious in all months with maximum salinity (>36 PSU) during summer monsoon season.

The reduction in salinity in the thermocline during the summer monsoon season (values less than 34.5 PSU) is possible only when there is an influx of low saline waters into the continental shelf. One of the characteristic features along the west coast of India during summer monsoon season is the presence of a northward flowing undercurrent in the depth range of 80-150m which are typically low saline (Mathew,1981 ; Antony,1990; Shetye et al.,1990; Hareesh Kumar and Mohan Kumar;1995). The recent studies of Hareesh Kumar and Mohan Kumar (1995) revealed that this undercurrent is of equatorial origin. The equatorial watermass brought by this poleward undercurrent is responsible for the reduction in

42

salinity in the thermocline during summer monsoon season. The existance of high saline ASHSW over the low saline equatorial Indian Ocean watermass produce large scatter in the T-S diagram during summer monsoon.

Several studies have reported the influx of Bay of Bengal/Equatorial Indian Ocean water (above 500 cl t^{-1}) into the shelf regions of the west coast of India during winter (Darbyshire,1967; Wyrtki,1971; Pankajakshan and Ramaraju,1987; Hareesh Kumar,1994). The T-S characteristics above 500 cl t^{-1} indicate uniform temperature (28°C) and rapidly decreasing salinity (35-33.5 PSU in March). However, this reduction in salinity is less compared to the values (35-32 PSU) reported by Hareesh Kumar (1994) for the entire water column. This suggests that the influence of Bay of Bengal/Equatorial Indian Ocean water is limited to the upper thermocline (with temperature above 27°C).

3.7 THERMOCLINE CHARACTERISTICS IN THE COASTAL REGIONS

The available temperature data in the coastal region (depth <200m) along the west coast of India (6° to 24°N) averaged in 0.25 x 0.25 degree square are utilised for this investigation. The thermocline characteristics, viz top of the thermocline, its average temperature and average gradient are presented in Figs.(3.(8-10)) to highlight its spatio-temporal variations.

Topography of the thermocline (Fig.3.8) exhibits large variations from December to March. Top of the thermocline ascends from February onwards (100m in February to 50m in March) in the lower latitudes (at 9°N) suggesting the beginning of upwelling. The thermocline is quite shallow (<50m) along the entire west coast of India during the
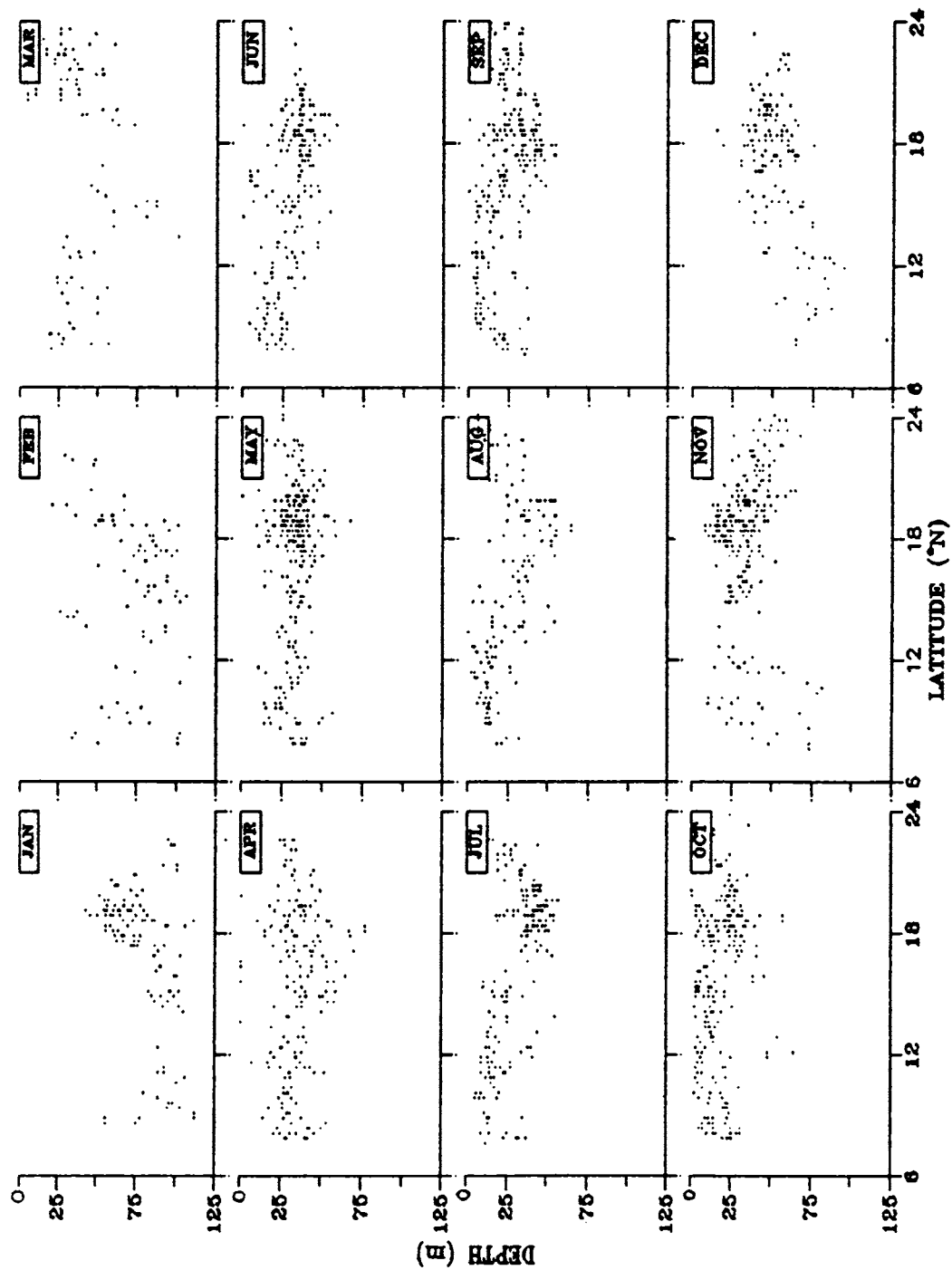
Fig. 3.8 Zonal distribution of thermocline top for coastal waters
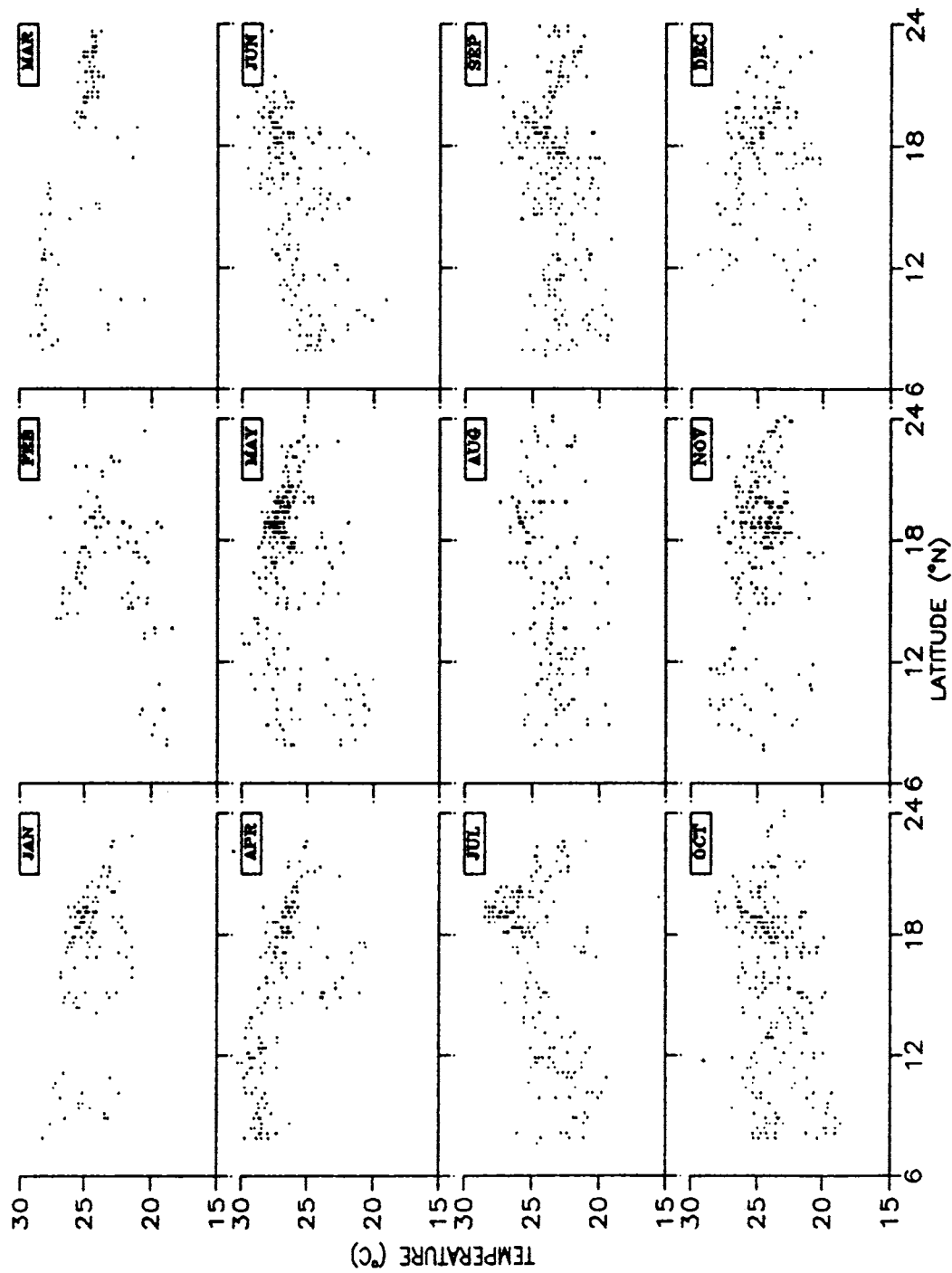
(depth <200m)

Fig. 3.9 Zonal distribution of thermocline temperature for coastal waters (depth <200m)

pre-monsoon   (April-May)   and   monsoon   (June-September)
seasons. The   shallow   thermocline   during   the   pre-monsoon
season is mainly caused by the accumulation of heat   in   the
surface layers (Hastenrath and Lamb,1979)   which   stabilises
the water column. However, during the summer monsoon   season
upwelling is the prime factor controlling   its   variability.
The effect of upwelling is more pronounced off the southwest
coast of India, where the thermocline shoals from $\cong$ 100m   in
February to less than 10m in September. One of   the   notable
features is that the shoaling   of   the   thermocline   is   not
significant between 16°N to 20°N suggesting weak upwelling.

When the process of sinking commences   along   the   west
coast of India (October-November onwards)   large   variations
are noticed in the top of the thermocline   especially in the
lower latitudes ($<12^{\circ}$N) which continues till March.   Another
important result to be noticed is that the   onshore-offshore
variations in the top of the thermocline is more during   the
periods of sinking compared to upwelling.   The   large
variations in the thermocline topography   from   November   to
March is   mainly   caused   by   variations   in   the
nearshore/offshore dynamics and the   latitudinal   variations
in the sinking process. During this period,   thermocline   is
noticed at deepest level (over   100m   in   January)   off   the
southwest coast of India and north of 20°N.

The   thermocline   temperature   (Fig.3.9)   also   exhibit
similar variations as that of top of thermocline.   Moreover,
large onshore-offshore and   latitudinal   variations   are
noticed during the periods of upwelling and sinking. This is
mainly due to the   variations   in   the   onshore-offshore
dynamics and the commencement of upwelling/sinking along the
west coast of India (Fig.3.6). During   winter   (December   to
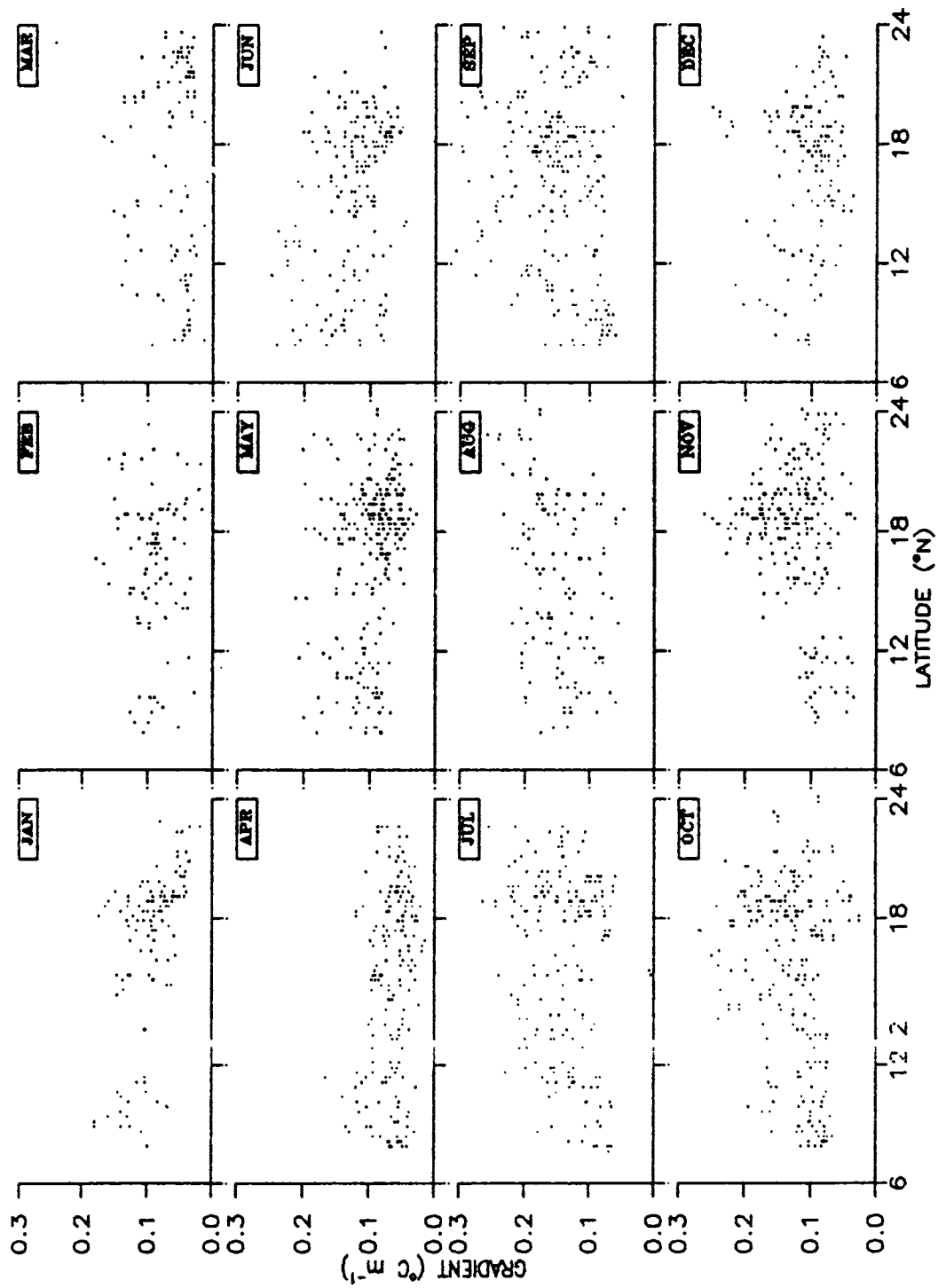February), thermocline temperature is greater than 27°C   off

44

Fig. 3.10 Zonal distribution of thermocline gradient for coastal
waters (depth <200m)

the southwest coast of India and decreases towards north ($\cong$ 23°C north of 20°N). In association with large heat input into the ocean during the pre-monsoon period (Hastenrath and Lamb,1979), temperature in the thermocline increases. If we closely examine the temperature pattern, occurrence of maximum temperature is found to be related to the periods of large heat gain. South of 14°N the maximum temperature (30°C) is found to occur in April. In the latitudinal band 14°N to 20°N the maxima occurs in May (28°C) while north of 20°N it occurs in June (30°C). With the onset of summer monsoon drastic cooling is noticed in the thermocline mainly due to upwelling. The cooling rate is found to be maximum south of 14° N (30°C in May to 20°C in September) and north of 20°N (30°C in June to 22°C in September). Such a cooling rate is not observed in the 14°-20°N latitudinal band. This suggests that cooling is more intense off the southwest coast of India and north of 20°N compared to any other regions along the west coast of India. The large variability north of 20°N is mainly due to the effect of winter cooling and pre-monsoon heating.

The thermocline gradient (Fig.3.10) also exhibits large variability in the continental shelf during greater part of the year. Minimum gradients (<0.1°C m^{-1}) are observed in April when shallow thermocline (Fig.3.6) and maximum heat input into the ocean is observed. Comparatively large gradients (>0.2°C m^{-1}) are observed during the summer monsoon season. Comparatively weak gradients ($\cong 0.15$°C m^{-1}) and minimum onshore-offshore variations are noticed north of 20°N. Another feature to be noticed is that the gradient in the thermocline decreased with the commencement of sinking, with minimum values (<0.05°C m^{-1}) occurring north of 20°N.

CHAPTER IV

SHORT-TERM VARIABILITY OF THERMOCLINE CHARACTERISTICS

4.1.INTRODUCTION

It is well known that the onset and progress of summer monsoon produces large scale spatio-temporal modifications in the thermal structure of the Arabian Sea (Wyrtki,1971; Robinson et al.,1979; Molinari, 1983; Shetye 1986; Rao et al.,1989; Rao et al.,1990; Hareesh Kumar,1994). Generally, the pre-monsoon season is characterised by fair weather conditions resulting in accumulation of heat with varying magnitudes across the basin. However, due to occasional thunder squall activities, marked variations are noticed in the meteorological (Sikka and Grossman,1980) and thermohaline fields (Rao,1987; Rao et al.,1993; Hareesh Kumar, 1994) on a synoptic scale. Active monsoonal spells and associated meteorological disturbances can cause short-term variability in the thermal structure (Rao,1986; Rao and Mathew,1990; Joseph et al.,1990; Murthy and Hareesh Kumar,1991). With the onset and progress of the summer monsoon, intense air-sea exchange processes (Hastenrath and Lamb,1979) and convergence induced by the negative wind stress curl (Hastenrath and Lamb, 1979;Bauer et al.,1991) deepens ($\simeq$ 100m) the thermocline in the central Arabian Sea (Sastry and D'Souza,1970; Hastenrath and Greischar,1989). However, significant warming occurs in the upper portion ofthermocline mainly due to the deepening of the mixed layer and mixing of the subsurface waters with surface waters. In the coastal regions, the process of upwelling results in the shoaling of isotherms towards the coast and cooling of the
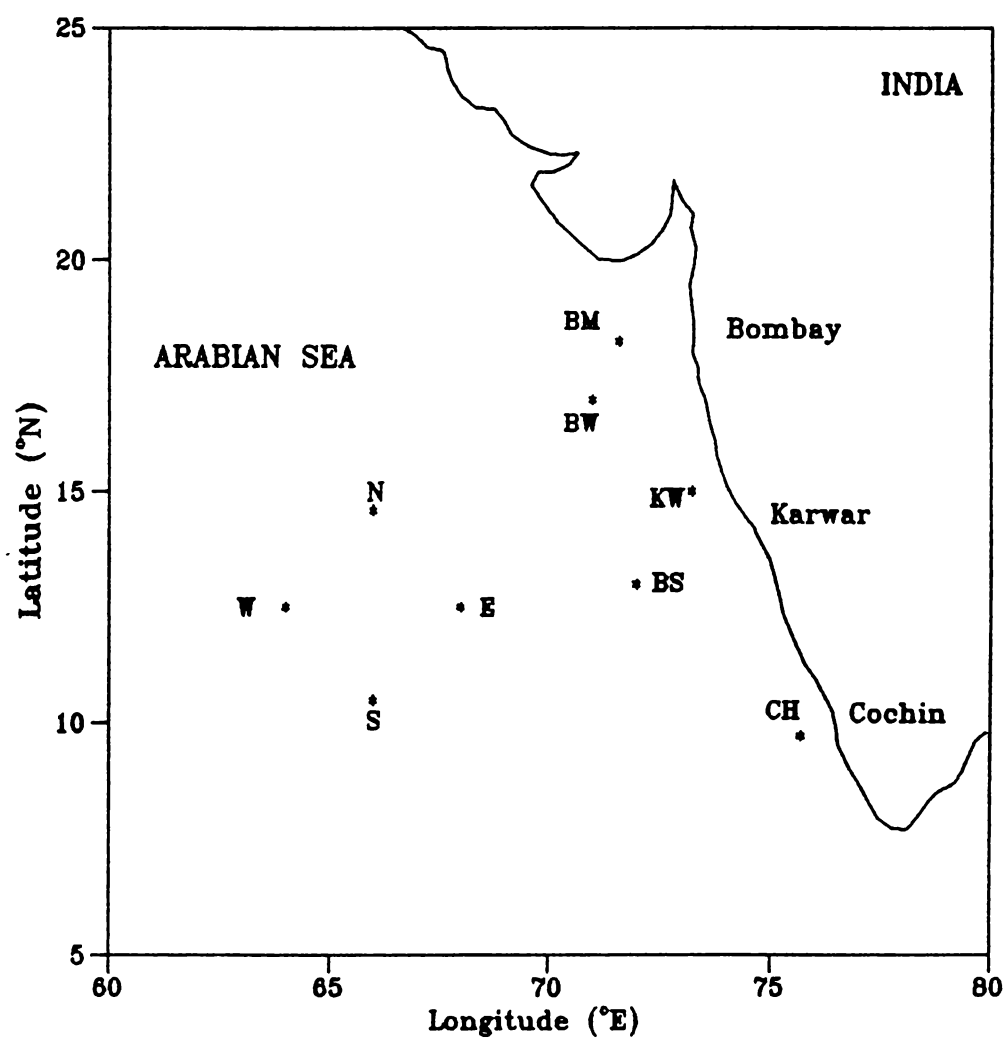
46

Fig. 4.1 Station location map of time series observations

water column (Warren et al.,1966; Swallow and Bruce,1966; Schott,1983; Mathew,1981; Shetye et al.,1991).

Prior to the conduct of summer monsoon experiments no systematic time series measurements were made to study the short term variability of thermal structure in the Arabian Sea. During these experimental programmes a systematic attempt was made to collect vertical temperature and salinity data at selected locations in the Arabian Sea. Although these data sets were collected at different locations over short duration, they provide important insight into the problem of thermocline variability.

In the Arabian Sea, several studies have been carried out to understand the time variation of the mixed layer and its causative factors (Rao,1986; Mc Creary and Kundu,1989; Joseph et al.,1990; Rao and Mathew,1990; Rao et al.,1991; Mohan Kumar et al.,1995; Hareesh Kumar,1994; Hareesh Kumar and Mohankumar,1995). However, the evolution of thermocline characteristics viz, top of the thermocline, thickness, gradient, mixing processes, oscillations is not adequately discribed or understood. In this chapter, the short term variability in the thermocline characteristics is studied utilising the time series data sets collected from selected locations in the Arabian Sea during the pre-monsoon and onset phases of the summer monsoon (Fig.4.1).

4.2. DATA

Most of the data sets utilised for this study correspond to open ocean conditions of the Arabian Sea were collected during MONSOON-77 and MONEX-79 field experimental programmes. In addition, data sets collected in the coastal zones off Bombay, Karwar and Cochin are utilised. The

47

Table 4.1
Station location, Symbol and observation period

Station location		Station	Observation
Latitude	Longitude	Symbol	Period
$18°15'$	$71°35'$	BM	28Jun.- 01Jul.'88
$14°45'$	$73°35'$	KW	28May - 01Jul.'89
			18Sep.- 25Sep.'89
			29Oct.- 10Nov.'86
$09°44'$	$75°42'$	CH	10Apr.- 17Apr.'91
			23May - 3Jun.'92
$13°00'$	$72°00'$	BS	26May - 7Jun.'77
			26Jun.- 14Jul.'77
$17°00'$	$71°00'$	BW	26May - 7Jun.'77
			26Jun.- 13Jul.'77
$14°30'$	$66°00'$	N	7Jun.- 19Jun.'77
			30Jun.- 15Jul.'77
$12°30'$	$68°00'$	E	7Jun.- 19Jun.'77
			30Jun.- 15Jul.'77
$10°30'$	$66°00'$	S	7Jun.- 19Jun.'77
			30Jun.- 15Jul.'77
$12°30'$	$64°00'$	W	7Jun.- 19Jun.'77
			30Jun.- 15Jul.'77

period, April-May represents pre-onset and June to September represents active phases of the summer monsoon. The station locations (Fig.4.1) are designated as N, E, S and W correspond to the four corners of the USSR polygon occupied in the central Arabian Sea during 1977 and BW and BS

represents two Indian ship locations in the eastern Arabian Sea during MONSOON-77. BM, KW and CH are the three coastal sations off Bombay, Karwar and Cochin respectively. Station locations, symbols and obervational periods are presented in Table 4.1. From these locations time series of the vertical profiles of temperature were collected at one/three/six hourly sampling interval. To study the role of mixing process in the thermocline region the subsurface currents obtained from selected depth levels by deploying Aanderaa RCM4 and RCM7 current meters at CH, KW, BM are also utilised.

4.3. RESULTS AND DISCUSSION

4.3.1 DEPTH-TIME SECTIONS OF THERMAL STRUCTURE

The depth-time sections of temperature presented in Fig.4.2 reveal the complex nature of spatio-temporal variability in the thermocline. One of the features that has to be noted is the occurrence of variable gradients and oscillatory nature in the thermocline. In the discussion, the depth-time sections of temperature for the coastal and deep stations are treated separately.

4.3.1.1 AT COASTAL STATIONS

The thermal sructure off Bombay (Fig.4.2a) is charactrised by a tri-layer structure with a sharp thermocline (2.5°C drop in 10m) sandwiched between upper (40m) and bottom (25m) isothermal layers. Formation of this feature can be explained in terms of air-sea interaction process. During winter, the thermal structure in the continental shelf off Bombay is characterised by deep isothermal layers ($\simeq$ 80m) with temperature $\simeq$ 26.5°C (Joseph
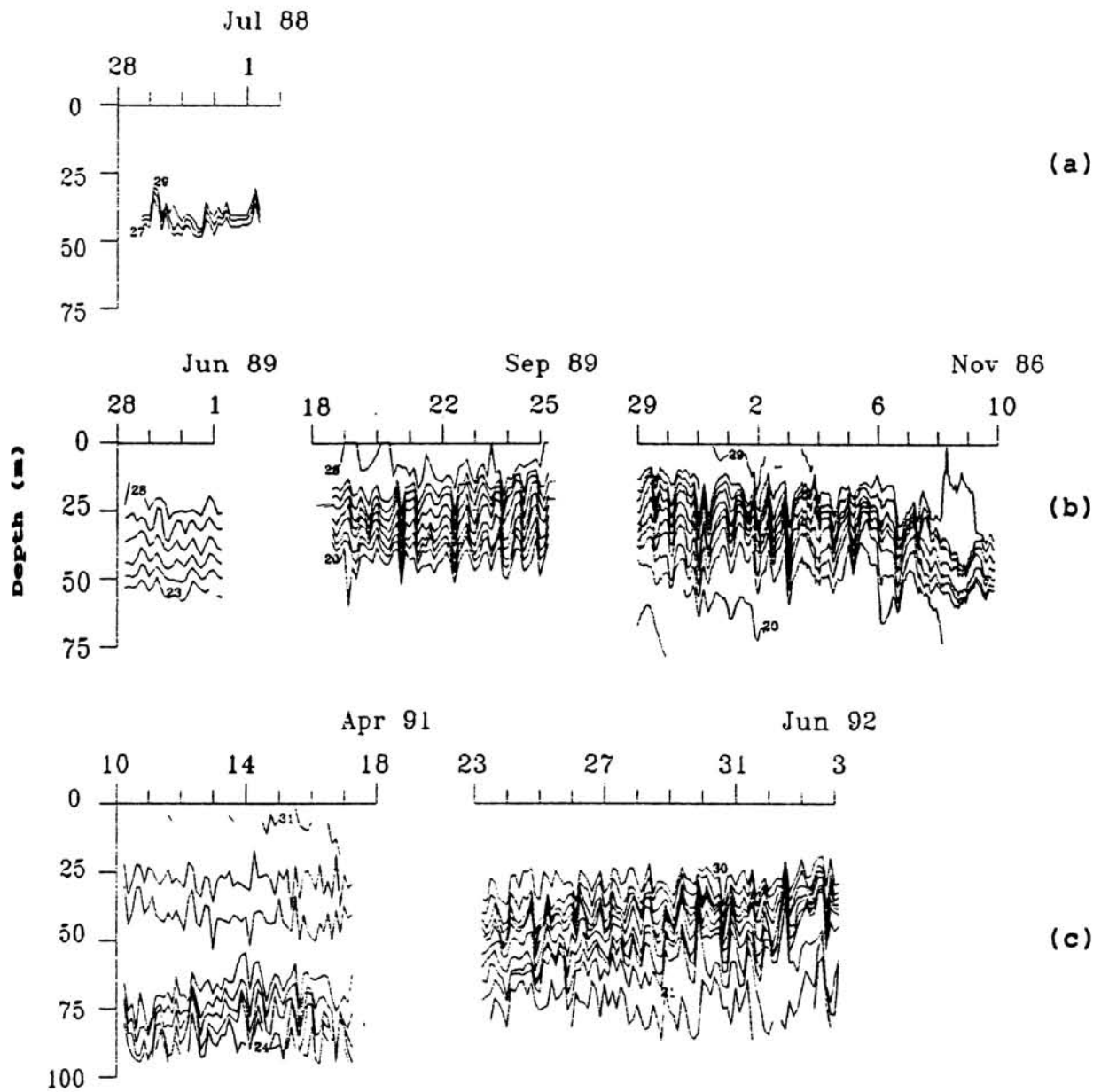
49

Fig. 4.2 Depth-time sections of temperature at (a) BM   (b) KW
(c) CH   representing shallow water (depth <200m) (°C)

and Hareesh Kumar,1990).. During the pre-monsoon period, climatological studies of Rao et al.(1990) reported a warming of $4°C$ in the surface layers. Intense vertical mixing (Hastenrath and Lamb,1979) of the surface warmer waters with subsurface cooler waters during the summer monsoon caused the re-distribution of heat, thereby deepening the surface mixed layer down to 40m with temperature $29.5°C$. Below 50m, the water column is isothermal $(26.5°C)$ having the characteristics reported by Joseph and Hareesh Kumar (1990). This indicated that the influence of surface forcings penetrate up to 50m depth. The analysis reveal that the pre-monsoonal heating in the surface layer and intense vertical mixing in the upper 50m over the remnants of the winter water with the onset of monsoon caused the formation of the tri-layer structure.

In the coastal waters off Karwar (Fig.4.2b), mixed layers of $\simeq$ 25m are noticed during the onset phase of summer monsoon (June) which shoal to 5m by the withdrawal phase (September) due to upwelling . The $25°C$ isotherm which lies in the middle of the thermocline shoaled from 40m during the onset phase to 20m by the end of monsoon season. The vertical displacements are more at the bottom layers as indicated by the displacement of $23°C$ isotherm which shoaled more than 30m. Due to upwelling there is a drastic reduction in temperature at subsurface levels (3 to $5°C$). It is interesting to note that there is a two fold increase in the thermocline gradient (0.15 to 0.3 m^{-1}), which will be discussed later in this chapter. During October-November, under the influence of a deep depression (Murthy and Hareesh Kumar,1991), top of the thermocline deepened by 25m (15m to 40m) due to drastic heat loss and convergence induced by the surface wind stress curl (Murthy and Hareesh Kumar,1991). Fast Fourier Transform (FFT) analysis of isotherm

displacement (October-November) in the thermocline revealed
oscillations with semi-diurnal (12 hrs), diurnal (24 hrs)
and inertial (46 hrs) periodicities. The oscillation with
inertial periodicity is caused by the distant storm centred
360km southwest of observational station and caused vertical
displacement of 15-20m in the isotherms. Pollard (1970) also
observed similar conditions during the passage of storm and
attributed the wind field as the main source of inertial
oscillation in the thermocline. As the station is located at
the periphery of the storm, continuous deepening of the
isotherms are observed mainly due to downwelling as
suggested by Leipper (1967).

Another interesting feature is the presence of a
prominent bottom isothermal layer (Fig.4.2b). By the end of
summer monsoon season, temperature of this layer decreased
by $3^{\circ}C$ ($23^{\circ}C$ to $20^{\circ}C$) mainly due to upwelling and its
thickness increased by 15 m (10 m to 25m) due to increased
shear mixing (Fig.4.6b). The presence of bottom isothermal
layer during October-November though with an increase in its
temperature compared to withdrawl phase suggest sinking.
Mohan Kumar et al.(1995) attributed the increase in
temperature near the bottom to the northward flowing under
currents, which are typical during the periods of upwelling.

The thermal structure off Cochin (Fig.4.2c) during
April is characterised by a shallow isothermal layer ($\cong 20$m),
a layer of weak stratification ($1.5^{\circ}C$ fall in 20m i.e.
$0.075^{\circ}C$ m^{-1}), a quasi-homogeneous layer (5 to 20m thickness
and gradient $<0.025^{\circ}C$ m^{-1}) and a layer of strong
stratification ($5^{\circ}C$ fall in 30m i.e. $0.17^{\circ}C$ m^{-1}). In the
regions of strong stratification, oscillations of inertial
(79 hrs), diurnal (24 hrs) and semi-diurnal (12 hrs)
periodicities are noticed, due to which the isotherms are

displaced by $\simeq$ 5-15m in the vertical. The layer of weak stratification is thought to be the result of deep mixed layer during winter followed by surface heating (Hareesh Kumar and Mohan Kumar,1995) during the pre-monsoon season. Thickness of the quasi-homogeneous layer decrease from 30m to 5m between 10 and 14 April and increase thereafter. By May, this quasi-homogeneous layer disappear and the thermocline becomes more stratified ($0.15^{\circ}C. m^{-1}$). Moreover there is an upward displacement of isotherms in the thermocline during this period. For instance, in the thermocline the $25^{\circ}C$ isotherm, which was at 85m on 17 April, shoaled to 35m by 3 June, with an average upward movement of 1.1 $m. day^{-1}$. This upward movement of isotherms are mainly due to the process of upwelling, results in cooling of $\simeq$ $0.8^{\circ}C$ at the surface and $4.5^{\circ}C$ at the bottom, with maximum cooling in the of $6^{\circ}C$ at 60m.

4.3.1.2 AT DEEP STATIONS

In the eastern Arabian Sea (BS and BW), intense solar heating during the pre-monsoon phase (Rao et al.,1990) resulting in the formation of near surface (<20m) thermocline (Fig.4.2(d,e)). The enhanced vertical mixing during the summer monsoon season deepens the thermocline to below 50m. However, the effect of upwelling is noticed within the thermocline at both locations as evident from the upward displacement of $24^{\circ}C$ isotherm which shoaled by 25m at BS (90m to 65m) and 20m at BW (80m to 60m). Several short period oscillations are also noticed in the thermocline in both the phases.

The observed thermal structure at the polygon stations (Figs.4.2(f-i)) in the central Arabian Sea is significantly different from the stations in the coastal regions in many
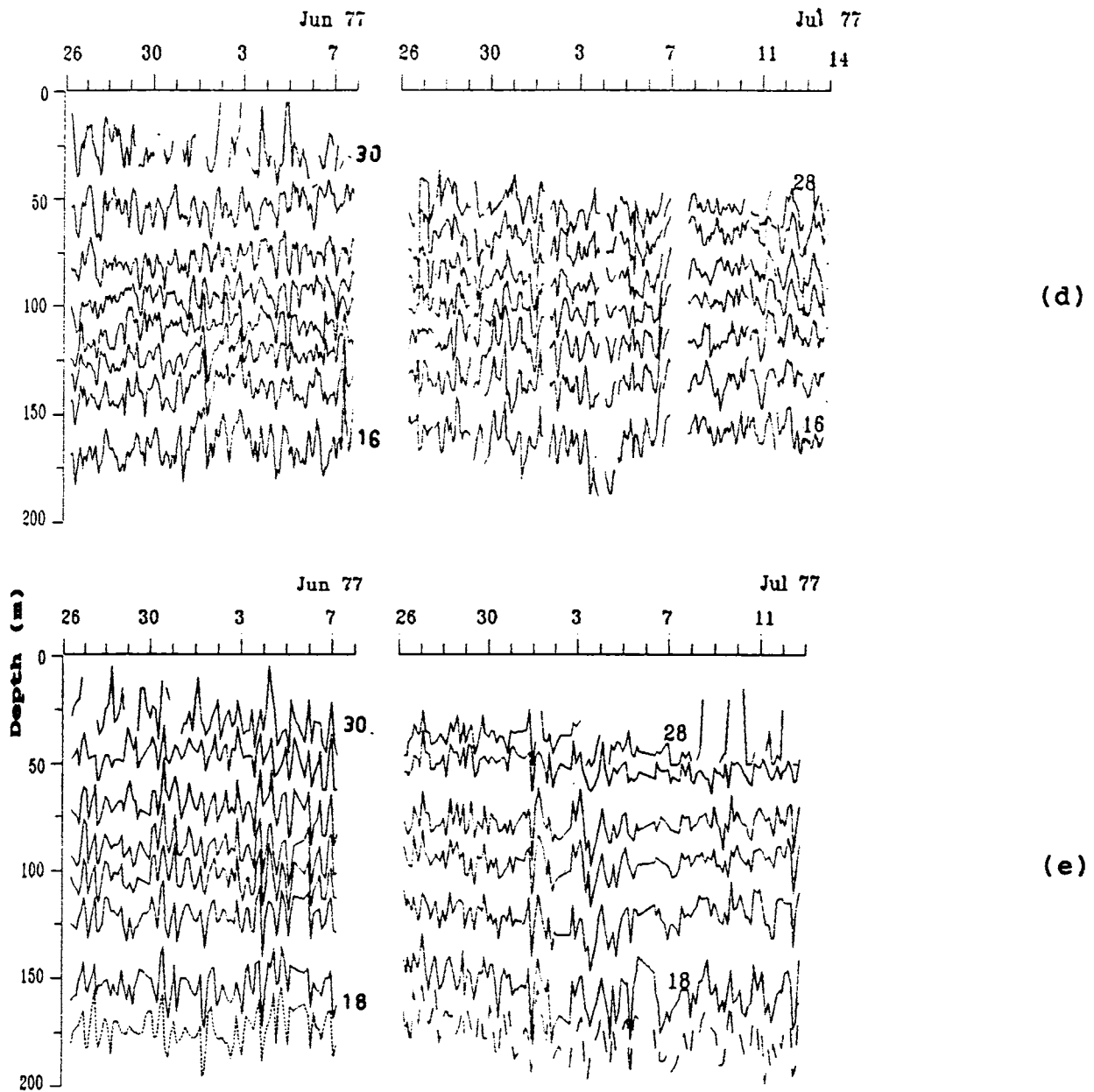
Fig. 4.2 Depth-time sections of temperature at (d) BS (e) BW

representing deep water (depth >1000m) (°C)

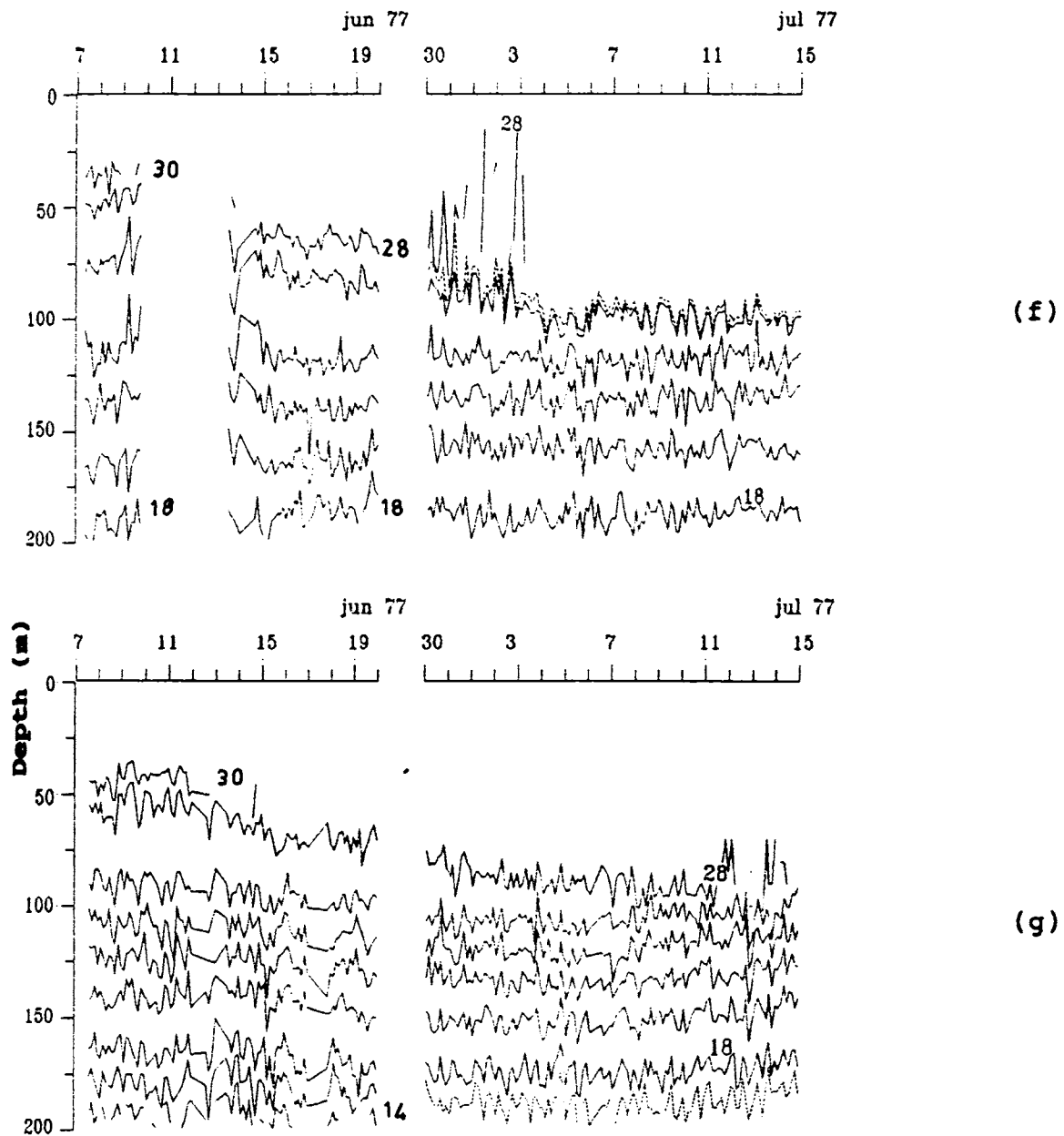Fig. 4.2 Depth-time sections of temperature at (f) N   (g) E
representing deep water (depth >1000m) (°C)
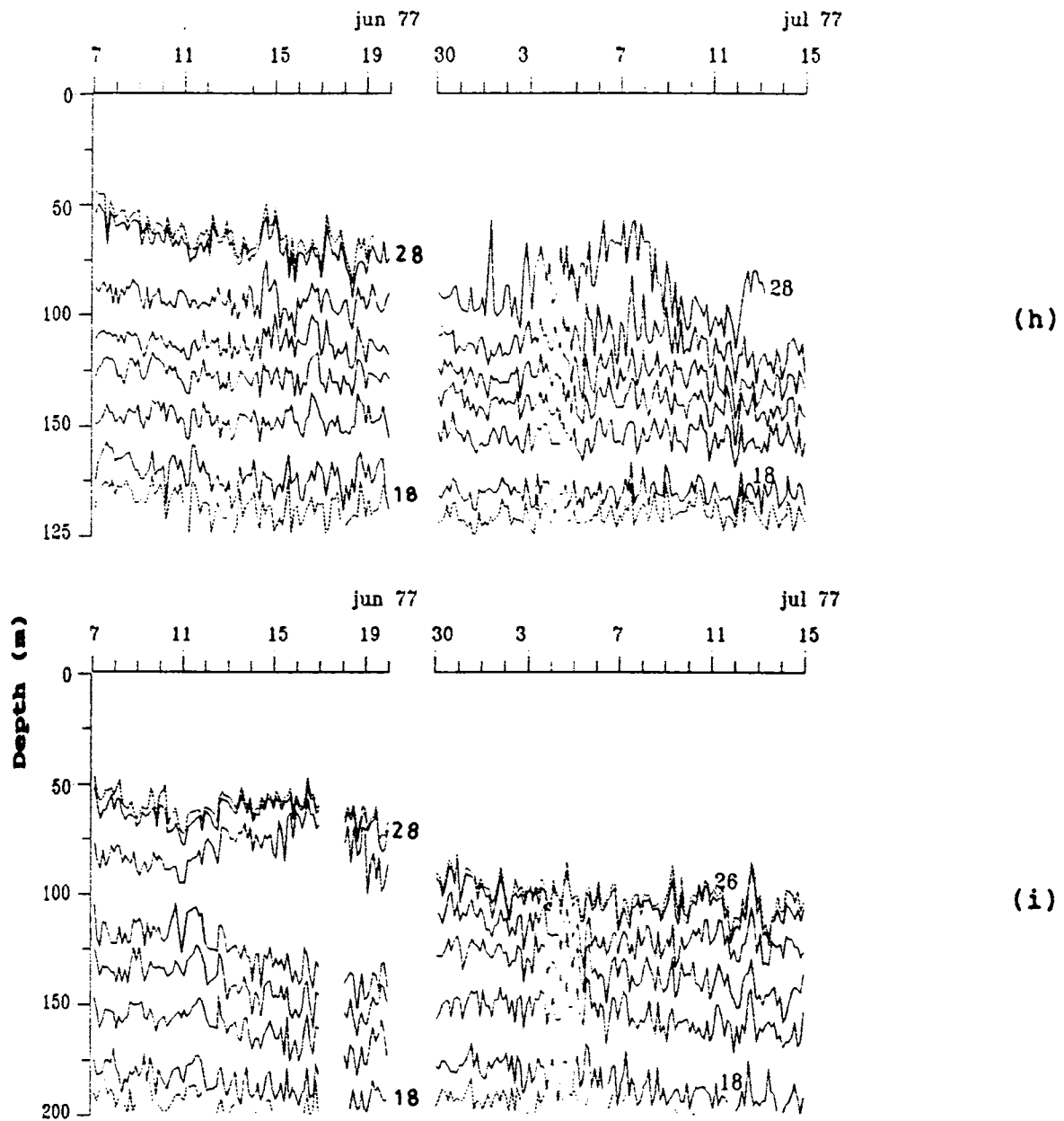
Fig. 4.2 Depth-time sections of temperature at (h) S (i) W
representing deep water (depth >1000m) (°C)

respects. A noteworthy feature is the deepening of thermocline in the central Arabian Sea, though with a varying magnitude in contrast to an ascend in the coastal regions (Figs.4.2(a-c)). Deepening of the thermocline is mainly due to enhanced vertical mixing (buoyant and mechanical) and sinking due to negative wind stress curl (Hastenrath and Lamb,1979; Rao et al.,1993). However, deepening is more rapid during the onset phase (7 to 19 June) than the active phase (30 June to 16 July). The onset phase over Arabian Sea is marked by a spurt in the turbulent kinetic energy in the lower atmospheric boundary layer (Mohanty et al.,1983). This results in the sudden increase of mechanical mixing on an otherwise calm ocean conditions. By the active phase, an equilibrium condition is attained and any further increase in the mechanical forcing will not penetrate much due to the deep mixed layers ($\cong$ 75m). All the available mechanical energy is distributed over the deep mixed layer without affecting top of the thermocline. The thermocline deepened by 45m (30m to 75m), 50m (40m to 90m), 45m (40m to 85)and 30m (50 to 80m) over a period of 12 days during the onset phase at N, E, S and W respectively while the corresponding values during the active phase are 40m (75m to 115m), 30m (80m to 110m), 20m (100m to 120m) and 40m (80m to 120m). Moreover, with the progress of summer monsoon the thermocline becomes more stratified ($<0.1^{\circ}$C m^{-1} to $>0.15^{\circ}$C m^{-1}). A more diffused thermocline is noticed at N ($<0.07^{\circ}$C m^{-1}) during the onset phase compared to other locations. Temporal variability in the isotherm depths in the thermocline shows oscillatory pattern caused by propagating internal waves and eddy fields etc. (Duing,1972; Swallow et al.,1983).

4.3.2 SHORT-TERM VARIATIONS OF THERMOCLINE CHARACTERISTICS

From the analysis of time series of thermal structure at selected locations it is found that there is significant variations in the thermocline characteristics. In the following sections the thermocline characteristics viz., top of thermocline, thickness, gradient, mixing in the thermocline and oscillations in the thermocline are discussed.

4.3.2.1 TOP OF THE THERMOCLINE

The time series of the top of thermocline at different locations are presented in Figs.4.3(a-i). Top of the thermocline exhibits large spatio-temporal variations. It is around 40m at BM in July, 25m/50m at KW in June/November and 20m at CH in April. With the progress of summer monsoon, top of the thermocline undergoes significant upward movement especially in the coastal regions due to upwelling. For instance, at CH thermocline top shoal from 25m on 10 April to 10m on 3 June, whereas at KW it moved up (25 to 5m) by the end of summer monsoon season (September). During October-November, it deepens to 70m due to convergence (sinking) induced by a deep depression. However, at BM top of the thermocline does not exhibit much variation (40m) during the short observational period (4days).

On the other hand, top of the thermocline is found below 35m at deep stations (Figs.4.3(d-i)) during the entire observational period. In the central (Figs.4.3(f-i)) and at the two stations in the eastern Arabian Sea (Figs.4.3(d&e)), it continuously deepened from 40-75m and 35-120m respectively due to intense vertical mixing (Hastenrath and Lamb,1979) and sinking with the onset and
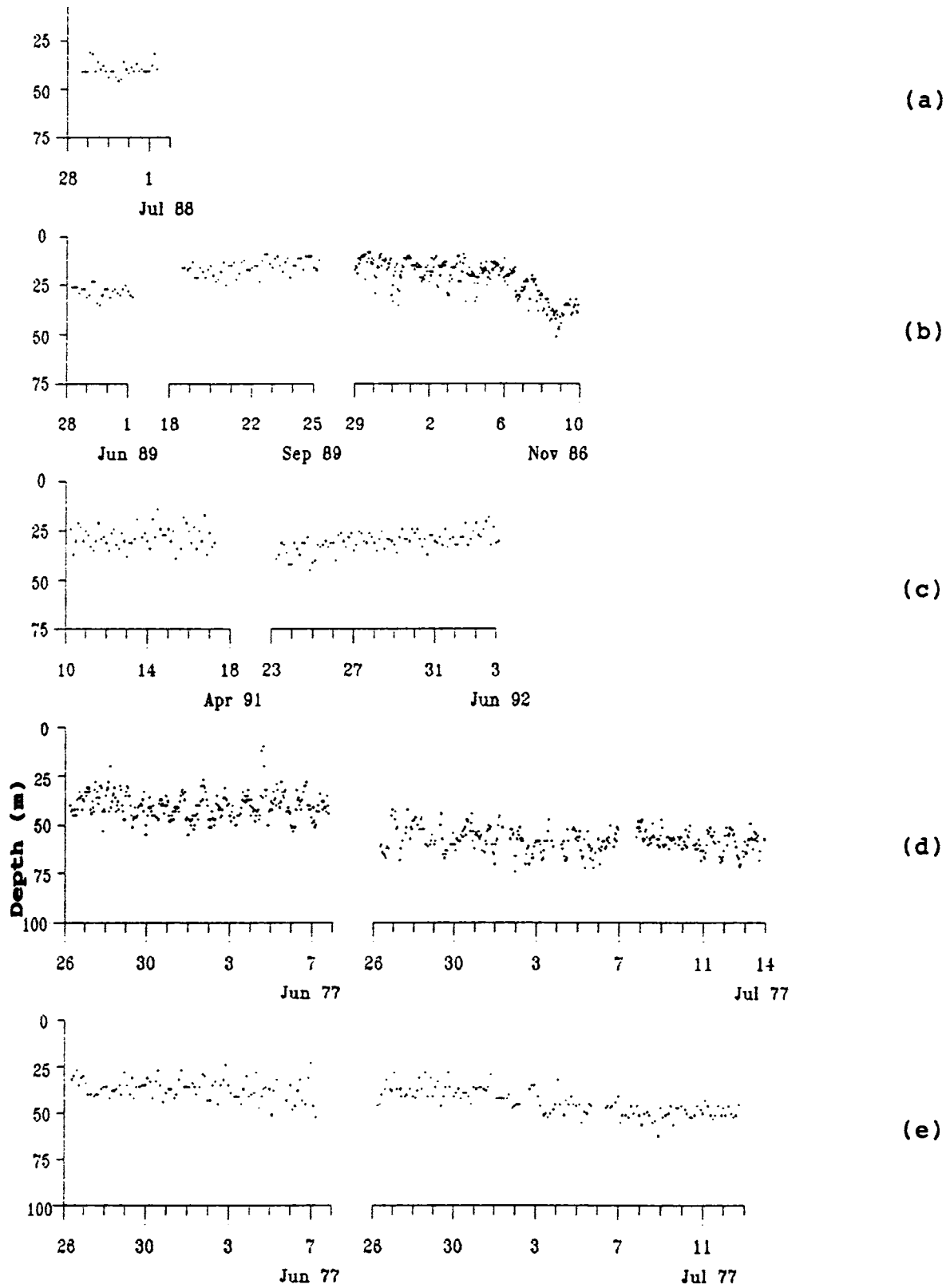
54

Fig.4.3 Time series of thermocline top at (a) BM   (b) KW
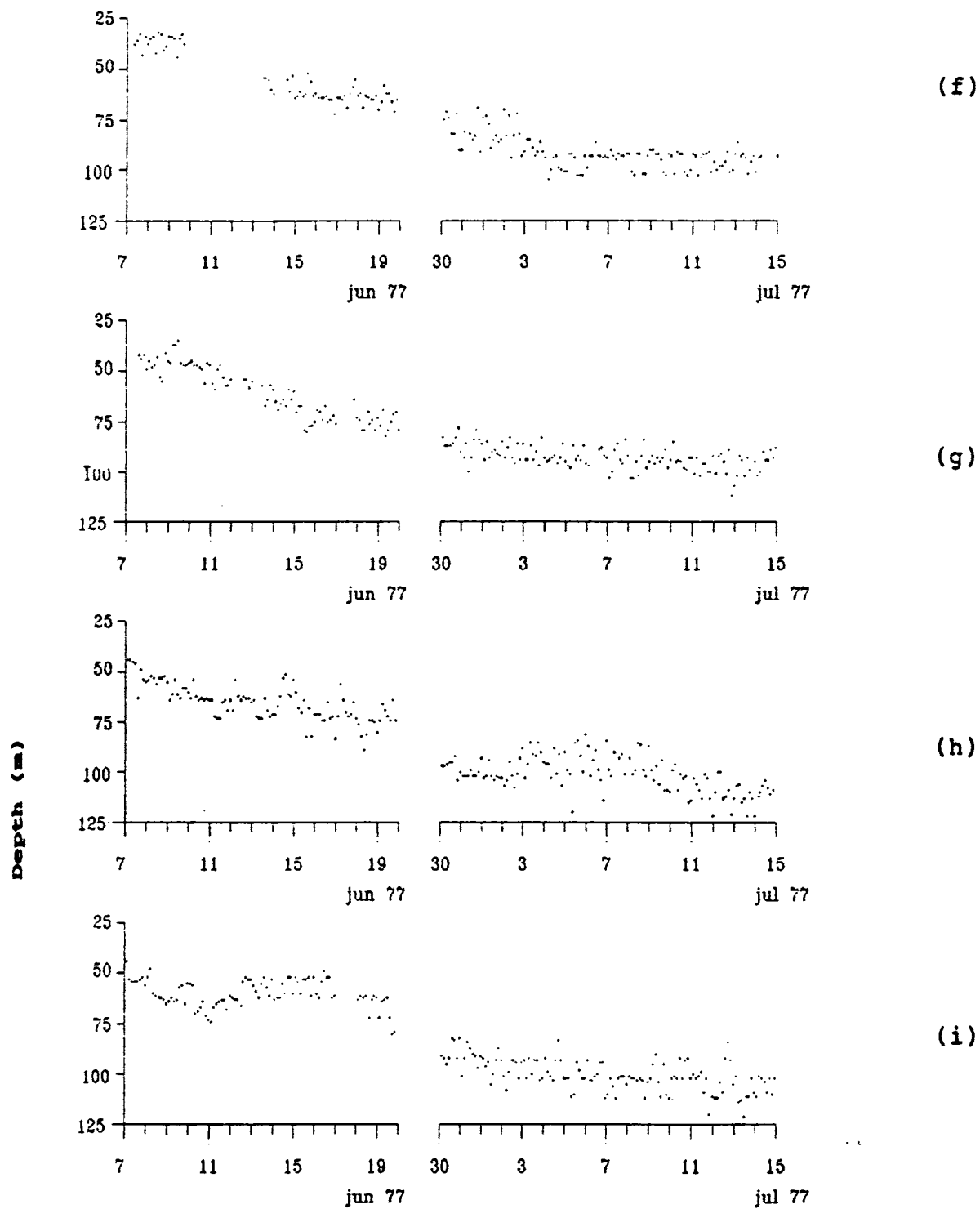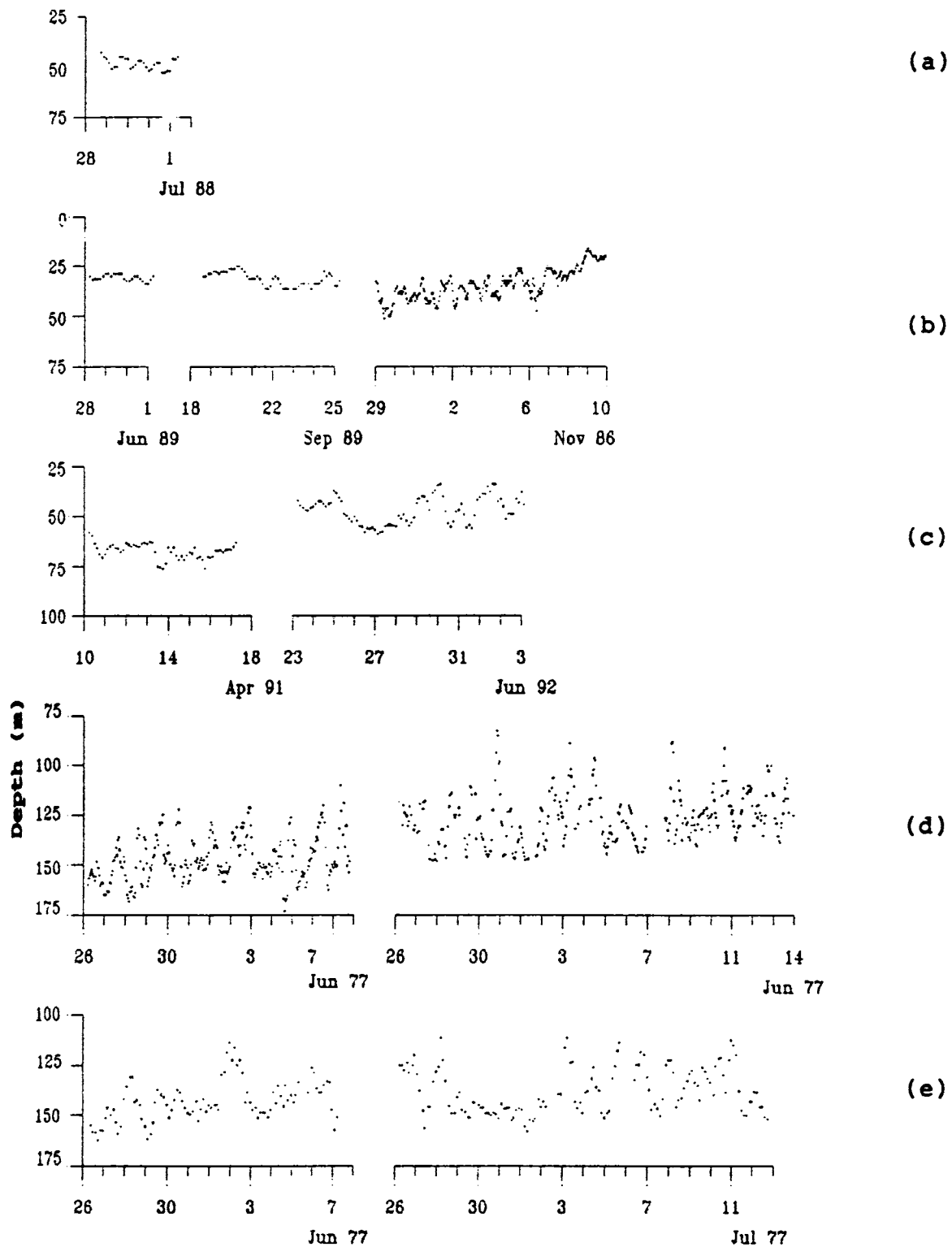(c) CH   (d) BS   (e) BW

Fig.4.3 Time series of thermocline top at (f) N (g) E
(h) S (i) W

progress of monsoon. During this period, top of the thermocline is observed at the deepest depth (>100m) in the central Arabian Sea compared to any other locations.

4.3.2.2 THICKNESS OF THE THERMOCLINE

Thickness of thermocline (Figs.4.4(a-i)) is minimum in the coastal zones. Even in the coastal regions marked variations are noticed between the southern (CH) and northern (BM) stations. The thermocline which was quite thick ($\simeq$ 70m) at CH in April (Fig.4.4c), gradually reduced to $\simeq$35m with the onset of monsoon (by June). The influence of upwelling is inhibited (the thermocline from surfacing) by the stabilising forces of buoyancy at both locations. While at KW it was around 30m during summer monsoon season. The increased current shears (Fig.4.6b) induced by the southerly surface currents (Hastenrath and Lamb,1979) and northerly undercurrent (Antony,1990; Hareesh Kumar and Mohan Kumar,1995) during the monsoon season erodes the thermocline forming a bottom iso-thermal layer. The combined effect of these two processes limits the thickness of the thermocline. At BM (Fig.4.4a) the thickness of the thermocline is 10m which is the minimum observed during this period.

On the contrary, thickness of the thermocline is greater than 100m at deep stations (Figs.4.4(d-i)) with maximum values noticed at N ($\simeq$ 220m). One of the noteworthy features is that the thermocline thickness gradually decreased with the progress of monsoon. The deepening of thermocline at these locations is caused by a variety of factors such as increased wind mixing, net heat loss at the surface, convergence due to negative wind stress curl (Hatenrath and Lamb, 1979) and entrainment at the bottom of mixed layer(Ramesh Babu and Sastry,1984). The convergence at

55

Fig.4.4 Time series of thermocline thickness at (a) BM (b) KW
(c) CH (d) BS (e) BW
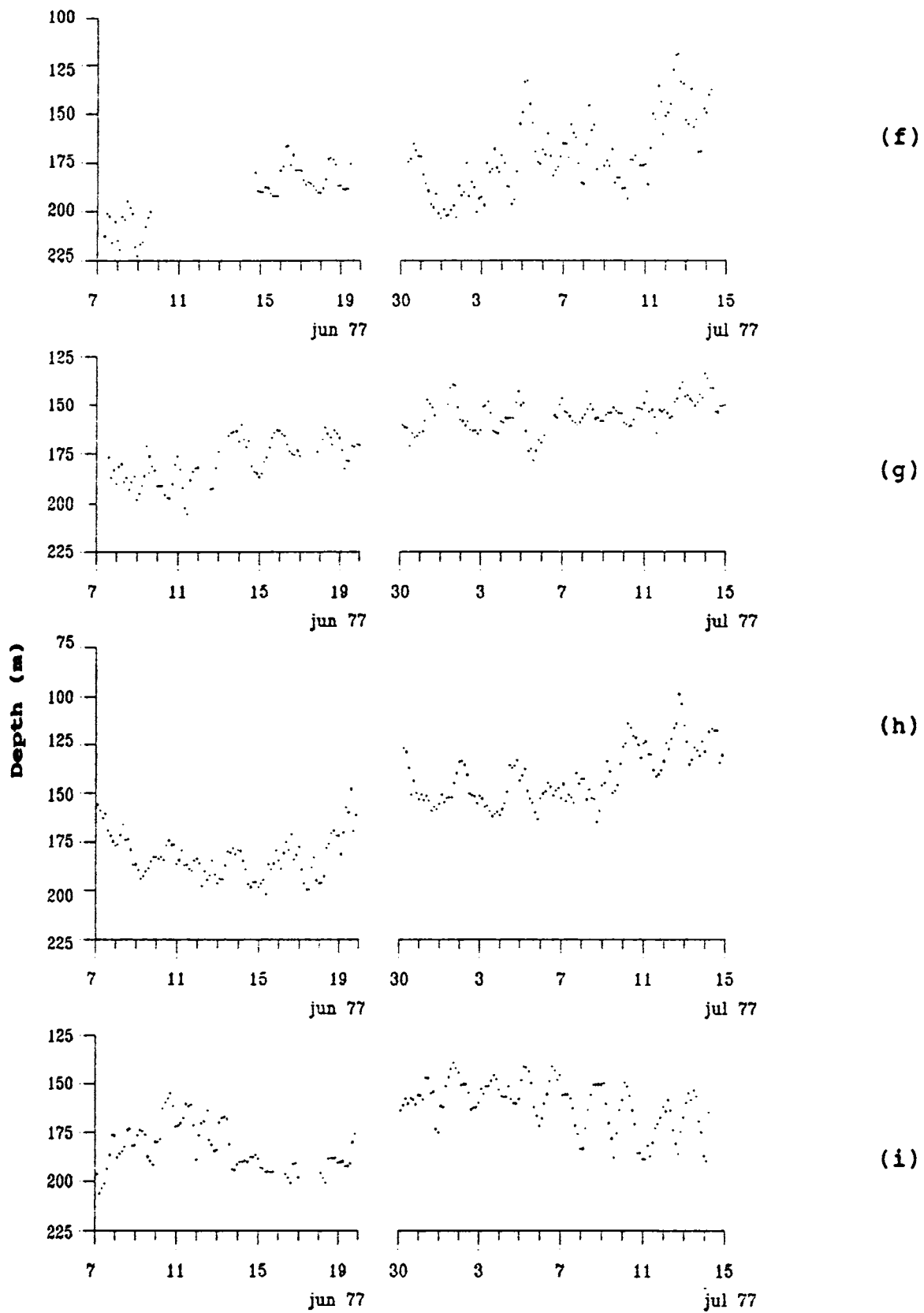
Fig.4.4 Time series of thermocline thickness at (f) N (g) E

(h) S (i) W

the upper layers is balanced by divergence at deeper layers (to maintain continuity) which erodes the bottom of the thermocline thereby reducing its thickness with the progress of monsoon. In the central Arabian Sea, maximum decrease in thickness is observed at N (220-120m) and minimum at W (200-150m). The corresponding values at E and S are 200-125m and 190-100m respectively.

4.3.2.3 THERMOCLINE GRADIENT

In general, the gradient is greater than $0.2^{\circ}C$ m^{-1} at the coastal stations (Fig.4.5(a-c)) except at KW in June and at CH in April and less than $0.1^{\circ}C$ m^{-1} at the deep stations (Figs.4.5(d-i)). The increased gradient in the coastal regions is due to the combined effect of upwelling which pushes the sub-surface waters towards the surface and net air-sea heat flux and wind mixing which inhibit its upward movement. The low gradients at the deep station is caused by the increased entrainment due to mixing of waters from upper thermocline and mixed layer (Philips,1977). The thermocline gradient more than doubled from pre-monsoon to active monsoon periods both at CH and KW. The thermocline gradient showed an increase from 0.1 to $0.15^{\circ}C$ m^{-1} in the central Arabian Sea. The thermocline gradient ($\cong 0.1^{\circ}C$) did not show much variation during both pre-monsoon and monsoon periods at BS and BW.

4.3.2.4 MIXING IN THE THERMOCLINE

Studies on mixing processes indicate that shear and static instabilities are the prime mechanisms governing the gradient in the thermocline (Miles,1961). As Richardson number (Ri) is the ratio of buoyancy to shear term, the thermocline stratification is studied in terms of Ri.

Fig.4.5 Time series of thermocline gradient at (a) BM (b) KW
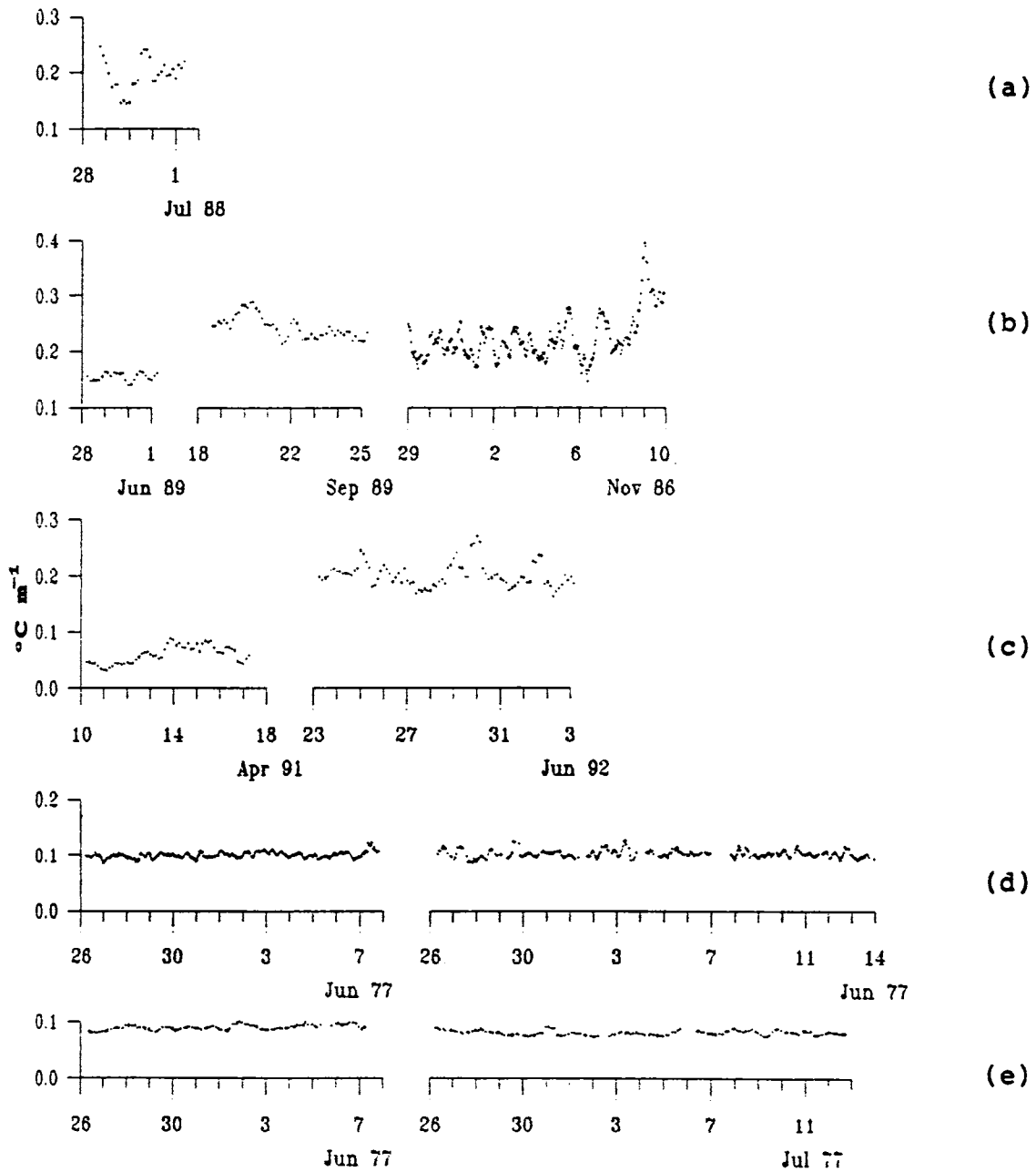
(c) CH (d) BS (e) BW
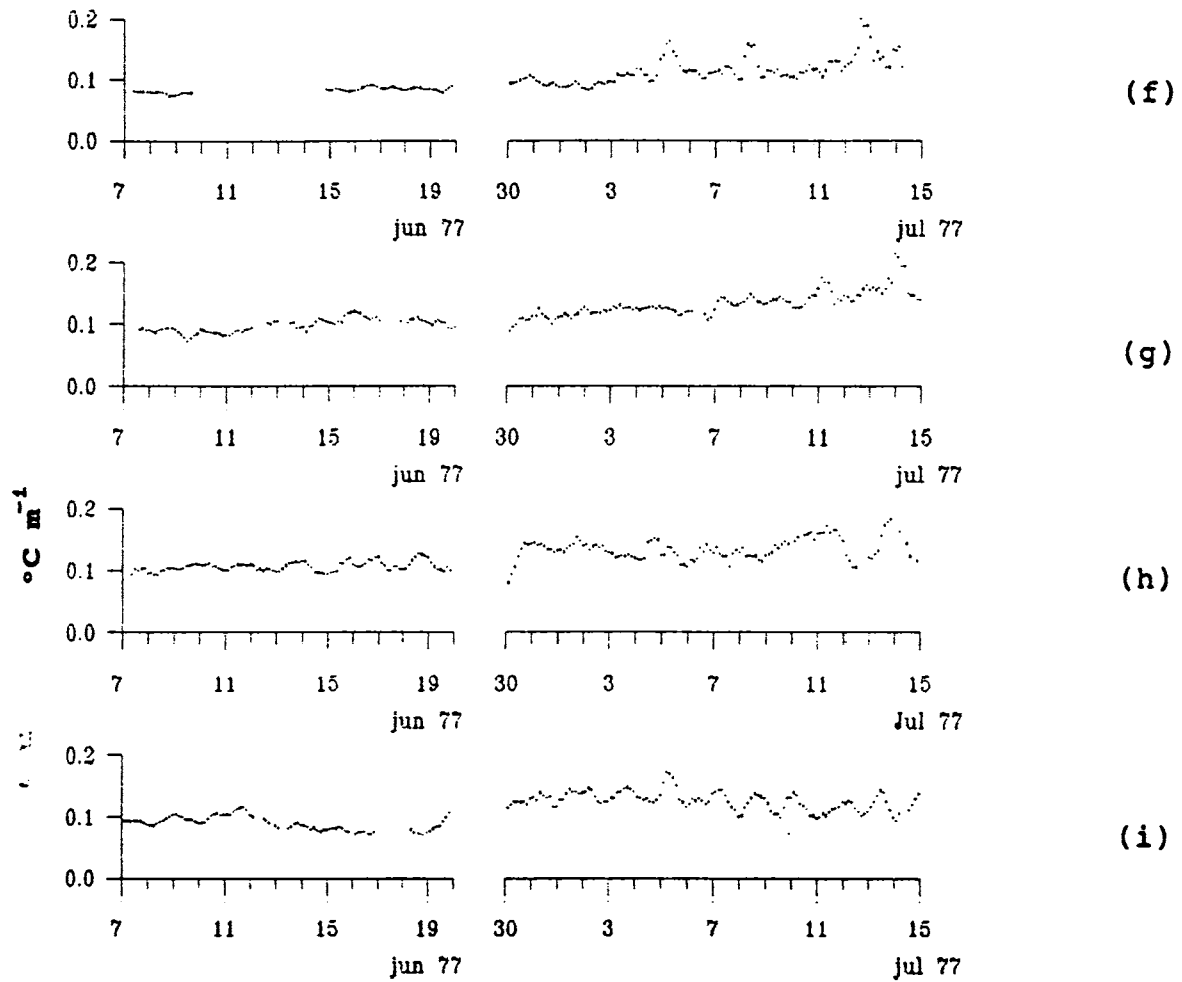
Fig.4.5 Time series of thermocline gradient at (f) N (g) E
(h) S (i) W

$$Ri = N^2 / S^2$$

where, N is Brunt-Vaisala frequency ($N^2 = -(g/\rho)(\delta\rho/\delta z)$) and S is the shear term ($S^2 = (\delta u/\delta z)^2 + (\delta v/\delta z)^2$)).

Laboratory and theoretical studies (Miles,1961) have revealed that high levels of turbulence and mixing are associated with low Ri (<0.25) and vice versa.

The Brunt-Vaisala frequency, which is a measure of static stability of the water column is maximum in the thermocline (15 cph between 65 and 85m in April and 18 cph between 30 and 50m in May-June at CH, 4.2 cph between 20 and 45m at BM during June/July and 17.6 between 15 and 60m and 28.8 cph between 15 and 40m at KW during June and September respectively) while, weak stratification is observed in the mixed layer and in the lower thermocline, i.e, in the region of undercurrent (< 6 cph). The depth ranges are chosen within the thermocline where current measurements are also available. The Shear and Ri in the thermocline at selected location are given in the table 4.2.

In order to obtain the nature of current at different levels, the current sticks off Cochin for April and May-June are presented in Fig.4.6a. In general, the currents were weak in the top 45m (10-20cm s^{-1}). The currents were stronger and opposing between 65 and 85m indicating a shear of 0.005 s^{-1}. However, the currents were stronger ($\cong 50$ cm s^{-1}) at all levels about 70m in June except between 23-28June at 30 and 50m. The drastic decrease of current speed from 30 to 50m between 23 and 28 June leads to large shear (0.025 S^{-1}). However the water column is statically stable during both the periods as indicated by negative $\delta\rho/\delta z$ (-0.03 to -0.09 kg m^{-4}). Further, there was a marked
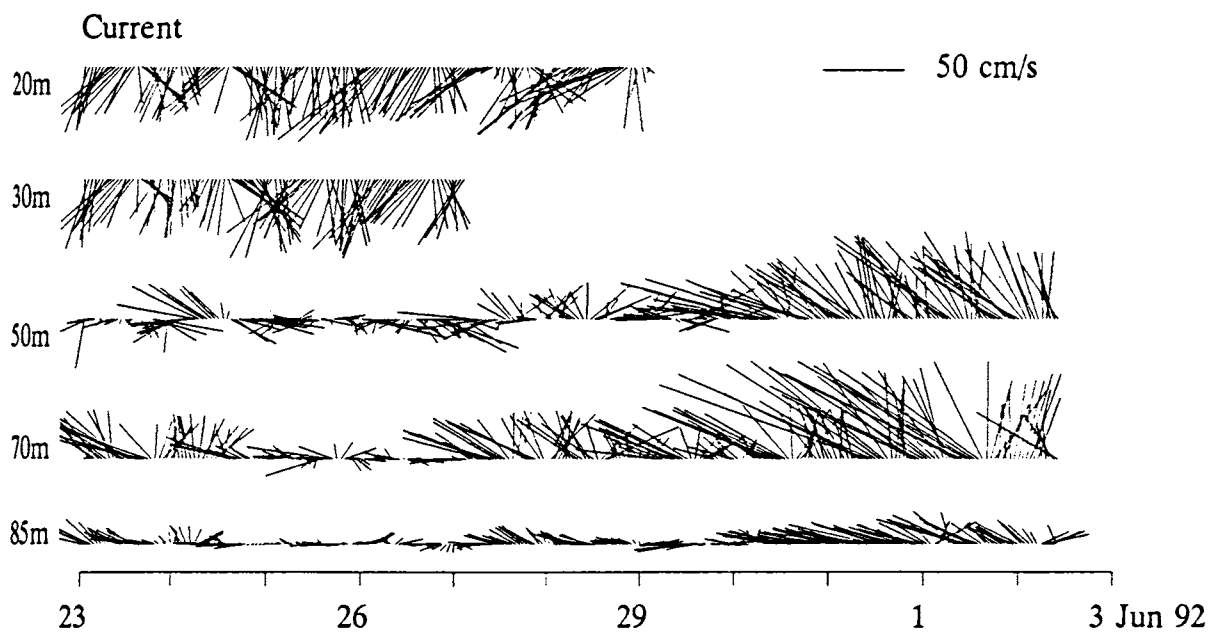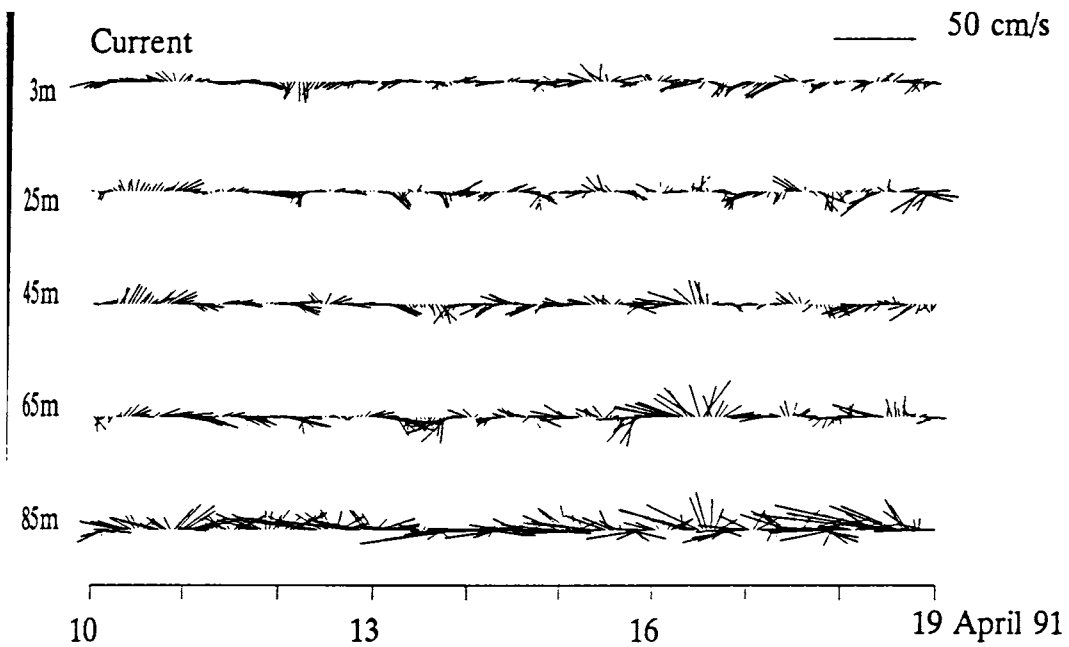
Fig. 4.6 Stick plots of sub-surface current at different levels

(a) April and May-June at CH
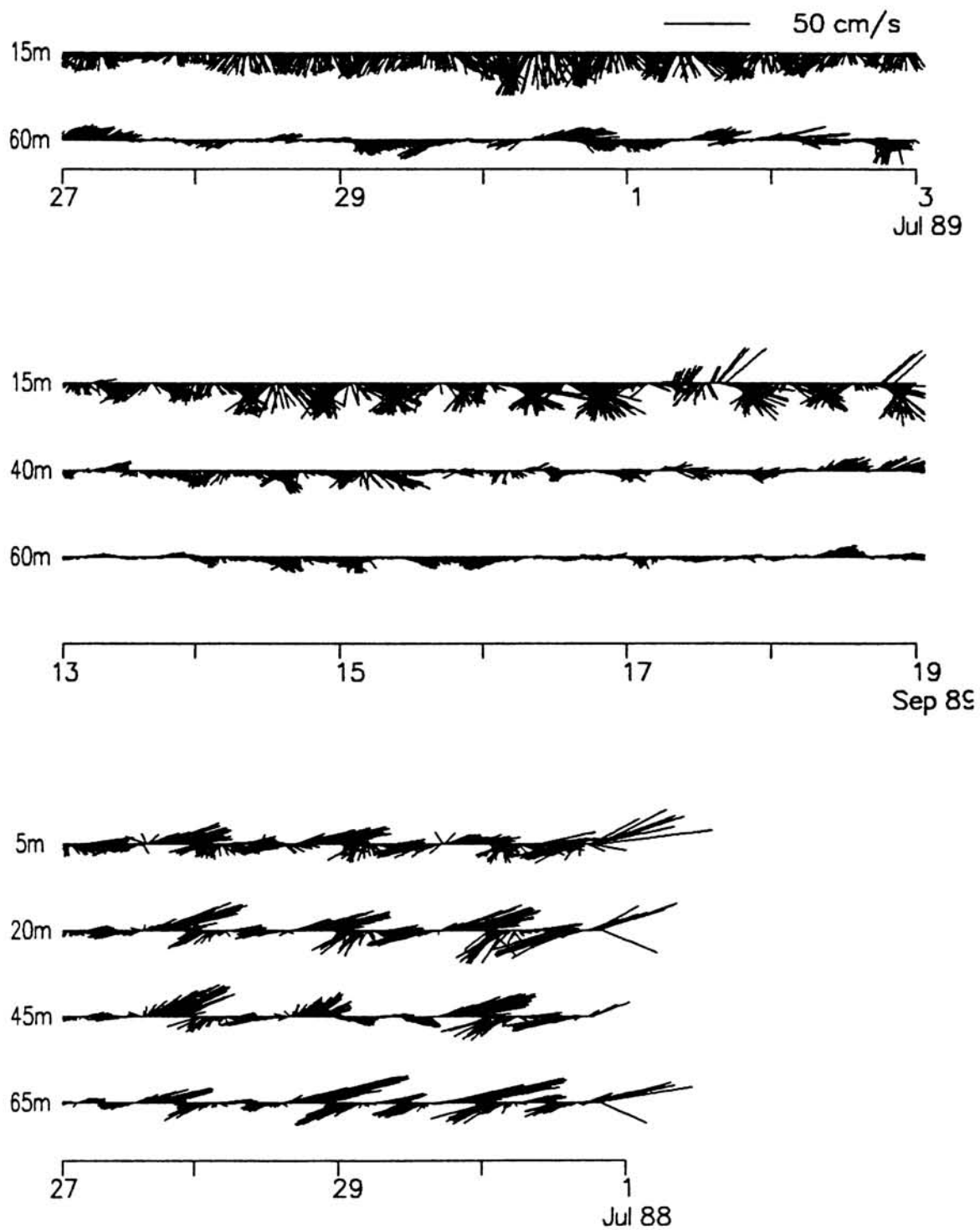
Fig. 4.6 Stick plots of sub-surface current at different levels
(b) July-September at KW   (c) June-July   at BM

reduction in thermocline gradient in the regions of undercurrent (>80m in April and >60m in May-June) due to strong shear. Since undercurrent strengthens with the progress of upwelling and it flows opposite to the currents above (Fig.4.6a), a secondary maximum in S is observed. Low Ri in this zone favoured the growth of turbulence and mixing process thereby reducing the vertical temperature gradient (Fig. 4.2c).

The current of KW could be obtained only at 15 and 60m during June while it was observed at 15,40 and 60m in September. The currents were less stronger and more oscillatory at 60m compared to 15m in June. From the current sticks (Fig.4.6b) at KW it is evident that the current strength decreased with depth in September indicating increased shear. At KW, the strong shear (0.008 s^{-1} in September) is noticed in the thermocline compared to other levels. In June, a low Ri (0.075) revealed increased turbulence, resulting in the weakening of thermal stratification. However, in September Ri (>0.29) indicated suppression of turbulence in the water column, suggesting a strong thermocline stratification, caused by the process of upwelling.

The current sticks at BM (Fig 4.6c) revealed nearly uniform currents at all levels)5m,20m,45m and 65m) with speed 30-40cm s^{-1}. At BM, though the shear in the thermocline is found to be 0.00099 s^{-1} and the high value of Ri (7.4) revealed suppression of turbulence in this region. This suggested that the vertical density gradient is sufficiently strong to overcome the instability caused by the flow. As a result, the three layer structure in this region is maintained throughout the observational period.

Table 4.2

Average shear (S), Richardson number (Ri) and Brunt-Vaisala frequency (N) at selected locations.

Observation location	Depth levels (m)	S (s^{-1})	Ri	N (cph)
BM (Jun.)	20-45	0.00099	7.400	4.2
KW (Jun.)	15-60	0.00490	0.075	17.6
KW (Sep.)	15-40	0.00800	0.290	28.8
CH (Apr.)	65-85	0.00500	0.200	15.0
CH (Jun.)	30-50	0.02500	0.050	18.0

4.3.2.5 SPECTRAL CHARACTERISTICS OF OSCILLATIONS IN THE THERMOCLINE

The thermocline zone is a region of large oscillations (Figs.4.2(a-i)) with frequencies ranging from Brunt Vaisala to inertial. To identify significant harmonics in the thermocline, the time series of the depth of $25^{\circ}C$ isotherm was subjected to FFT analysis . The analysis were carried out at CH and BS representing coastal and deep stations during pre-monsoon and monsoon phases (Figs.4.7(a-b)). The most dominant harmonics noticed at all locations are inertial, diurnal and semi-diurnal, though with varying spectral magnitudes. In addition to these periodicities, high frequency oscillations are also observed in the thermocline. In general, diurnal and semi-diurnal components contain maximum energy during pre-monsoon phase at CH (Fig. 4.7a) and BS (Fig.4.7b) while, the inertial components have maximum energy during the monsoon phase. This can be attributed to the fact that during monsoon phase, more energy is utilised to disturb strong thermocline
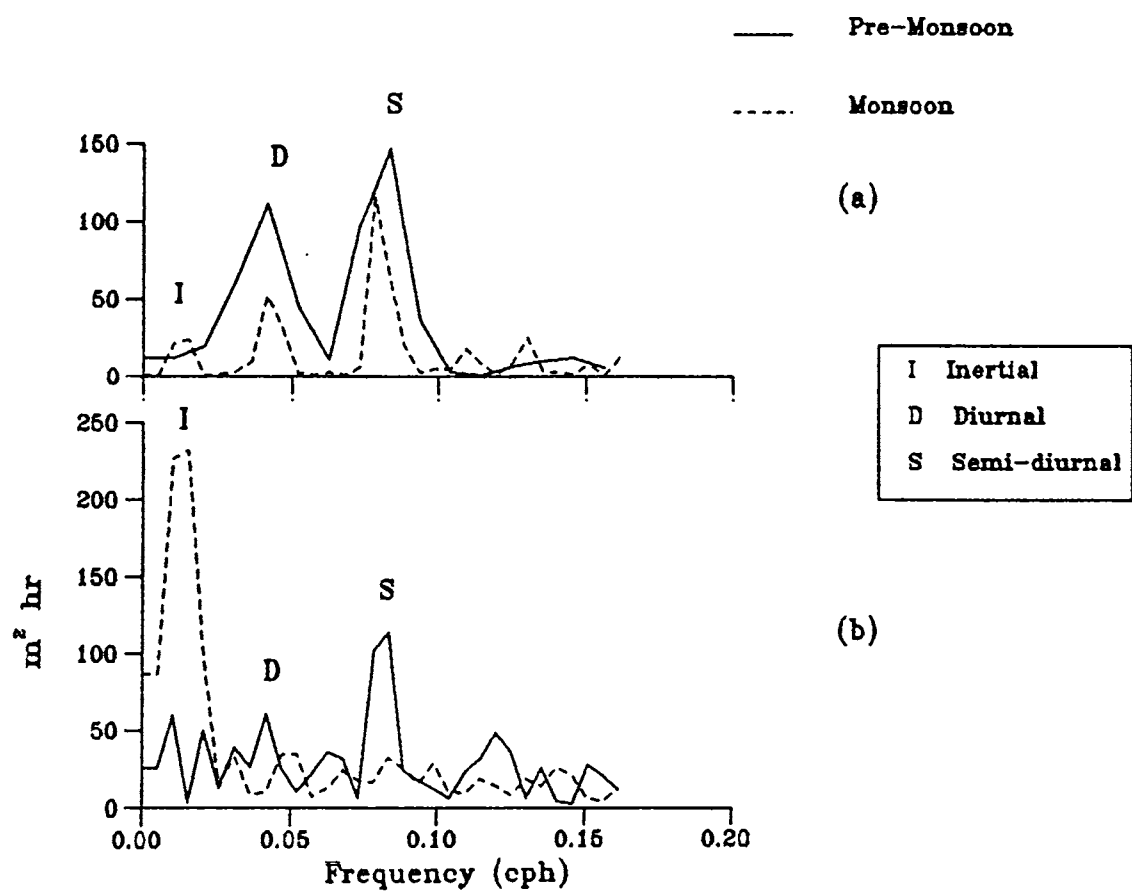
Fig. 4.7 Spectral density of the depth of $25^\circ C$ isotherm at (a) CH
(b) BS

stratification (Fig.4.2b). Moreover, the inertial oscillation (70.9 hrs at CH;53.3 hrs at BS) noted during the summer monsoon phase, is absent (Fig.4.7a) or weak (Fig.4.7b) during pre-monsoon. This can be due to the fact that, during the monsoon phase, the strong winds blow in pulses, which is favourable for the generation of inertial oscillations. The diurnal and semi-diurnal component contain more energy in the coastal region mainly caused by the internal tides during the pre-monsoon phase.

CHAPTER V

INFLUENCE OF OCEANIC INHOMOGENITIES ON SOUND PROPAGATION
-SOME CASE STUDIES

5.1 INTRODUCTION

5.1.1 Oceanic inhomogenities and acoustics

In reality, the ocean is an extremely complex and variable medium. In such a complex environment more complex models of propagation incorporating statistical characteristics of the variations might be necessary to obtain reliable predictions of the sound field. Ocean currents, internal waves and small-scale turbulence perturb the horizontally stratified character of the sound speed and cause spatial and temporal fluctuations in sound propagation. Boundaries of large currents, such as the Gulf Stream and Kuroshio, represent frontal zones separating watermasses with essentially different characteristics. Within these frontal zones, temperature, salinity, density and sound speed suffer strong variations and hence the acoustic propagation (Levenson and Doblar,1976). Large eddies in the ocean are mostly observed near intense frontal currents. The parameters of synoptic eddies vary over rather wide range. The diameter of an eddy ranges from 25 to 500km. Analysis of propagation studies through a cyclonic Gulf Stream eddy revealed considerable variations in the propagation conditions (Vastano and Owens, 1973). Considerable fluctuations of the intensity and phase of sound waves arise in the presence of internal waves (Stanford,1974). We know that such characteristics of the

ocean water as salinity, temperature, density, and current velocity do not vary smoothly with depth, but in discontinuous fashion. Such fine layered structure leads to multipath of sound transmission and hence cause additional fluctuations of phase and amplitude to the sound signal (Stanford,1974). Thicknesses of these layers typically vary from tens of centimetres to tens of metres.

From the previous chapters it is inferred that the thermocline characteristics at deep and shallow regions in the Arabian Sea are influenced by a number of oceanographic phenomena namely meso-scale eddies, internal waves, upwelling, sinking, undercurrent etc. These processes result in the formation of various thermocline features such as step structures, sharp vertical gradient and bottom quasi-homogeneous layer with varying thermocline gradient and thickness. In association with the temporal and spatial variabilities in the thermocline one can expect fluctuations in the amplitude and phase of acoustic signals transmitted through the medium.

In the present study, some of the typical thermocline features identified from the previous chapters are used to delineate their role on acoustic propagation. A range-dependent numerical model is used for the simulation of propagation conditions.

5.1.2 DESCRIPTION OF THE MODEL

The basis of all the theoretical models of underwater sound propagation is the wave equation.

$$\nabla^2 \phi = \frac{1}{c^2} \cdot \frac{\partial \phi^2}{\partial t^2}$$

62

where ∇^2 : Laplacian operator, ϕ :Velocity potential, c : speed of sound and t: time

The parabolic equation to the wave equation is of the form

$$\frac{\partial^2 p}{\partial z^2} + 2ik_o \frac{\partial p}{\partial r} + k_o^2 (n^2 - 1)p = 0$$

where n : refraction index which is a function of depth(z), range(r) and azimuth(θ), p : pressure field (function of range and depth), k_o :reference wave number (ω/c_o), ω :source frequency and c_o : reference sound speed.

This equation is numerically solved by implicit finite difference technique (Lee and McDaniel,1988) which is a *marching solutions*. An advantage of this solution is that the calculation necessarily includes many receiver depths and is therefore the results are directly suitable for contouring.

The parabolic equation model (PE-IFD) is quite distinct from the other two main classes of models that are commonly used. The ray theoretical models are based on the assumption that acoustic wavelengths are small enough so that diffraction effects are negligible. The normal mode model is based on the approximation that the ocean is horizontally stratified so that coupling between the waveguide modes is negligible. The PE-IFD model retain these two so that it is valid to much lower frequencies and for more realistic, non-stratified oceans.

This model is used for computing acoustic propagation loss in both range-dependent and range-independent

environments. An important feature of this model is that it can handle arbitrary surface boundary conditions and an irregular bottom with arbitrary bottom boundary conditions. Another important feature of the model is that it can handle horizontal interfaces of layered media.

The inputs to the model are frequency (Hz), source depth (m), receiver depth (m) and range (m) as operational parameters. The environmental inputs are sound speed (m s^{-1}) profile, water depth (m), density (g/cc) atttenuation (dB/wave length) in the water and sediment layers. Reference sound speed and depth/range step sizes are the tuning factors of the model. The usual step sizes are one-fourth of a wave length and half wave length in depth and range respectively.

The model output is the transmission losses to the specified points in the depth-range plane. The model was implemented and validated using the transmission loss measurements made during an acoustic experiment off Cochin (Balasubramanian and Radhakrishnan, 1989;1990). They found good agreement between the experimental and simulations using the model.

The model described above is applied to simulate the propagation conditions under different oceanic environments. Several studies were carried out for the range-dependenet environments for other oceanic regions (Davis et al.,1982). The propagation under range-dependent scenario is not reported for Arabian Sea. This aspect is investigated using the PE-IFD model for a wide variety of oceanic features such as layered micro-structure, internal waves and eddy in the following sections.

To delineate the effect of the water born features, the influences of surface and bottom boundaries are kept minimum in the model. A pressure release sea surface is assumed so that the fields will vanish at the surface. An artificial absorbing bottom (Lee and Mc Daniel, 1988) was also assumed in the model to minimise the bottom effect.

5.2 THERMOCLINE AS AN ACOUSTIC BARRIER

As sound propagates, its energy gets refracted in water column depending on the prevalent sound speed gradients. Strong refractions and hence changes in the insonification pattern occur as the relative position of the source/receiver changes. In the ocean vertical gradient are more compared to horizontal. Most commonly large sound speed gradients occur in the thermocline region which in effect can act as a barrier for the sound energy propagating across it. For a given sound speed gradient in the thermocline, refraction increases with increase of the thickness of thermocline. Similarly, for a given thermocline thickness, higher the sound speed gradient higher the refraction. An important feature associated with this kind of refraction is the formation of shadow zones beneath the thermocline depth, which occur for a high frequency sound located near the sea surface.

The results in previous chapters indicate that the gradients and thickness of thermocline change drastically on climatic and synoptic time scales. The variations in gradient is of the order of $0.05^{\circ}C$ m^{-1} to $0.14^{\circ}C$ m^{-1} on climatic scale whereas it is of the order of $0.05^{\circ}C$ m^{-1} to $0.3^{\circ}C$ m^{-1} in the synoptic scale. Similarly, the thermocline thickness varies from 40 to 100m and 10 to 190m on synoptic and climatic scales respectively. Correspondingly, the

65

Source depth : 5 m Freqency : 2000 Hz

☐ <70 dB　　　▨ 70-80 dB　　　■ >80 dB
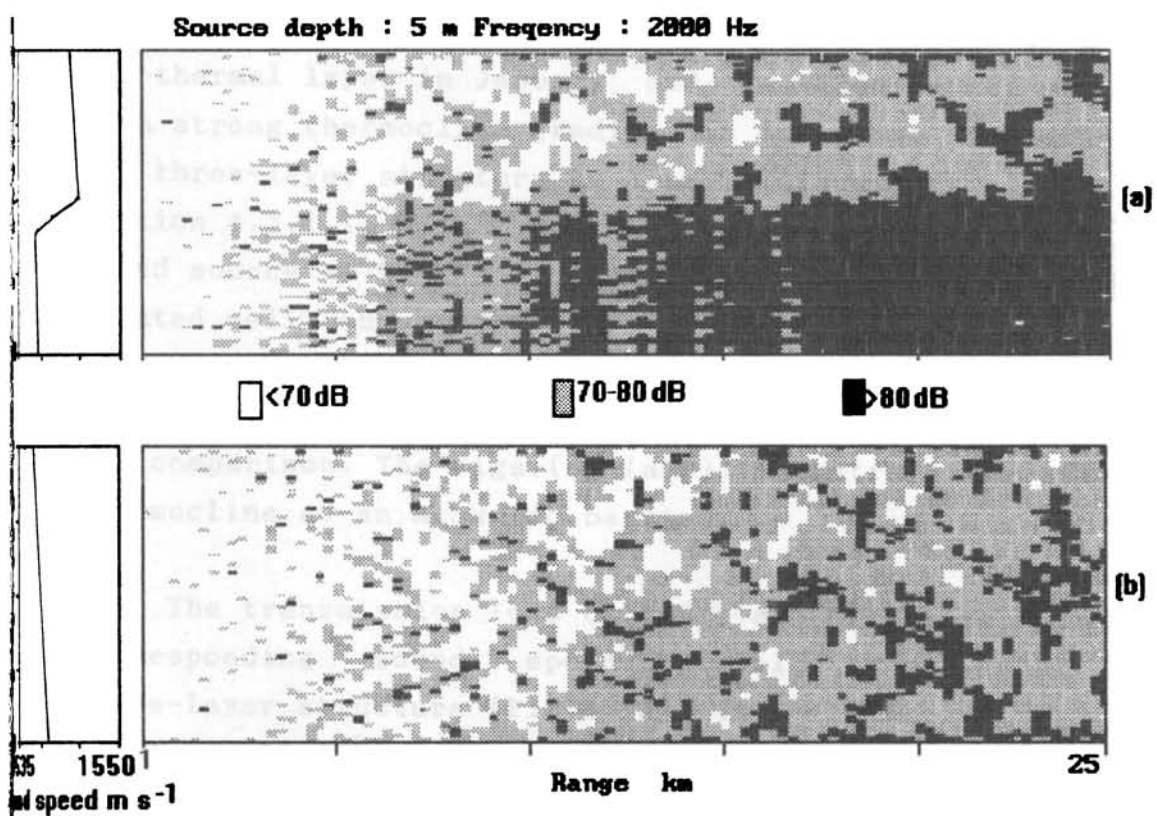
1535　1550

und speed m s⁻¹

Range　km

Fig.5.1 Iso-loss contours determined by PE-IFD model
(a) water column having thermocline
(b) water column having near iso-thermal condition

shadow zone variability also will be more.

5.2.1 MODEL SIMULATIONS OF TRANSMISSION LOSS

To simulate the sound propagation for different
thermocline structure, two typical profiles are identified
in the regions off Bombay (18°50'N, 71°35'E; depth <80m)
during January and June. Temperature profiles were obtained
using MBT. The thermal structure is characterised by a near
iso-thermal layer in January and a three-layer structure
with strong thermocline gradient in June. The formation of
the three-layer structure in June is discussed in detail in
Section 4.3.1.1. Model runs were performed by choosing a
sound source of 2 kHz frequency at 5m depth, which is
located well above the thermocline. A range-independent
environment is assumed for the computations. The
transmission loss contours for these two cases are presented
for comparison. The Figs.(5.1(a&b)) illustrate the effect of
thermocline as an acoustic barrier..

The transmission loss contours are presented along with
corresponding sound speed profiles containing the
three-layer structure (Fig.5.1a). The thermocline gradient
is strong (0.25°C m^{-1}) and found at a depth of 40m. The
transmission loss contours show significant difference above
and below the thermocline depth. The transmission loss
increases slowly with range above thermocline depth, whereas
it increases rapidly below it. This indicate that the energy
below thermocline is very less compared to above it.
Similarly, the profile without thermocline and corresponding
transmission loss contours are presented in Fig.5.1b. Unlike
the other case, this contours show that the transmission
loss increases slowly with range for the entire water
column. For instance, the 80dB contour found at a range of

11km below thermocline(70m), which is absent at same depth (where the loss is about 70dB) in the near isothermal case. This clearly indicates that the energy available below thermocline is very much limited for an acoustic source above thermocline. Moreover, a well marked shadow zone (transmission loss >80dB) is present below thermocline depth from 11km onwards, which is absent in the other case. The model runs were performed with the source below thermocline also indicated similar results. This suggests that thermocline act as an acoustic barrier for the passage of energy across it.

5.3 LAYERED OCEANIC MICROSTRUCTURE

Studies conducted by several authors indicate that the high frequency sound propagation is drastically affected by small scale oceanic features like inversions, step like structures, etc. (Melberg and Johannessen,1973; Ewart,1980; Unni and Kaufman,1983). This is mainly due to the fact that the inhomogeneities in the oceanic environment cause scattering and hence loss of energy for the transmitted signal. A recent study of Hareesh Kumar et al.(1995) clearly indicated the presence of step like structures in the thermocline in the Arabian Sea. The study also brought out sharp sound speed gradient associated with these step like structures.

During the 101th cruise of FORV *Sagar Sampada* fine scale measurements of temperature and salinity at close depth intervals (using Seabird CTD system; accuracy $\pm 0.001^{\circ}C$) were made in the coastal waters of Cochin ($9^{\circ}75'N;75^{\circ}75'E$) from 23 May to 3 June 1992. Vertical profiles of temperature and salinity are characterised by multiple subsurface maxima in salinity corresponding to the

Temperature (°C)

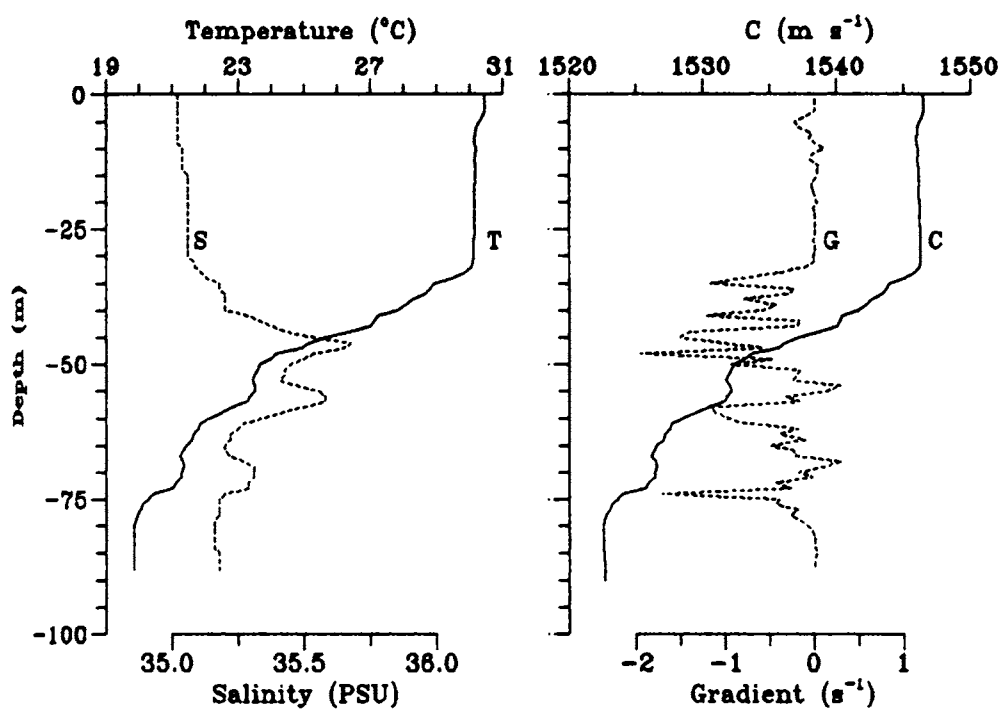19   23   27   31   1520   1530   1540   1550

C (m s⁻¹)

Fig.5.2 Vertical profiles of temperature, salinity, sound speed and sound speed gradient showing micro-structure in the thermocline.

thermocline region (Fig.5.2). These maxima are separated by
pockets of low saline waters. Vertical separation between
these multiple maxima varies from 10 to 15 m and their
salinity progressively decreased with increasing depth.
Among these, the upper maximum is more pronounced. The
occurrence of the multiple maxima mostly coincided with the
reversal of flow from southerly to northerly at 50m (Hareesh
Kumar et al.,1995). Thus the prevailing flow pattern may be
mainly responsible for the formation of multiple maxima.
Temperature and salinity values of these maxima corresponds
to 23.5 kg m^{-3} sigma-t surface, which is obviously the
Arabian Sea High Salinity Watermass. Below the subsurface
maxima, salinity reduced by 0.3 PSU (35.7 to 35.4 PSU). It
is interesting to note that in association with the
occurrence of these multiple maxima, either inversions ($\simeq$
0.2°C) or step like structures (5 to 10m thickness) are
noticed in the temperature field (Fig.5.2).

The temperature profile containing step structure in
the thermocline and the corresponding salinity profile
consisting of multiple maxima are used in computing the
sound speed profle (Fig.5.2). A surface layer of near
iso-speed conditions (the sonic layer or surface duct), of
about 35 m is noticed. In the thermocline, sound speed
varied from 1525 to 1546 m s^{-1}. The sound speed gradients
(Fig.5.2) exhibited rapid fluctuations within the
thermocline (-2 to 1 s^{-1}) caused by thermal inversions and
multiple subsurface salinity maxima. The positive gradient
in sound speed, caused by the advection of warm and low
saline waters, coincided with the depths of multiple maxima.

5.3.1 MODEL SIMULATIONS OF TRANSMISSION LOSS
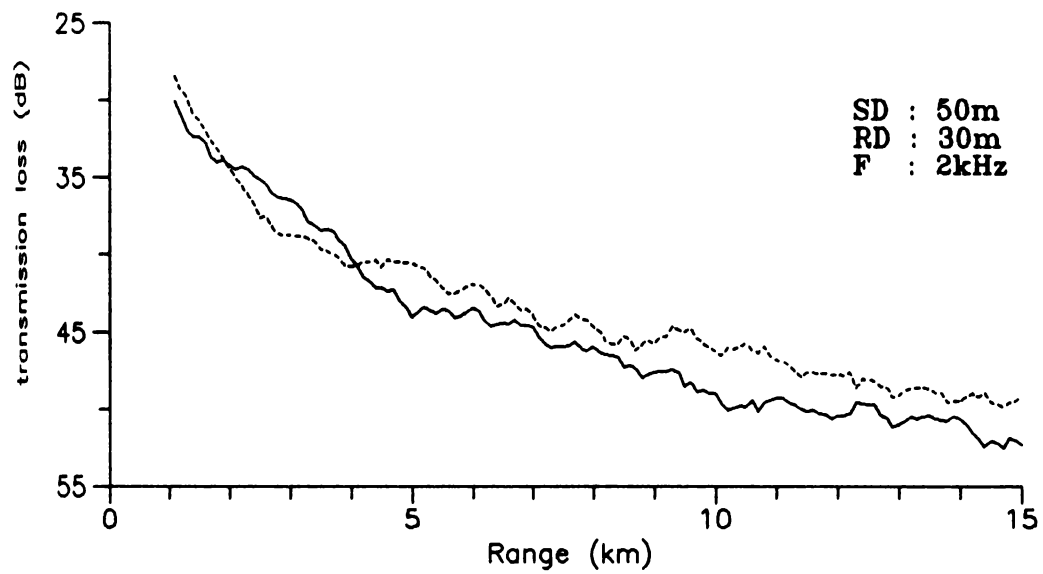
The influence of this layered micro-structure upon

Fig.5.3 Propagation loss versus range from PE-IFD model for
the thermocline with (continuous line) and without
(dash) microstructure.

sound propagation is dependent on the sound speed gradients, the physical size and dynamics of the microstrucutre. As the vertical dimensions of the fine structures were of the order of 1 to 10m (Fig.5.2), their variability would be expected to affect sound scattering in frequency ranges from approximately one to tens of kilo hertz. This would lead to loss of coherence and fluctuations in phase and amplitude in the acoustic signals which in turn will degrade the performance of high frequency systems. This stresses the importance of the inclusion of the fine structure variations in acoustic propagation modelling.

A sound source of 2kHz frequency located (50m depth) within the thermocline where the layered micro-structure is seen, is used for transmission loss simulation. The sound speed gradient in this region show maximum fluctuations. The transmission loss values are simulated using the model. To delineate the effect of micro-structure, the transmission loss values are also simulated for the profile with smoothed microstrcture. The transmission loss with range (Fig.5.3) are presented for a receiver within the sonic layer (30m). This show the intensity fluctuation due to microstrcture in the thermocline. The transmission loss due to micro-structure in the thermocline is appreciably higher (2 to 4 dB)than the other case without micro-structure. However, for the ranges of 2km to 4km a reverse trend is noticed. This suggests the importance of fine structure in temperature and salinity on high frequency sound propagation.

5.4 INTERNAL WAVES

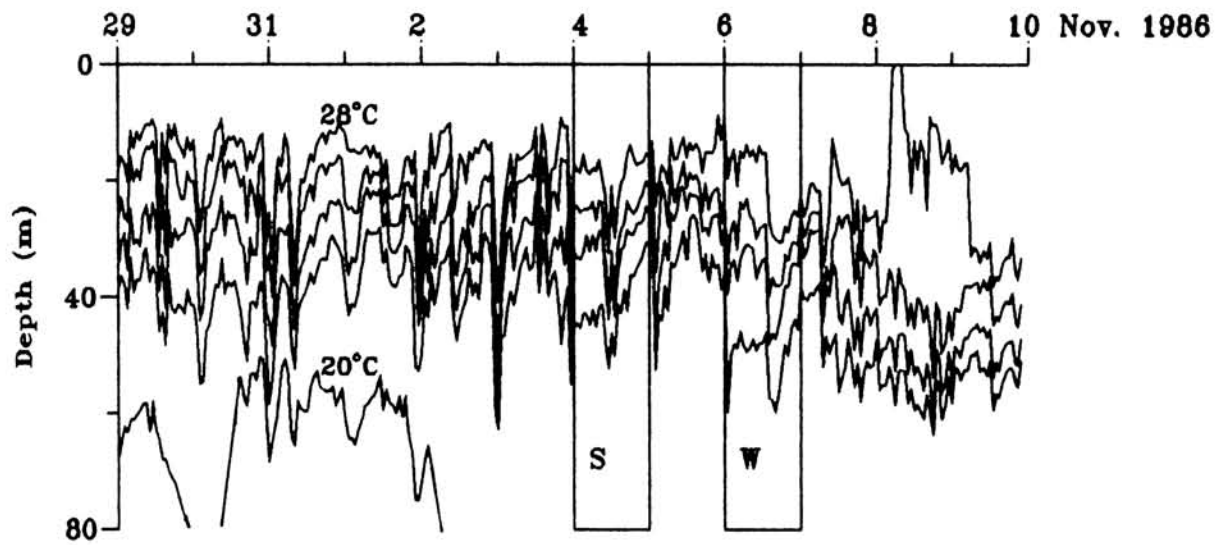Previous studies indicated that the internal waves have got profound influence on acoustic propagation (Lee,1961;

Fig.5.4a Passage of internal waves past a stationary observation point as evidenced by temporal fluctuations in isotherm patterns.

Frequency response curve
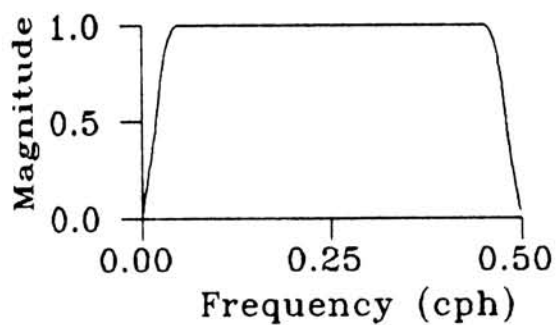
Fig.5.4b Freqency response curve of the Yulwalker digital filter design.

Porter et al.,1974; Baxter and Orr,1982; Murthy and Murthy,1986; Pinkel and Sherman,1991). This aspect was not studied for the Arabian Sea, though several studies (Varkey,1980; Murthy et al.,1992; Rao et al.,1995) reported the dominance of internal waves in this region. Hence, an attempt is made to analyse influence of internal waves on acoustic propagation based on observations and model simulation of transmission loss for this environment.

An oceanographic experiment was conducted off Karwar, west coast of India during October-November 1986 in order to study the internal wave activity. Measurements were carried out onboard RV Gaveshani, which was anchored at $15^{\circ}01'N$ and $73^{\circ}21'E$ (depth $\simeq$ 90m) for a period of 12 days (29 October to 10 November, 1996). Vertical profiles of temperature were collected using a TSK Micom Bathythermograph (accuracy :$\pm 0.05^{\circ}C$) at hourly interval. The salinity data was obtained from hydrocasts taken once a day. During the experiment, a deep depression was formed in the vicinity of the observational point. Under the influence of this deep depression, the convergence induced at its periphery caused deepening of thermocline (Fig.5.4a). FFT analysis of temperature at different depth levels revealed low frequency harmonics (lower than inertial, $\simeq$ 46 hrs), which was induced by the continuous deepening of the thermocline. To remove this low frequency component, the temperature data set is high pass filtered using a Yulwalker digital filter. The frequency response of the digital filter is shown in Fig.5.4b.

In order to identify oscillations in the thermocline, the isotherm within the thermocline are subjected to FFT. The most dominant harmonics are inertial (46 hour), diurnal (24 hour) and semi-diurnal (12 hour). The harmonics of the
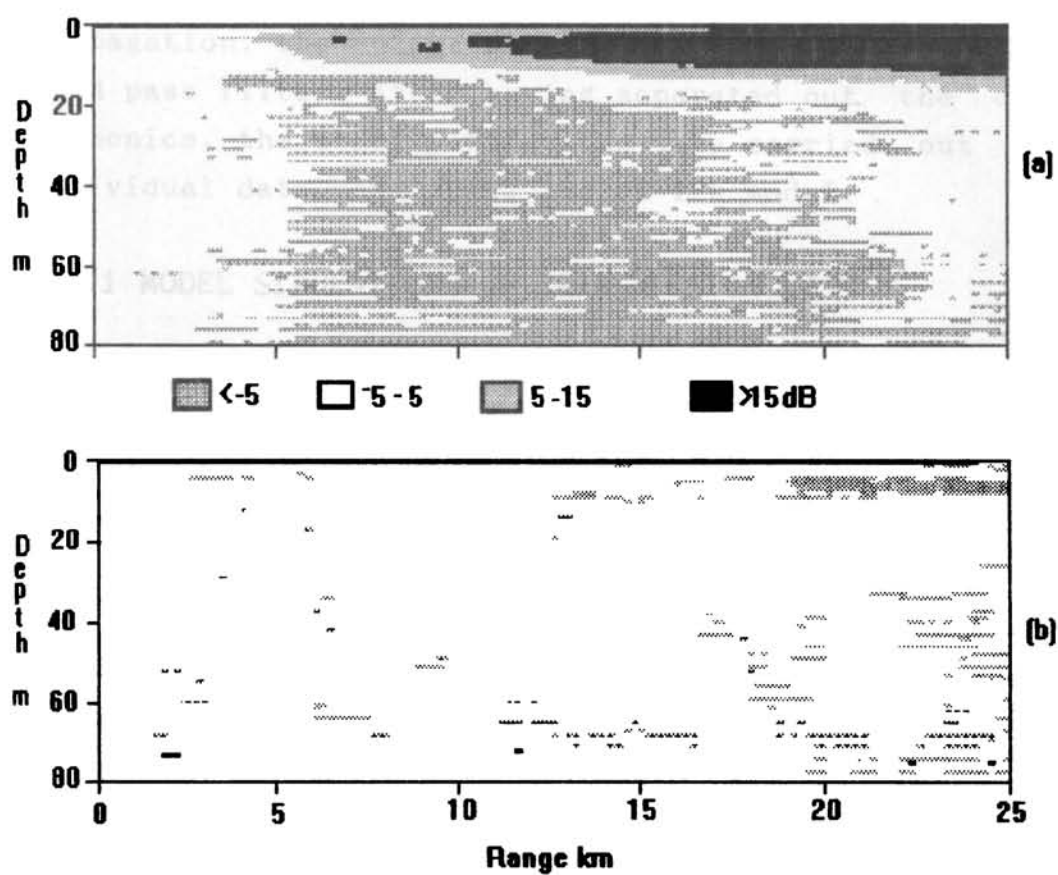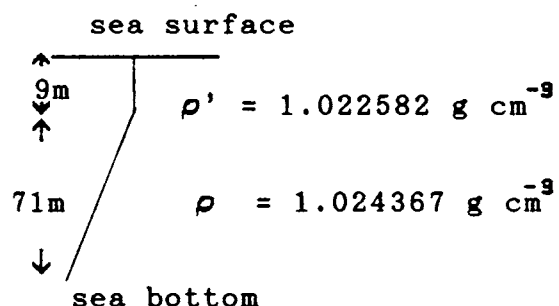
Fig.5.5 Intensity fluctuations due to internal wave fields
(a) strong internal wave field (b) weak internal
wave field

inertial periodicity are generated by storm-induced wind field. Pollard (1970) also has observed inertial oscillations in connection with a sudden change of the wind speed and rapid changes in barometric pressure. In order to identify the influence of different harmonics on sound propagation, the entire data set is subjected to Yulwalker band pass filter. After having separated out the different harmonics, the model simulations were carried out for the individual data sets using the PE-IFD model.

5.4.1 MODEL SIMULATIONS OF TRANSMISSION LOSS

The internal wave spectrum occupies a continuum in scale; from the Brunt Vaisala period to the inertial period having all horizontal wavelengths and vertical wavelengths, possibly from a few centimetres to the depth of the ocean. To bring out the amplitude of the internal waves the depth-time section of the temperature at the observation point is shown in Fig.(5.4a). Fluctuations in temperature field is quite evident in the thermocline region and is due to internal wave propagation. In the absence of direct measurements, a two-layer approximation of the ocean was made for the computation of internal wave speed. Based on this approximation (Pond and Pickard, 1983) the speed (v), of the internal wave can be computed from

$$v^2 = gh \left[(\rho - \rho')/\rho' \right]$$

sea surface

9m

$\rho' = 1.022582$ g cm^{-3}

71m

$\rho = 1.024367$ g cm^{-3}

sea bottom

71
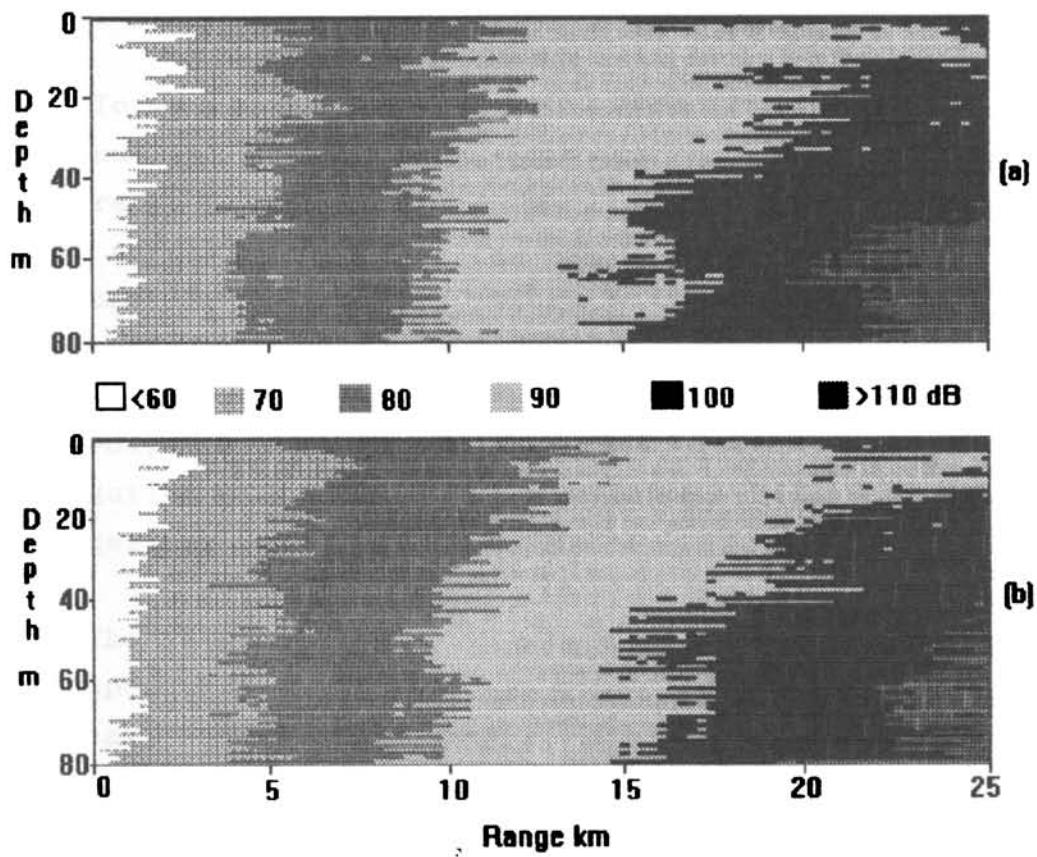
Fig.5.6 Contours of propagation loss as a function of range
and depth for internal wave with (a) all the
harmonics (b) high frequency harmonics (periods
greater than 12hrs).

where g is the acceleration due to gravity, h is the thickness of the top layer of weak density gradient, ρ is the mean density of the bottom layer of strong density gradient, and ρ' is the mean density of the top layer. The average speed of the internal wave computed to be 40 cm s^{-1}.

To model the acoustic fluctuations, basic assumptions are made which allow to relate the time series measurements to a range-dependent field (Rubenstein and Brill,1991). The first assumption is that the temperature field is made up of soliton-like internal waves. Since solitons are dispersionless the temperature fluctuations with a constant speed (internal wave speed) can advect to yield a range-dependent field. Secondly, the direction of propagation of the waves is assumed to be that of acoustic propagation.

The hourly sound speed profiles were computed corresponding to the temperature profiles following Mackenzie(1981). The entire sound speed profiles are separated into discrete sets of 24. With an internal wave speed of 40 cm s^{-1} this corresponds to 33.6 km of horizontal range. The effects of internal waves on sound propagation is more in the frequency range 50Hz-20kHz (Etter,1991). A 3kHz source frequency source selected at 5m depth to simulate the transmission loss.

Acoustic intensity fields are simulated under range-dependent (with 24 profiles) and range-independent environments (with single profile). The first profile in the set of 24 is taken for the range-independent model simulation. The simulation of transmission loss is performed for all the sets. The array of transmission loss values
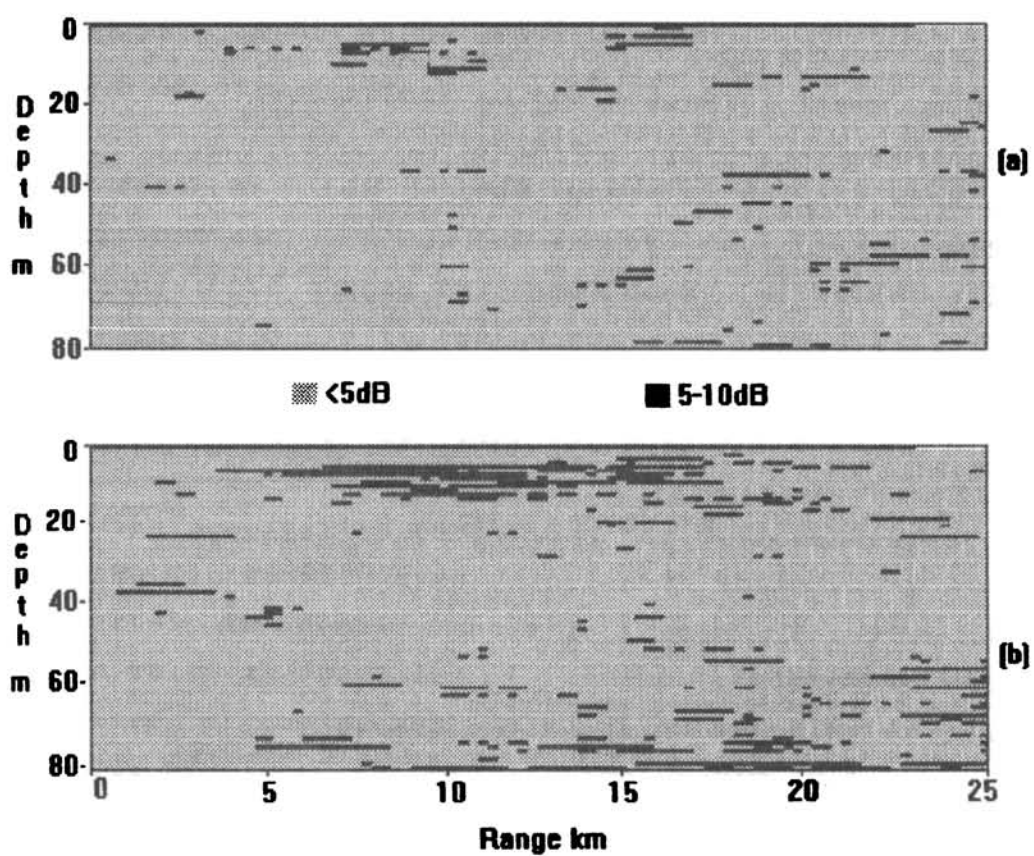
Fig.5.7 Difference contours of propagation loss values (a)
high frequency harmonics (period greater than 12hrs)
(b) diurnal frequency (period 24hrs)

obtained from simulation for range-independent environment is subtracted from the corresponding array for the range-dependent environment to obtain a loss difference array. This difference array of transmission loss is contoured (difference contour) for all the individual sets. The difference contours indicate strong (Fig.5.5a) and weak (Fig.5.5b) fluctuations in the acoustic field. The strong fluctuations are associated with transmission loss difference of -15dB to 25dB, where as for the weak field it mostly between -5dB and 5dB except few higher differences (5-15dB).These strong (S) and weak (W) fluctuations are clearly evident in thermal structure (Fig.5.4a). Thus the internal wave field can cause an acoustic intensity fluctuation of -15 to 25dB, which is appreciably high.

The propagation conditions for different spectral bands of the internal waves mentioned above are simulated separately to identify their influence. It may be noted that since only 24 profiles (33.6 km horizontal range) are utilised for the present simulation spanning one day, the effects of inertial oscillation could not be resolved. Simulations are carried out for all the remaining sets of data in the similar manner.

The transmission loss contours for two sets viz., the set containing all the harmonics (Fig.5.6a) and for the higher frequency (higher than semi-diurnal) harmonics (Fig.5.6b) indicate that they are almost similar but with certain minor variations. To investigate further this aspect, the difference contours for two harmonics (diurnal and higher) are presented in Figs.(5.7(a & b)). The contours greater than 10dB difference are shaded black in the diagram. The difference field show large variations corresponding to the diurnal harmonics than the high
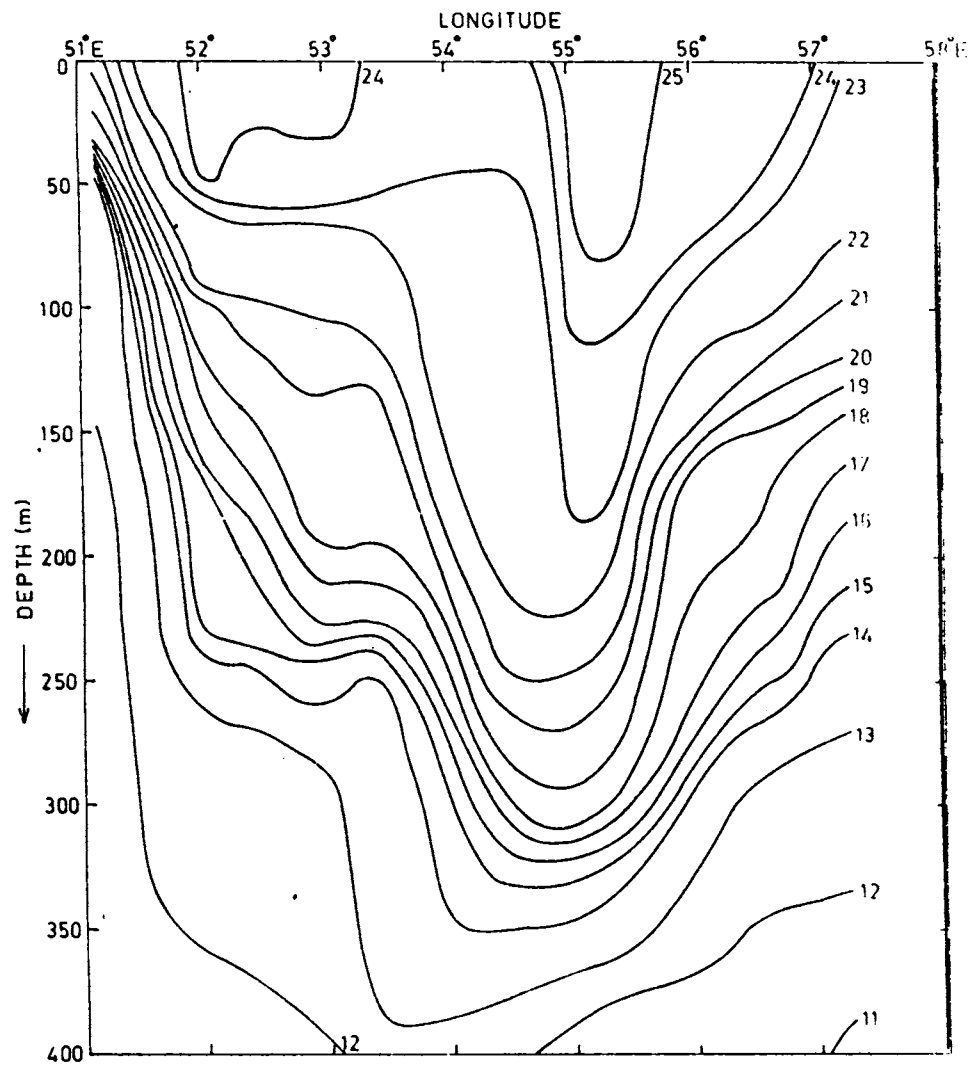
Fig.5.8 Presence of a warm core eddy evidenced by the spatial
fluctuations in isotherm patterns.

frequency internal waves. This clearly suggest that the influence of high frequency harmonics closely resemble with internal wave field containing all harmonics. This established that to study the acoustic field in the presence of internal wave, major focus has to be given to high frequency harmonics (greater than semi-diurnal frequency) compared to low frequency internal wave harmonics.

5.5 MESO-SCALE EDDIES

Influence of eddies on sound propagation was studied by several authors (Weinberg and Zabalgogeazcoa,1977; mellberg at al.,1990) and found that the eddies play a vital role in the long range propagation. Hence, an attempt is made to understand the influence of an eddy on sound propagation. During MONEX-79 temperature data were collected off Somalia normal to the coast along 8°N from west to east using XBT. The station located near to the coast was having a depth of 300m and it increased to 4500m at a distance of 130km from the shore and thereafter it maintained the same depth. The vertical structure of temperature (Fig.5.8) reveals the presence of a warm core eddy with its core temperature of about 25°C (anticyclonic) which has an horizontal extent of approximately 600km and vertical extent of about 400m. The individual sound speed profiles across the eddy is presented in Fig.5.9. A sonic layer depth of about 220m is noticed corresponds to the trough of the eddy, where the sound speed is about 1531 cm s^{-1}. The sonic layer depths are vary from one end of the eddy to the other. Corresponding to this a sharp thermocline ($\cong$ 0.25°C m^{-1}) at a shallow depth ($\cong$ 20m) at the western periphery compared to a diffused ($< 0.06^{\circ}$C m^{-1}) and deeper ($\cong$ 40m) at the eastern side. However the core of the eddy is characterised by a deep thermocline ($\cong$ 220m) with a thermocline gradient of $\cong 0.1^{\circ}$C m^{-1}. Since the
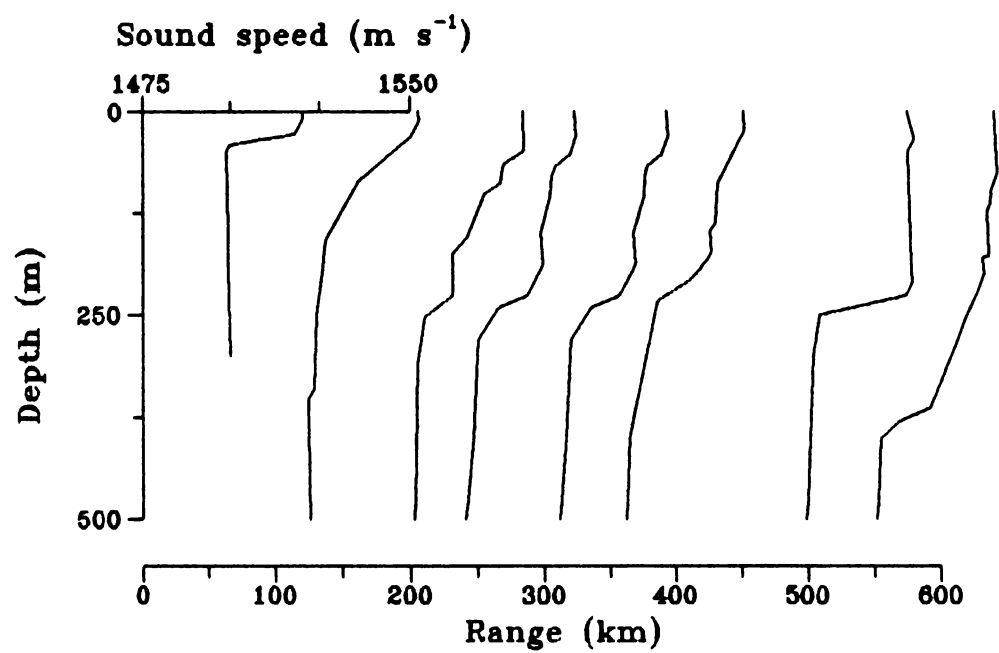
Fig.5.9 Vertical temperature profiles across the eddy

eddy was identified using hydrographic measurements without repeating the same stations, it is difficult to compute its movements. Thus for the present study a stationary eddy is assumed for transmission loss computations. In order to get the vertical profile up to station depth, a climatological mean profile available for the region is appended to the bottom of the observed profiles.

5.5.1 MODEL SIMULATIONS OF TRANSMISSION LOSS

In order to investigate the effect of this warm core eddy on sound propagation, transmission loss simulation were carried out using the PE-IFD model. Here, the effect of eddies on solely waterborne effect is studied. As the horizontal extent of the eddy is very large (600 km), high frequency sound would not propagate across the eddy. Such large ranges are attained only at low frequencies of the order of few tens of hertz. Hence, in the simulation a source frequency of 100Hz is used. The source is assumed to be positioned at 150m depth, well within the eddy and deep sound channel. Computed transmission loss for the entire range and upto a depth of 500m is presented in Fig.5.10(a & b), which covers the extent of the eddy. In order to bring out the influence of the eddy on sound propagation, the computations were repeated for an identical environment except that the water column is assumed laterally homogeneous. This is achieved by taking the initial sound speed profile to be representative of the entire range.

Transmission loss result obtained for both these cases are presented in Figs.5.10(a&b). Here, the shaded area represents regions with transmission loss higher than 100dB. The 100dB value was selected arbitrarily, such that all the convergence zones are represented in the figures. The
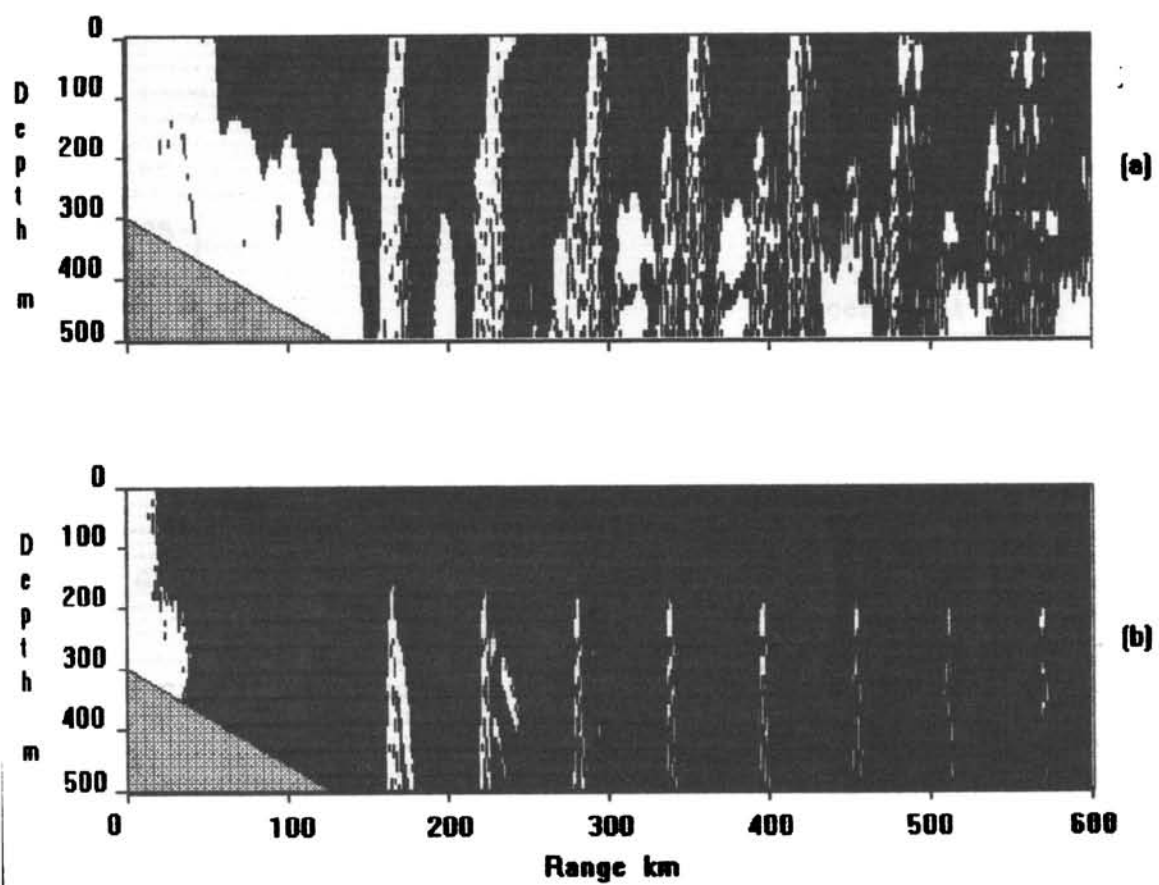
Fig.5.10 Iso-loss contours determined by PE-IFD model
(a) propagation across the eddy (b) propagation
without eddy. Shaded (black) area represent loss
higher than 100 dB
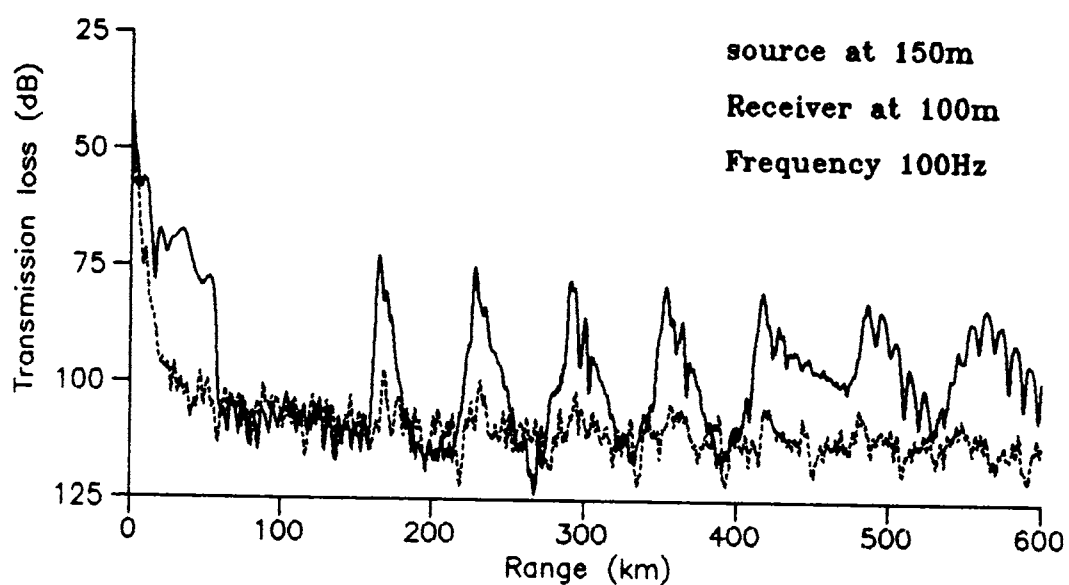
Fig.5.11 Propagation loss versus range from PE-IFD model for 100 Hz Frquency source at 150m depth and receiver at 100m depth. The Continous line for propagation across eddy and dash line for without eddy.

periodic narrow (10km wide at the surface) white vertical bands occurring in Fig.(5.10a) are the convergence zones which occur at a regular range interval of about 60km. The pattern is some what smeared as the depth increases but a high degree of insonification is evident at depths more than 250m. In contrast, Fig.5.10b, which corresponds to a range-independent, eddy-free environment does not show evidence of such convergence zones except at deeper levels than the source depth. The zones are well defined and sharp compared to the previous case. Also, the area of insonification is much less especially at longer ranges from the sound source. Almost similar observations were made by Lawrence (1983) in a modelling study of acoustic propagation across warm core eddy in the Tasman sea, where the convergence zones rose to near surface in the presence of a warm core eddy. The results of the simulation show the significance of the eddy on long range sound propagation characteristics.

In order to highlight the magnitude of acoustic intensity variation caused by the presence of the eddy, transmission loss as a function of range at a depth of 100m for both the cases are presented in Fig.5.11. About 15-20dB convergence gain is evident from the figure. Lateral shift in the pattern of the convergence zones of the order of about 10km is also noticed. The width of the convergence zone and lateral shift in the zone are all depend on the detailed nature of the eddy field.

CHAPTER VI

SUMMARY AND CONCLUSIONS

The present study has been undertaken with the objectives to understand the thermocline variability in the Arabian Sea and to investigate its influences on acoustic propagation. Though this type of study has been carried out for the other oceanic regions, the thermocline variability and associated acoustic propagation were not understood well for the Arabian Sea. One of the preliminary tasks was to identify the various oceanographic features that are responsible for the thermocline variability. The outcome of this study was that various factors such as eddies, internal waves, water masses, upwelling/sinking, undercurrents, summer/winter cooling and monsoon effects influence the structure of thermocline in the Arabian Sea, in the spatial and temporal domains.

In the present study major focus has been given to understand thermocline variability in the Arabian Sea as a whole. The typical parameters which are used to describe the thermocline characteristics are its top, thickness, gradient and oscillations. Subsequently to investigate the different processes prominent in the the coastal waters which have bearing on the thermocline characteristics, transects of temperature normal to the coast were analysed. The uniqueness of this data set is that several hydrographic sections were repeatedly made to cover the same stations. As the variabilities observed in the thermocline was found to be occurring on different time scales, the investigation was further extended to cover the short term aspects also. This

was achieved by analysing time series measurements made at several locations in the Arabian Sea. These data sets were collected for coastal as well as deep waters covering monsoon and non monsoon periods. After having described the thermocline variability, the propagation characteristics for different types of thermocline were investigated.

Climatological studies indicated that during pre-monsoon periods entire Arabian Sea was characterised by shallow thermocline (30-40m) due to surface heating. With the commencement of summer monsoon thermocline further shoaled in the the coastal regions due to upwelling. On the other hand deep thermoclines (>120 m) were noticed for the same period in the central Arabian Sea due to sinking and increased vertical mixing. One of the major findings is that strong spatial variability was noticed from July to September in the entire Arabian Sea. The scenario changed as the winter sets in. The thermocline was pushed down (>70m) in the coastal region. Thermocline thickness suggested that it is less than 40m in the northern Arabian Sea throughout the year. It increased (>100m) and average thermocline temperature drops to less than $20^{\circ}C$ during summer monsoon. The thermocline gradient was found to be between 0.04° and $0.14^{\circ}Cm^{-1}$. Weak gradients are noticed in the northern Arabian Sea due to interaction of two different watermasses (Arabian Sea High Salinity and Persian Gulf watermasses). The decrease of gradient in the equatorial Arabian Sea from January to June is attributed to equatorial undercurrent which caused the spreading of isotherms in the thermocline.

Large variations in thermocline characteristics are noticed off the west coast of India on an annual cycle. Large cross shore and onshore dynamic processes were found to be responsible for the observed thermocline variability.

In response to these processes the thermocline was found to shoal and deepen along the entire west coast. One of the important findings of this study is that on an annual cycle the thermocline characteristics were found to exhibit a time lags from southern to northern locations.

Deep thermocline (>60m) is noticed off Ratnagiri from January to March. From May onwards the thermocline moved up due to upwelling and it almost surfaces ($\cong$10m) during summer monsoon. The shallow thermocline is noticed even up to December. The thermocline gradient also increases during this period (0.3^{o}C m^{-1} in October) which decrease to 0.08^{o}C m^{-1} in January. The influence of northward flowing undercurrent on thermocline variability was found to be negligible north of Ratnagiri.

Deep thermocline (>60m) is noticed off Kasargod from December to February. During pre-monsoon months it shoals to less than 25m due to accumulation of heat in the upper layers with very warm SST (>30°C) associated with Indian Ocean warm pool. The thermocline during this period was thick (>190m) with weak vertical gradient (0.075 ^{o}Cm^{-1}). With the progress of upwelling the gradient in the upper thermocline increases to over 0.2^{o}C m^{-1}. However, in the lower thermocline the gradient was weak ($\gtrsim$0.08^{o}C m^{-1}). This is due to increased shear mixing associated with southerly surface currents and northerly undercurrent.

The deep thermocline observed during December-February shoals during pre-monsoon due to intense surface heating off Cochin. The upward movement of isotherms in the thermocline is evident from March and it surfaces by July/August, with strong vertical temperature gradient (>0.2^{o}C m^{-1}). Upwelling continues up to October. The down slopping of the isotherms

towards the coast in the lower thermocline is an indirect evidence of the presence of sub-surface northward undercurrent. As a result, in the lower thermocline weak temperature gradient $(0.03^\circ C \ m^{-1})$ are noticed due to strong shear mixing. The commencement of sinking results in the deepening of thermocline ($>100m$) in December. During this period the temperature gradient increased $(0.15^\circ Cm^{-1})$ which was an unique feature observed in this region.

Off Cape Comorin deep thermocline is observed ($>70m$) from December to January. Another important result that can be seen from vertical section of temperature was the occurrence of a clockwise eddy (warm core) centered about 150 km from the coast. The core temperature of the eddy was found to be $27^\circ C$ and its radius about 50 km. At the centre of the eddy thermocline was deeper by about 50m compared to its peripheries. The thermocline surfaces by July/August due to upwelling as off Cochin and Kasargod. During major part of the year upwelling dominated (March-October) compared to sinking (November-February) process.

The analysis further revealed that surfacing of thermocline leads to significant cooling in the surface layers ($\approx 6^\circ C$ off Cape and Cochin, $4^\circ C$ off Kasargod). However, the thermocline did not surface off Ratnagiri. The downward movement of thermocline (sinking) starts by October, October-November, November and January off Cape, Cochin, Kasargod and Ratnagiri respectively. Thus it was observed that there was a time lag of about a month for the commencement of sinking process from south to north.

The average temperature decreases sharply at all locations due to upwelling compared to periods of sinking. The annual range of average temperature of thermocline is

maximum off Cochin (5°C) and minimum (3°C) off Ratnagiri. Average rate (per month) of upward movement of isotherms was found to be 30m, 23m, 29m and 11m off Cape, Cochin, Kasargod and Ratnagiri respectively, suggesting stronger upwelling off the south west coast of India. The deepening rate isotherm was found to be about 2 to 5 times faster during the period of sinking, compared to that of upwelling.

The T-S analysis indicated the presence of Arabian Sea high salinity watermass in the thermocline throughout the year. However, the effect of Bay of Bengal watermass was marginal in the thermocline. The low saline equatorial Indian Ocean watermass is also evident in the thermocline.

The average temperature of thermocline indicated drastic cooling from pre-monsoon to monsoon. The cooling is found to be maximum south of 14°N and north of 20°N. The strong upwelling off the south west coast of India and winter cooling north of 20°N coupled with pre-monsoon heating induced large annual ranges in thermocline temperature ($\gtrsim 10^{\circ}$C).

The analysis of short-term variability of thermocline at selected locations in the Arabian Sea brought out several interesting features. A three-layer vertical temperature profile with strong thermocline (2.5°C in 10m) was observed off Bombay in June/July, whereas much weaker thermoclines were observed in the central Arabian Sea. This strong thermocline off Bombay was the result of intense pre-monsoon heating followed by vertical mixing in the upper 50m (due to monsoon activity) over the remenant of winter water. The dynamic aspects of three layer structure investigated with the help of Richardson number indicated high values (7.4 in thermocline) off Bombay. This is an evidence of the

81

suppression of turbulence which enabled the three layer structure with strong thermocline gradient to be maintained throughout the period of observation. Further the thickness of the thermocline was only 10m at this location.

The thermocline was shallower off Karwar in September (5m) compared to June (20m) mainly due to the effect of upwelling. The thermocline gradient also showed a higher value of 0.3°C m^{-1} in September compared to January (0.15 $^\circ$C m^{-1}. Another note worthy feature at this location was the presence of bottom isothermal layer. The spectral characteristics indicated that oscillations of inertial, diurnal and semi-diurnal periodicity occur in the thermocline.

The effect of upwelling on thermocline characteristics is clearly evident in the temperature profiles off Cochin. The thermocline shoaled and the isotherms moved up between April and June. The temperature at 60m dropped by as much as 6°C during this period. The 25°C isotherm moved up at an average speed of 1.1 m day^{-1} and thermocline gradient also doubled (0.1 to 0.2 $^\circ$C m^{-1}) during this period. The vertical current shear increased from 0.005 s^{-1} to 0.25 s^{-1} from April to June showing increased turbulence in the lower thermocline. This suggested increased mixing in the thermocline due to southerly surface flow and northerly undercurrent in June. The Richardson number decreased from 0.2 to 0.05 during this period suggesting dynamic instability.

The thermocline variations on short time scales differed markedly in the deep stations compared to coastal stations. In the eastern Arabian Sea intense surface heating produced a shallow thermocline ($\cong$20m) during pre-monsoon.

With the progress of the monsoon though thermocline deepens to 100m the isotherms within it moved up. This resulted in the increase of thermocline gradient (<0.1 to >0.02 $^{\circ}C$ m^{-1}).

Oceanographic aspects of thermolcine characteristics for the Arabian Sea indicated that large variabilities in both spatial and temporal domains exist. In association with these variabilities one can expect large variations in the acoustic propagation characteristics also. This is due to the fact that temperature is one of the important parameters determining sound speed in the ocean. This clearly indicate that *apriori* knowledge of thermocline characteristics is very much essential to understand the propagation conditions in the sea. Transmission loss and sound speed are the two important parameters which are commonly used to describe the propagation conditions in the ocean medium.

Simulation of transmission loss carried out with the help of a range dependent model (PE-IFD) for different features associated with thermocline indicated that each of them affect propagation in a distinct manner. As the thermocline acts as a barrier for the passage of acoustic energy from either side, occurrence of shadow zones are associated with its characteristics. Shadow zones, the regions of weak sound intensity, were found to exhibit large variations depending on the thermocline gradient and thickness. When thermocline gradients were sharp it was found that a prominent shadow zone occurred at near ranges and vice versa. Sharp gradients in thermocline were generally found to exist during the periods of upwelling in the coastal Arabian Sea. Thus one can expect prominent shadow zones during this period.

Numerical experiments carried out with different

thermocline features indicated large fluctuations in the intensity of acoustic energy. Typical case studies were carried out to simulate the propagation conditions for oceanic layered microstructure, internal waves, meso-scale eddy field.

The results indicated that inclusion of layered microstucture in the propagation model is important as it was found to influence intensity fluctuation in the acoustic field. A deference (with and without microstructuree) of 2-4 dB transmission loss was found to exist for a source of 2 kHz frequency when the layer thickness was $\cong 10m$. The oscillations associated with thermocline (internal waves) are found to influence propagation to a large extent. In the presence of weak internal wave activities (identified from thermal structure) the transmission loss fluctuation was found to be -5 to 5 dB. On the contrary, it was -15 to >20 dB for strong internal wave field. This clearly establishes that internal waves can cause large fluctuations (3 to 4 times) in the acoustic intensity. Further, influence of different harmonics on sound propagation suggested that periods higher than the semi-diurnal (12 hrs) were predominant compared to low frequencies. This also establish major focus has to be given to high frequency harmonics compared to low frequency harmonics. Simulations carried out for a warm core eddy with a source of 100Hz frequency at 150m depth revealed that convergent zones are found to extend to the surface. This suggest that more energy would be available in the near surface region compared to a situation where eddy is absent. Moreover the area of insonifications is found to be much less and sharp in the absence of an eddy field and vice versa. Another important result is that there was a convergence gain of 15-20 dB at 100m depth in presence of eddy. A lateral shift of about

10km was noticed in this pattern at this depth.

FUTURE OUTLOOK

In the present study the problem of thermocline variability in the Arabian Sea has been addressed in terms of various oceanographic factors and their influence on acoustic propagation. Though a number of oceanographic factors could be identified from the data sets used, specific data collection programme need to be planned to address the thermocline aspects in greater detail. In this programme the aspects like layered microstructure, directional internal waves, eddies, currents etc need to be monitored for basin wide at close spatial and temporal resolutions. However, the tremendous logistics involved for carrying out such a programme prevented us from taking up this task. Systematic observations of thermocline with relevent data on various physical processes would enable to develop a numerical model of the thermocline.

The study could be further extended using the fine scale measurements to study more realistic transmission loss characteristics which can be used as a back ground to asses the propagation conditions. The transmission loss studies carried out in the frame work of a range dependent model need to be validated with proper experimental data. This would improve the capability of underwater surveillance.

REFERENCES

Ali H B (1993) Oceanographic variability in shallow water acoustic and the dual role of the bottom. *IEEE Journal of oceanic engineering*, 18,(1) 31-41.

Antony M K (1990) Northward undercurrent along the west coast of India during upwelling - Some inferences. *Indian Journal of Marine Sciences*, 19, 95-101.

Baer R N (1981) Propagation through a three dimensional eddy including the effect on an array. *Journal of Acoustical Society of America*, 69, 70-75.

Balasubramanian P and K G Radhakrishnan (1989). Implementation of a range dependent transmission loss model based on Parabolic equation method. *Departmental report No.RR*-13/89, Naval Physical and Oceanographic Laboratory, Kochi.pp25.

Balasubramanian P and K G Radhakrishnan (1990) PE:IFD model versus off Cochin experimental data *Journal of Acoustical Society of India,* XVIII, 78-82.

Banse K (1968) Hydrography of the Arabian Sea shelf of India and Pakistan and effects on demersal fishes. *Deep-Sea Research*, 15, 45-79.

Bauer S, G L Hitcock and D B Olson (1991) Influence of monsoonally forced Ekman dynamics upon surface layer depth and plankton biomass distribution in the Arabian Sea. *Deep Sea Research*, 38, 531-553.

Baxter L,II and M H Orr (1982) Fluctuations in Sound transmission through internal waves associated with the thermocline: A computer model for acoustic transmission through sound velocity fields calculated from thermistor chain, CTD,XBT,and acoustic backscattering. *Journal of Acoustical Society of America* 71(1) 61-66.

Beckerle J, Baxter L, Porter R, Spindel R(1980) Sound channel propagation through eddies South West Off the Gulf Stream. *Journal of Acoustical Society of America* 68 : 1750-1767

Brekhovskikh L and Lysanov Yu (1982) *Fundamentals of ocean Acoustics* springer-Verlag, Berlin Heidabbery- pp250.

Brock J C, C R McClain, M E Luther and WW Hay (1991) The phytoplankton bloom in the northwestern Arabian Sea during the southwest monsoon of 1979. *Journal of Geophysical Research*, 96, 20613-20622.

Brock J C, C R McClain and W W Hay (1992) A Southwest monsoon hydrographic climatology for the Northwestern Arabian sea. *Journal of Geophysical Research* 97 (CO) 9455-9465.

Bruce J G (1974) Some details of upwelling off the Somali and Arabian coasts. *Journal of Marine Research*, 32, 419-423.

Bruce J C, Quadfasel D R, Swallow J C (1980) Somali eddy formation during the commencement of the South West monsoon of 1978. *Journal of Geophysical Research* 85 (C11): 6654-6660.

Charyulu R J, Y V B Sarma, M S S Sarma and L V G Rao (1994) Temperature oscillations in the upper thermocline region - A case of internal wave off Kalpeni island in the southern Arabian Sea. *Indian Journal of Marine Sciences*, 23, 14-17.

Chen CT, and F J Millero(1977) Speed of sound in sea water at high pressures. *Journal of Acoustical Society of America.* 62, 1129-1135.

Clark J G and M Kronengold (1974) Long period fluctuations of CW signals in deep and shallow water *Journal of Acoustical Society of America*, 56,1071-1083.

Colborn J G (1975) The thermal structure of the Indian Ocean. University Press of Hawaii, Honolulu, pp173.

Colosi J A, S M Flatte and C Bracher (1994) Internal wave effects on 1000 km oceanic acoustic pulse propagation, simulation and comparison with experiment. *Journal of Acoustical Society of America*, 96, 452-468.

Currie R I, A E Fisher and P M Hargreaves (1973) Arabian Sea upwelling. In : The biology of the Indian Ocean, B Zeitzchel and S A Gerlach (Ed.),Springer-Verlag, 37-53.

Cutler A and J Swallow (1984) Surface currents of the Indian Ocean (to $25^{\circ}S,100^{\circ}E$) (Compiled from Achieved historical data). (UK Institute of Oceanographic Sciences, Bracknell) pp 8 and charts 36. 36.

Das V K Gouveia A D, Varma K K (1980) Circulation of Water characteristics on isanosteric surfaces in the Nothern Arabian Sea during February -April.*Indian journal of Marine Science* 9(3) 156-165.

Davis J A , White D and Cavanagh R C,(1982) Norda parabolic equation workshop, 31 March- 3 April 1981. *Naval Ocean Research and Development Activity, Technical Note* pp143.

Darbyshire M (1967) The surface waters off the coast of Kerala, southwest India. *Deep-Sea Research*, 14, 295-320.

Defant (1936) Die troposphare des Atlantaschen Ozeans. Schichtung und Zirkulation des Atlantischen Ozeans. Deutsche Atlantische Expedition "Meteor" 1925-1927 Wissenschaaftl . Erg;6(1): pp289.

Del Grosso V A (1974) New equation for the speed in natural water (with comparison to other equations), *Journal of Acoustical Society of America* 56, 1084.

Del Grosso, V A and C W Mader (1972) Speed of sound in sea water samples. *Journal of Acoustical Society of America.* 52 961-974

Desaubies Y J F (1976) Acoustic phase fluctuations induced by internal waves in the Ocean. *Journal of Acoustical Society of America* 60(4) 795-799

Desaubies Y J F (1978) On the scattering of sound by internal waves in the ocean. *Journal of Acoustical Society of America*, 64, 1461-1469.

Duing W (1972) The structure of sea surface temperature in monsoonal areas. In : Studies in Physical Oceanography, A L Gordon (Ed.) 1-18.

Duing W and A Leetmaa (1980) Arabian Sea cooling : A
preliminary Heat Budget. *Journal of Physical
Oceanography*, 10, 307-312.

Elliot A J and G Savidge (1990) Some features of the
upwelling off Oman. *Journal of Marine Research*, 48,
319-333.

Etter P C (1991) Underwater Acoustic Modeling : Principles,
techniques and applications. **Elseiver Applied Science,
New York** pp297.

Ewart T E (1980) A Numerical simulations of the effects of
Oceanic Fine structure on the acoustic transmission,
Journal of Acoustical Society of America, 67(2),
496-503.

Flatte S M, Dashen R, W H Munk, K M Waston and F Zachariasen
(1979) Sound transmission through a fluctuating
Ocean. **Cambridge University Press, Cambridge UK** ,85-161.

Flatte S M and F D Tappert (1975) Calculation of the effect
of internal waves on oceanic sound transmission.
Journal of Acoustical Society of America, 58,
1151-1159.

Gallagher J F (1966) The variability of watermasses in the
Indian Ocean. **Publication National Oceanographic Data
Centre**, G-11, 1-74.

Hamilton G R (1974) The variations of sound speed over long paths in the Ocean :International workshop on low frequency propagation and noise, Woods Hole, M.A. 7-30.

Hareesh Kumar P V (1994) Thermohaline variability in the upper layers of the Arabian Sea, Ph.D thesis, Cochin University of Science and Technology, pp108.

Hareesh Kumar P V and N Mohan Kumar (1995) On the flow and thermohaline structure off Cochin during the pre-monsoon season, Continental Shelf Research (in press).

Hareesh Kumar P V, N Mohan Kumar and K G Radhakrishnan (1995) Multiple subsurface maxima in vertical salinity structure - A case study. *Indian Journal of Marine Sciences*, 24, 77-81.

Hart T J and R I Currie (1960) The Benguela Current. *Discovery Report*, 8, 437-457.457.

Hastenrath S and L Grieschar (1989) Climatic Atlas of the Indian Ocean - Part III : Upper - ocean structure. (University of Winsconsin press,Madison) pp247.

Hastenrath S and P Lamb (1979) Climatic Atlas of the Indian Ocean - Part I : Surface Climate and Atmospheric circulation (Wisconsin University Press Madison, p 11 and Figs 97.

Hasternath S and J Merle (1987) Annual cycle of subsurface thermal structure in the tropical Atlantic Ocean. *Journal of Physical Oceanography*, 17, 1518-1538.

Henrick R F (1980) General effects of currents and sound speed variations on short range acoustic transmission in cyclonic eddies.*Journal of Acoustical Society of America* 67 No:1 121-134.

Itzikowitz S, M J Jacobson and W L Stiegmann (1982) Short range acoustic transmission through cyclonic eddies between a submerged source and receiver. *Journal of Acoustical Society of America*, 71, 1131.

Johannessen O M, G Subbaraju and J Blindheim (1981) Seasonal variation of the oceanographic conditions off the southwest coast of India during 1971-75. *FiskeriDir. Skr. Ser.*, 18, 247-261.

Joseph M G, P V Hareesh Kumar and B Mathew (1990) Short term pre-onset southwest monsoonal transformations in upper western equatorial Indian Ocean. *Indian Journal of Marine Sciences*, 19, 251-256.

KNMI, (1952), Indische Ocean Oceanographische and Meteorologische gevens., 2Ed. Publ. No. 135, pp (31) and 24 Charts.

Krishnamurti T N (1981) Cooling of the Arabian Sea and the onset vortex during 1979 In: **Recent Progress in equatorial oceanography**, Report of final meeting of SCOR Working Group 47 Venice, Italy.

Lawarence M W (1983) Modeling of acoustic propagation across warm core eddies. *Journal of Acoustical Society of America*. Vol 73(2), 427-485.

Lee D and S T Daniel (1988) Ocean Acoustic Propagation by finite difference methods. **Pergamon Press New York,** pp423.

Lee O S (1961) Effect of an internal wave on sound in the ocean. *Journal of Acoustical Society. of America,* 33, 677-681.

Leetmaa A and H Stommel (1980) Equatorial current observations in the western Indian Ocean in 1975 and 1976. *Journal of Physical Oceanography,* 10, 258-269.

Leetmaa A, D R Quadfasel and D Wilson (1982) Development of the flow field during the onset of the Somali Current,1979. *Journal of Physical Oceanography,* 12, 1325-1342.

Leipper D F (1967) Observed ocean conditions and hurricane Hilda, 1964. *Journal of Atmospheric Science,* 24, 182-196.

Levenson, C and R A Doblar (1976) Long range acoustic propagation in the Gulf Stream. *Journal of Acousical Society of America.* 59, 1134.

Levitus S (1982) Climatological Atlas of the world ocean. (US Government Printing Office, Washington DC) pp213

Mackenzie K V (1981) Nine-term equation for sound speed in the Oceans. *Journal of Acoustical Society of America.* 70, 807.

Medwin H (1975) Speed of sound in water : A simple equation for realistic parameters. *Journal of Acoustical Society of America* 58, 1318

Mathew B (1981) Studies on upwelling and sinking in the seas around India, Ph.D Thesis, University of Cochin pp159.

McCreary J and P K Kundu (1989) A numerical Investigation of Sea Surface Temperature Variability in the Arabian Sea. *Journal of Geophysical Research*, 94, 16097-16114.

Mellberg L E, A R Robinson and G Bostew (1990) Modeled time variability of acoustic propagation through a Gulf stream meander and eddies. *Journal of Acoustical Society of America*, 87, 1044-1053.

Mellberg L E and O M Johanessen (1973) Layered oceanic microstructure - its effect on sound propagation. *Journal of Acoustical Society of America*, 53, 571-580.

Miles J W (1961) On the stability of heterogeneous shear flows. *Journal of Fluid Mechanics*, 10, 496-508.

Mohan Kumar N (1991) A study on air-sea interaction processes over the Indian Seas, Ph.D thesis, Indian Institute of Technology, Delhi. pp132.

Mohan Kumar N, P V Hareesh Kumar and M X Joseph (1995) Response of the coastal waters off Karwar to summer monsoonal forcing during 1989. *Continental Shelf Research*, 15, 883-888.

Mohanty U C, Dubey, S K and Singh M P (1983) A study of heat and mositure budget over the Arabian Sea and their role in the onset of maintenance of summer monsoon. *Journal of Meteorological Society of Japan,* 61, 208-221.

Molinari R L (1983) Somali Basin response to the monsoon and the feed back effect of the atmosphere. (CCCO Panel on Indian Ocean Climatic Studies, First Session,Paris)

Molinari R L, J F Festa and J C Swallow (1986a) Mixed layer and thermocline climatologies in the western Indian Ocean (Atlantic Oceanographic and Meteorological Laboratory, Miami), pp40.

Molinari R L, J C Swallow and J F Festa (1986b) Evolution of near surface thermal structure in the western Indian Ocean during FGGE 1979. *Journal of Marine Research,* 44, 739-763.

Montgomery R B and Stroup E D (1962) Equatorial waters and currents at $150^{\circ}W$ in July-August 1952. Johns Hopk Oceanogr. studies, 1-68.

Munk W H (1980) Horizontal deflections of acoustic fronts by mesoscale eddies. *Journal of Physical oceanography* 10, 596-604.

Munk W H and Zachariasen (1976) Sound propagation through a fluctuating ocean theory and observation. *Journal of Acoustical Society of America,* 59, 818-838.

Muraleedharan P M, M R Ramesh Kumar and L V G Rao (1995) A note on poleward undercurrent along the southwest coast of India. *Continental Shelf Research,* 15, 165-184.

Murthy P G K and G R K Murthy (1986) A case study on the
    influence of internal waves on sound propagation in the
    sea. *Journal of Sound and Vibration*, 108, 447-454.

Murthy P G K, G S Sharma, V V James and K V Suseela (1992)
    Internal wave characteristics in the eastern Arabian
    Sea during summer monsoon. *Proceeding of the Indian
    Academy of Sciences*, 101, 317-327.

Murthy P G K and P N Ananth (1994) Internal waves and their
    diurnal activity in the coastal waters around India
    Symposium on Underwater systems, NSTL, Vizag

Murthy P G K and P V Hareesh Kumar (1991) Response of
    coastal waters off Karwar to a deep depression.
    Continental Shelf Research, 11, 239-250.

Murthy P G K and V V James (1995) Some aspects of internal
    waves in the coastal waters off Cochin. *Indian Journal
    of Marine Sciences* (in press)

Narayana Pillai V, P K Vijayarajan and A Nandakumar (1980)
    Oceanographic investigations off the southwest coast of
    India. *FAO/UNDP Report*, (FAO, Rome),pp51.

Pankajakshan T and D V Ramaraju (1987) In : Contributions in
    Marine Sciences. T S S Rao et al (Editors),pp237.

Phillips O M (1977) The dynamics of the upper ocean.
    Cambridge University Press, New York, pp336.

Pickard G L and W J Emery (1982) Descriptive Physical
    Oceanography. An Introduction, Pergamon Press, Oxford,
    pp249.

Pinkel R and J T Sherman (1991) Internal wave induced
        fluctuations in the oceanic density and sound speed
        fields. *Ocean Variability and acoustic propagation*,
        Potter J and A Warn-Varnas (eds) Kluwer Publishers,
        Netherlands, 103-118.

Pollard R T (1970) On the generation by wind of internal
        waves in the ocean. *Deep Sea research*, 17, 795-812.

Pond S Pickard G L (1983) Introductory Dynamical
        oceanography **Pergamon Press, Newyork, pp321.**

Porter R P, R C Spindel and R J Jafee (1974) Acoustic
        internal wave interaction at long ranges in the ocean.
        Journal of Acoustical Society of America, 56, 1424-1436.

Prasannakumar S, M T Babu and Ramanamurthy T V (1992) Sound
        speed structure and propagational characteristics of a
        cold core eddy in the Bay of Bengal. *Physical Processes
        in the INDIAN SEAS proceedings, ISPSO,* 1990, 51-55.

Prasannakumar S, T V Ramana Murthy, R K Somayajulu, P V
        Chodankar and C S Murthy (1994) Reference sound speed
        profile and related ray Acoustics of Bay of Bengal for
        tomographic studies. *Acoustics*, 80, 127-137.

Quadfasel D R and F Schott (1982) Watermass distribution at
        intermediate layers off the Somali Coast during the
        southwest monsoon 1979. *Journal of Physical
        Oceanography*, 12, 1358-1372.

Quadfasel D R and F Schott (1983) Southward subsurface flow
        below the Somali current. *Journal of Geophysical
        Research*, 88, 5973

Ramana Murthy T V, Y K Somayajalu, P V Chodankar and C S
    Murthy (1993) Acoustic characteristics of the waters
    of the Bay of Bengal. *Indian Journal of Marine
    Sciences*, 22, 263-267.

Ramesh Babu V and J S Sastry (1984) Summer cooling in the
    east central Arabian Sea - A process of dynamic
    response to the southwest monsoon. *Mausam*, 35, 17-26.

Rao D P, R V N Sarma, J S Sastry and K Premchand (1976) On
    the lowering of the sea surface temperature in the
    Arabian Sea with the advance of southwest monsoon.
    Proceeding of the symposium on *Tropical Monsoons*
    (Indian Institute of Tropical Meteorology, Pune)
    106-115.

Rao R R (1986) Cooling and deepening of the mixed layer in
    the central Arabian Sea during MONSOON-77 :
    Observations and simulations. *Deep-Sea Research*, 33,
    1413-1424.

Rao R R (1987) The observed variability of the cooling and
    deepening of the mixed layer in the central Arabian Sea
    during monsoon-77. *Mausam*, 38, 43-48.

Rao R R and B Mathew (1990) A case study on the mixed layer
    variability in the south central Arabian Sea during the
    onset phase of MONEX-79. *Deep-Sea Research*, 37,
    227-243.

Rao R R, B Mathew and P V Hareesh Kumar (1993) A summary of results on thermohaline variability in the upper layers of the east central Arabian Sea and Bay of Bengal during summer monsoon experiments. *Deep Sea Research*, 40, 1647-1672.

Rao R R, P V Hareesh Kumar and B Mathew (1990) Watermass modification in the upper layers of the Arabian Sea during ISMEX-73. *Mausam*, 41, 611-620.

Rao R R, R L Molinari and J F Festa (1989) Evolution of the Climatological Near-Surface Thermal Structure of the Tropical Indian Ocean I : Description of Mean Monthly Mixed Layer Depth, Sea Surface Temperature, Surface Current and Surface Meteorological Fields. *Journal of Geophysical Research*, 94, 10801-10815.

Rao R R, R L Molinari and J F Festa (1991) Surface meteorological and near surface oceanographic Atlas of the tropical Indian Ocean. (NOAA Technical Memorandum, ERL AOML-69) pp59.

Rao Tatavarti, N Mohan Kumar and P V Hareesh Kumar (1995) Mixing processes and internal waves on the continental shelf off Cochin. *Indian Journal of Marine Sciences* (in press)

Reverdin G (1987) The upper equatorial Indian Ocean : The climatological seasonal cycle. *Journal of Physical Oceanography*, 17, 903-927.

Robinson A R(1983) Overview and summery of Eddy science. *Eddies in Marine Sciences* (Ed.by Robinson A R) Springer-Verlag, Berlin Heidelberg. pp609.
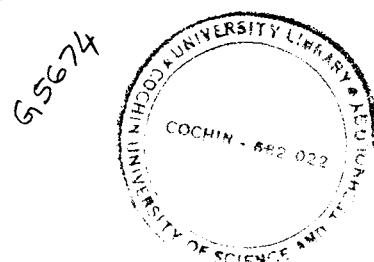
Robinson M K, R A Baur and E H Schroeder (1979) Atlas of North Atlantic-Indian Ocean monthly mean temperature and mean salinities of the surface layer. (Naval Oceanographic Office, Washington DC) pp213.

Rochford D J (1964) Salinity maxima in the upper 1000m of the north Indian Ocean. *Australian Journal of Marine and Freshwater Research*, 15, 1-24.

Rubestein D and M H Brill (1991) Acoustic variability due to internal waves and surfaces waves in shallow water. *Ocean variability and acoustic propagation*, J Potter and A Warn-Varnas (eds) Kluwer Academic Publishers, Netherlands, 215-228.

Saha K R (1974) Some aspects of the Arabian Sea summer monsoon. *Tellus*, 26, 464-476.

Sastry J S and R S D'Souza (1970) Oceanography of the Arabian Sea during southwest monsoon season - Part I : Thermal structure. *Indian Journal of meteorology and Geophysics*, 21, 367-382.

Sastry J S and R S D'Souza (1971) Oceanography of the Arabian Sea during southwest monsoon season - Part II : Stratification and Circulation. *Indian Journal of Meteorology and Geophysics*, 22, 23-34.

Sastry J S and R S D'Souza (1972) Oceanography of the Arabian Sea during southwest monsoon season - Part III : Salinity. *Indian Journal of Meteorology and Geophysics*, 23, 479-490.

Sastry J S and V Ramesh Babu (1979) Convergence of Ekman wind driven layer and surface circulation in the Arabian Sea during southwest monsoon. *Mahasagar*, 12, 201-211.

Schott F (1983) Monsoon response of the Somali Current and associated upwelling. *Progress in Oceanography*, 12, 357-381.

Schott F and D R Quadfasel (1982) Variability of the Somali current system during the Onset of the South west Monsoon.12, 1343-1357.

Schott F and D R Quadfasel (1983) Variability of Somali current system during the onset of southwest monsoon of 1979. *Journal of Physical Oceanography*, 12, 1343-1357.

Sharma G S (1966) Thermocline as an indicator of upwelling. *Journal of Marine Biological Association India*, 3, 8-19.

Sharma G S (1968) Seasonal variation of some hydrographic properties of the shelf water off the west coast of India. *Bulletin of the National Institute of Sciences*, 38, 263-275.

Sharma G S (1976) Transequatorial movement of watermasses in the Indian Ocean. *Journal of Marine Research*, 34, 143-154.

Sharma G S (1978) Upwelling off the southwest coast of India. *Indian Journal of Marine Sciences*, 7, 207-218.

Shenoi S S C and M K Antony (1991) Current measurements over western continental shelf of India. *Continental Shelf Research*, 11, 81-94.

Shetye S R (1986) A model study of the seasonal cycle of the Arabian Sea surface temperature. *Journal of Marine Research*, 44, 521-542.

Shetye S R, A D Gouveia, S S C Shenoi, D sundar, G S Michael, A M Almeida and K Santanam (1990) Hydrography and Circulation off the west coast of India during the Southwest Monsoon 1987. *Journal of Marine Research*, 48, 359-378.

Shetye S R, S S C Shenoi and D Sundar (1991) Observed low frequency currents in the deep mid-Arabian Sea. *Deep Sea Research*, 38, 57-65.

Sikka D R and R Grossman (1980) Summer MONEX Chronological weather summary. *International MONEX management Center, New Delhi*

Smith R L and J S Bottero (1977). On upwelling in the Arabian Sea. In : A voyage of Discovery, M Angel (Ed.), Pergamon Press, 291-304.

Somayajalu Y K, T V R Murthy, S P Kumar and C S Murthy (1994) Simulation studies related to acoustic propagation in the Arabian Sea. *Acoustic Letters*, 17, 173-183.

Stanford G,(1974) Low frequency fluctuations of a CW signal in the Ocean, *Journal of Acoustical Society of America*,55,968-976.

Swallow J C(1983) Eddies in Indian Ocean, Eddies in marine sicence (ed by AR Robinson) Springer-Verlag Berlin Heidelberg 200-218.

Swallow J C (1984) Some aspects of physical oceanography of the Indian Ocean. *Deep Sea Research*, 31, 639-650.

Swallow J C and J G Bruce (1966) Current measurements off the Somali Coast during the southwest monsoon in 1964. *Deep-Sea Research*, 13, 861-888.

Swallow J C, R L Molinari, J G Bruce, O B Brown and R H Evans (1983) Development of near surface flow pattern and watermass distribution in the Somali Basin in response to the southwest monsoon of 1979. *Journal of Physical Oceanography*, 13, 1398-1415.

Taft B A and J A Knauss (1967) The Equatorial Undercurrent of the Indian Ocean as observed by the Lusiad expedition. *Bulletin of Scripps Institution of Oceanography*, 9, pp 163.

Unni S and C Kaufman(1981) Acoustic fluctuations due to the temperature fine structure of the ocean. *Journal of Acoustical Society of America* 69(3) 676-680.

Urick R J (1982) Sound Propagation in the Sea, Peninsula Publisher, California pp215.

Urick R J (1983) Principles of Underwater sound McGraw-Hill Book Company, New York .pp423.

Varkey M J (1980) Power spectra of currents off Bombay. *Indian Journal of Marine Sciences*, 9, 278-280.

Vastanov A C and G E Owens (1973) On the acoustic characteristics of a gulf stream cyclonic ring. *Journal of Physical Oceanography*, 3, 470-478.

Warren B, H Stommel and J C Swallow (1966) Watermasses and patterns of flow in the Somali Basin during the southwest monsoon of 1964. *Deep-Sea Research*, 13, 825-860.

Weinberg N L and J G Clark (1980) Horizontal acoustic refraction through ocean mesoscale eddies and fronts. *Journal of Acoustical Society of America*, 68, 703-706.

Weinberg L and X Zabalagogeazcoa (1977) Coherent ray propagation through a Gulf Stream. *Journal of Acoustical Society of America*, 62, 888-894.

Wilson W D (1960) Equation for the speed of sound in Sea water . *Journal of Acoustical Society of America* 32 1357

Wyrtki K (1964) Thermal structure of the Eastern Pacific Ocean. Deutsche Hydr.Zeit.,Erganzungsheft Reihe $A(8^{\circ})$,Nr.6. Hamburg.

Wyrtki K (1971) Oceanographic Atlas of the International Indian Ocean Expedition (US Government Printing Office, Washington DC) pp531.

Wyrtki K (1973) An equatorial Jet in the Indian Ocean. *Science*, 11, 262-264.

Yoshida K and H L Mao (1957) A theory of upwelling of large
    horizontal extent. *Journal of Marine Research*, 16,
    40-54.